UNIVERSITY OF CALIFORNIA
RIVERSIDE

Forward Genetic Studies Towards the Understanding of the Molecular Mechanisms Underlying Floral Meristem Determinacy and Small RNA Function in *Arabidopsis*

A Dissertation submitted in partial satisfaction
of the requirements for the degree of

Doctor of Philosophy

in

Plant Biology

by

Yun Ju Kim

March 2010

Dissertation Committee:
Dr. Xuemei Chen, Chairperson
Dr. Patricia S. Springer
Dr. Harley M.S. Smith

The Dissertation of Yun Ju Kim is approved:

_____

_____

_____

Committee Chairperson

University of California, Riverside

ACKNOWLEDGEMENTS

This work would not have been possible without the help and support of everyone around me.

First, I am deeply grateful to my adviser, Professor Xuemei Chen. From her, I have learned the process of scientific thinking and obtained invaluable techniques throughout my doctoral career. However, the most important thing that I have learned from her is the mentality of a scientist, mentor, advisor, and leader. The summary of aforementioned skills will provide a strong foundation for my future success.

I also would like to thank the other members of my dissertation committee: Professors Patricia Springer and Harley Smith. They have provided valuable comments, honest advice, and positive feedback, to keep me on track for my dissertation work. I would also like to thank Professor Venugopala Reddy for his helpful discussion.

In addition, I especially want to thank every member of Dr. Chen's lab. I am very fortunate to have such wonderful people around me during my doctoral career. They were not only there to share the happy moments, but were also there through the hardships of both my personal and professional life. I will never forget the memories generated with my loving colleagues. I would also like to thank my friends with their love, encouragement, and support I was able to partake this long journey.

Last but not the least, I would like to thank my family for their unconditional support. They were my motivation through every moment of this process. I want to express the love I have for my parents, sisters, and brother. Specifically, I would like to deeply thank my husband, Younghoon, for his endless love and support and the dearest,

my Keul. I would like to dedicate my thesis to them because without them, I would not have made it.

Yun Ju Kim
Riverside, California
March 2010

ABSTRACT OF THE DISSERTATION

Forward Genetic Studies Towards the Understanding of the Molecular Mechanisms Underlying Floral Meristem Determinacy and Small RNA Function in *Arabidopsis*

by

Yun Ju Kim

Doctor of Philosophy, Graduate Program in Plant Biology
University of California, Riverside, March 2010
Dr. Xuemei Chen, Chairperson

Forward genetics is a powerful tool to identify genes involved in particular biological processes. In my thesis work, I participated in forward genetic screens to identify genes involved in two biological processes in plants, stem cell maintenance in the floral meristem and small RNA biogenesis/function. First, I characterized a Polycomb (PcG) gene, *CURLY LEAF* (*CLF*) as a factor required for floral meristem termination. A mutation in *CLF* enhances the floral determinacy defects of *ag-10*, a weak allele in *AGAMOUS* (*AG*), a gene essential for floral stem cell termination. *CLF* acts in the *AG* pathway to repress the stem cell identity gene, *WUSCHEL* (*WUS*) to result in floral stem cell termination. In addition, I show that this role of *CLF* reflects the role of the PcG complex in the control of floral meristem determinacy. Taken together, I provide a link between epigenetic regulation and stem cell maintenance in the floral meristem. Second, I identified two genes, *MED20a* and *STERILE APETALA* (*SAP*) that promote small RNA biogenesis and modulate small RNA activities, respectively. MED20a is a subunit of the

Mediator complex, which is thought to bridge transcription factors and the RNA Polymerase II (Pol II) transcriptional machinery. In *med20a* and mutants in two other Mediator subunits, *med17* and *med18*, miRNA accumulation is generally reduced. In the *med20a* mutant, the levels of pri-miRNA are also lower and the promoter activity of *MIR167a* is reduced, suggesting that the Mediator promotes *MIR* gene expression at the transcriptional level. I show that *SAP* is a negative regulator of the activities of a subset of miRNAs. In *sap* mutants, the mRNA and protein levels of several miRNA target genes are reduced despite no changes in miRNA accumulation. In addition, some miRNAs are more active in *sap* mutants, resulting in more 3' cleavage products from target mRNAs. This indicates that *SAP* negatively regulates the activities of a subset of miRNAs at the posttranscriptional level. These studies extend our understanding of the dynamic control of small RNA biogenesis and function.

Table of Contents

List of Figures

Chapter 1

Chapter 2

Chapter 3

List of Tables

Chapter 1

Chapter 2

Chapter 3

CHAPTER 1

The Polycomb Group proteins act in concert with *AGAMOUS* in the temporal regulation of floral meristem determinacy in *Arabidopsis*

ABSTRACT

Unlike the SAM, the floral meristem is determinate such that it produces a fixed number of floral organs. The floral homeotic gene *AGAMOUS* (*AG*) is a key temporal regulator of the stem cell identity gene, *WUSCHEL* (*WUS*); it shuts off *WUS* expression at a precise time in flower development to result in floral determinacy. Here we show that Polycomb Group (PcG)-mediated gene silencing is required for the temporal floral meristem termination. A mutation in *CURLY LEAF* (*CLF*), a PcG gene, enhances the floral determinacy defects of *ag-10*, a weak *ag* allele. Genetic and biochemical studies show that *CLF* acts in the same genetic pathway with *AG* and it is required for the initial repression of *WUS* by *AG*. In addition, the role of *CLF* reflects that of the PcG complex in the control of floral determinacy as a mutation of another PcG gene, *TFL2*, also enhances the floral determinacy defects of *ag-10*. Taken together, our studies provide a link between epigenetic regulation and the control of floral meristem determinacy.

INTRODUCTION

The meristem is a place where cells continuously divide and give rise to new cells to produce organs throughout the life cycle of the plant (Steeves and Sussex, 1989). How meristem identity is precisely maintained during cell proliferation and organogenesis is a fundamental question in developmental biology that has been intensively pursued in the model plant *Arabidopsis*. *Arabidopsis* has two important meristems for postembryonic plant development. The shoot apical meristem (SAM) harbors stem cells to produce all aerial organs and the root apical meristem (RAM) results in continuous root growth (Scofield and Murray, 2006). The SAM undergoes developmental transitions, the most obvious being the vegetative to reproductive transition. During the vegetative stage, the SAM produces rosette leaves on its flanks. After perceiving external and internal cues, the vegetative meristem is converted to an inflorescence meristem, which produces cauline leaves with inflorescences and flowers in the axils (Blazquez et al., 2006). After being initiated on the flank of an inflorescence meristem, a floral meristem produces a fixed number of floral organs in whorls: four sepals, four petals, six stamens and two fused carpels from the outside to the inside of the flower (reviewed by Sablowski, 2007). While the SAM and floral meristems probably share similar molecular mechanisms for their homeostasis, there is one apparent difference between floral meristems and the SAM - floral meristems are determinate. When carpel promordia are formed, the floral meristem is terminated at stage 6 and stops producing any other organs, resulting in a fixed number of organs and whorls (Mayer et al., 1998). What are the molecular mechanisms that specify floral meristem determinacy? Although several regulators that

play a role in floral meristem determinacy and their functions have been uncovered through genetic studies (see below), a molecular framework underlying floral determinacy still remains to be established.

Molecular mechanisms to maintain meristem stability

Although the stem cells in meristems continuously divide and some daughter cells participate in organogenesis, stem cell number and meristem size remain largely constant (Scofield and Murray, 2006). It suggests that meristem homeostasis and organogenesis are very well balanced and a mechanism exists to ensure meristem identity. *WUSCHEL* (*WUS*) and *SHOOT MERISTEMLESS* (*STM*) are two key regulators acting in parallel to regulate shoot meristem identity and stability (Lenhard et al., 2002).

WUS encodes a homeodomain-containing protein and is crucial for stem cell identity (Mayer et al., 1998). *wus* mutants fail to initiate the SAM during embryogenesis. Later, adventitious SAMs develop to result in shoots and inflorescences. The floral meristems are terminated prematurely: flowers fail to initiate the fourth whorl and usually terminate in a single stamen. On the other hand, ectopic expression of *WUS* results in an enlarged shoot apical meristem and numerous floral organs (Schoof et al., 2000; Gallois et al., 2004). *WUS* is expressed in a small number of cells (termed the organizing center) underneath stem cells and presumably regulates stem cell identity in a non-cell autonomous manner (Laux et al., 1996; Mayer et al., 1998). It is not clear how *WUS* acts non-cell autonomously to maintain stem cell identity.

CLAVATA (*CLV*) genes negatively modulate *WUS* activity (reviewed by Carles and Fletcher, 2003). *clv1, clv2* and *clv3* mutants show phenotypes that suggest enhanced meristem activity such as shoot fasciation, enlarged floral meristems and increased number of floral organs. In any of the *clv* mutants, the *wus* expression domain expands and meristem size is gradually enlarged. In contrast, increased *CLV* expression rapidly represses *WUS* expression and terminates meristem activity. *CLV1* and *CLV2* encode membrane-associated receptor like proteins (Clark et al. 1997; Jeong et al., 1999). They form a putative CLV1/CLV2 receptor complex that perceives CLV3 as a small ligand. *CLV3* encodes a 96 amino acid protein with a putative secretary signal in its N-terminal region (Fletcher et al., 1999). However, recently, biochemical studies demonstrated that a 12 amino acid peptide with two hydroxy prolines near its C-terminal region acts as the mature form of CLV3, which physically interacts with the LRR domain of CLV1 (Kondo et al., 2006; Sawa et al., 2006; Ogawa et al., 2008). This finding confirmed that CLV3 and CLV1/CLV2 act as a ligand and receptor complex to restrict *WUS* expression. In turn, WUS activates *CLV3* expression, which causes limitation of *WUS* expression itself. This *CLV-WUS* regulatory loop is a key mechanism to maintain stem cell homeostasis (Fletcher et al., 1999; Brand et al., 2000).

SHOOT MERISTEMLESS (*STM*) encodes a *KNOTTED*-like homeobox (*KNOX*) transcription factor, which is expressed throughout the meristem (Long et al., 1996). Similar to *wus* mutants, *stm* mutants exhibit premature termination of meristems, which is indicative of loss of stem cells. *STM* is thought to keep stem cells and their daughter cells

undifferentiated to bulk them up before organogenesis, while *WUS* is required to maintain stem cell identity (Lenhard et al., 2002).

Modulators of floral meristem determinacy

Floral meristems, which are derived from the SAM, share with the SAM many regulators of stem cell homeostasis such as *WUS*, *STM* and *CLV*. One difference between these two is that a floral meristem is determinate. *WUS* expression is shut down at stage 6 when carpel primordia are initiated, resulting in floral meristem termination (Mayer et al., 1998). *wus* mutant flowers terminate floral meristems prematurely. This shows that *WUS* is a central factor in floral meristem maintenance and there must be negative regulators to control *WUS* activity in floral meristems to result in proper floral meristem termination. In the past two to three decades, several regulators have been identified through genetic studies.

AGAMOUS (AG) is a main switch to turn off *WUS* expression at the proper time. It was identified as a homeotic gene that is expressed in the inner two whorls to specify stamen and carpel identities (Bowman et al., 1989; Yanofsky et al., 1990). However, in strong *ag* mutants, the flowers show not only homeotic transformation of floral organs but also floral meristem indeterminacy with a flowers-within-flower phenotype – *ag* flowers have repeating patterns of sepal-petal-petal. This phenotype suggested that *AG* might be a negative regulator of *WUS* for floral determinacy. *WUS* expression starts from floral stage 1 and begins to decrease at stage 3 when *AG* starts to be expressed (Mayer et al., 1998). *WUS* expression is completely terminated at stage 6. In the *ag-1* mutant, *WUS*

expression is prolonged in the indeterminate floral meristems well beyond stage 6 (Lenhard et al., 2001; Lohmann et al., 2001). This prolonged *WUS* expression is required for the indeterminate floral meristem activity in *ag-1* because *wus-1* is epistatic to *ag-1* (Laux et al., 1996). In turn, *WUS* activates *AG* expression together with *LEAFY* (*LFY*), a floral meristem identity gene. *WUS* directly binds to cis-elements of *AG* and can activate a reporter gene under the control of the *AG* regulatory sequence in the presence of *LFY* in yeast (Lenhard et al., 2001; Lohmann et al., 2001). Therefore, the *AG-WUS* negative feedback loop is a floral specific mechanism that designates floral meristems as determinate.

The *CLV* genes are well known *WUS* repressors in the SAM. In the floral meristem, their function is quite different from that of *AG*. The *clv3-1* mutant shows enlarged floral meristems and increased floral organ numbers but the floral meristems do terminate (Clark et al., 1995; Brand et al., 2000). Conversely, *ag* mutants have a fixed number of floral organs in each whorl but have prolonged floral meristem activity, resulting in a flowers-within-flower phenotype (Bowman et al., 1989; Yanofsky et al., 1990). This implies that *AG* controls the expression of *WUS* temporally, whereas the *CLV* genes control the spatial patterns of *WUS* expression. Consistently, the *clv1-1 ag-2* double mutant shows a synergistic effect on the floral meristem, which indicates that the two acts in parallel (Clark et al., 1993).

SUPERMAN (*SUP*), which is expressed specifically in whorl 3, encodes a C2H2 zinc finger protein (Schultz et al., 1991; Bowman et al., 1992; Sakai et al., 1995). It plays a role in boundary maintenance between whorl 3 and whorl 4 in the floral meristem. In

sup mutants, the expression domains of whorl 2- and whorl 3-specific homeotic genes, *AP3* and *PI,* are expanded to whorl 4, which causes extra stamen development between whorl 3 and whorl 4. *WUS* is required for the determinacy defects in *sup* flowers because *wus-1* is epistatic to *sup-6* (Laux et al., 1996). However, the synergistic effect of *ag-1 sup-1* double mutants on the floral meristem indicates that the two genes act in parallel (Bowman et al., 1992).

ULTRAPETALA1 (*ULT1*), which encodes a novel cystein-rich protein with a B box-like box, is expressed in the SAM and floral meristems and also in developing stamens and carpels. *ult1* mutants show an enlarged inflorescence meristem and increased number of floral organs (Fletcher, 2001). *ULT1* acts in the *AG-WUS* regulatory loop to maintain floral meristem determinacy because delayed *WUS* transcriptional repression is observed in *ult1-1* and both *wus-1* and *ag-1* are epistatic to *ult1-1* with respect to floral determinacy (Carles et al., 2004). However, the floral meristem is eventually terminated in *utl1-1* although it is delayed, which indicates that *ULT1* is not essential for *AG* activity.

Transgenic lines carrying miR172-resistant *AP2* (*AP2m3*) have indeterminate floral meristems that produce numerous stamens (Chen, 2004). *APETALA 2* (*AP2*) was identified as a homeotic gene that is required for perianth organ identities. miR172, which is present in the inner two whorls, is a negative regulator of *AP2* to reduce *AP2* levels in the inner two whorls The floral phenotype of *AP2m3* transgenic lines suggests that miRNA172-mediated repression of *AP2* is required to maintain floral meristem size and temporal stem cell termination (Chen 2004; Zhao et al., 2007). Genetic studies

indicate that miR172-mediated *AP2* repression acts in both *AG*-dependant and *AG*-independent pathways to control floral meristem determinacy.

KNUCKLES (*KNU*) is a putative transcriptional repressor, which encodes a C2H2 zinc finger protein (Payne et al., 2004). The *knu* mutant flowers have additional floral organs growing inside of whorl 4 and abnormal gynoecium development. *KNU* expression is initiated at stage 6 in the sepals, pedicels and at the base of carpel primordia. Later, its expression is expanded into all floral organs including male and female gametophytes. On the other hand, expression of a *KNU::GUS* translational fusion transgene is more restricted than that of *KNU* transcripts in that it appears to mimic the spatial pattern of *WUS* expression and to contrast the temporal pattern of *WUS* expression. This indicates that *KNU* might be post-transcriptionally regulated to maintain floral meristem determinacy.

Recently, several regulators of floral determinacy have been identified and found to act upstream of *AG* to activate *AG* transcription. *REBELOTE* (*RBL*), *SQUINT* (*SQN*) and *UTL1* were isolated from a forward genetic screen as *CRABS CLAW* (*CRC*) modifiers (Prunet et al., 2008). *CRC* is a member of the *YABBY* gene family (Bowman and Smyth, 1999). Genetic studies implicated *CRC* in the regulation of floral meristem determinacy. While each single mutant in *RBL*, *SQN*, and *UTL* does not show any floral meristem determinacy defects, each of the mutations in combination with *crc* causes strong floral meristem determinacy defects. In all double mutants, *AG* expression is reduced in whorl 4, which presumably causes prolonged *WUS* expression to result in floral meristem indeterminacy. *PERIANTHIA* (*PAN*) is also involved in the maintenance

of floral meristem determinacy as an activator of *AG* expression (Das et al., 2009). *pan* mutants show very similar floral determinacy defects as those of *ag* mutants under short day conditions. In addition, *PAN* expression overlaps with that of *AG* and *PAN* directly binds to regulatory sequences in the *AG* second intron. Similarly, *RBL*, *SQN* and *ULT1* act in combination with *CRC* and *PAN* to promote *AG* expression in whorl 4 to repress *WUS* expression for floral meristem determinacy. These findings imply that several independent inputs exist to control *AG* activity to result in the precise regulation of *WUS* to terminate the floral meristem.

Unsolved puzzles in floral meristem determinacy

AG is the only gene that is able to shut down *WUS* expression at the right timing for proper floral determinacy. Although several regulators of floral determinacy have been identified, which act in the same or parallel pathways, almost nothing is known about the molecular mechanism underlying the repression of *WUS* expression by *AG*.

One puzzle is the temporal gap between *AG* and *WUS* expression. *AG* expression is initiated at stage 3, but *AG* does not turn off *WUS* until stage 6 (Lenhard et al., 2001; Lohmann et al., 2001). If *AG* acts as a transcription factor to directly repress *WUS* expression, it is hard to explain this temporal gap.

Most recently, it has been uncovered that *KNU* is a key mediator in the *AG-WUS* regulatory loop (Sun et al., 2009). *KNU* is expressed in the center of floral meristems at stage 6, at the same place where *WUS* is normally expressed and at the same time when *WUS* is repressed. *AG* directly binds to *KNU* promoter, which results in reduced histone

H3K27 methylation to activate *KNU* transcription. Then *KNU* may act as a transcription repressor to shut down *WUS*. However, *knu* mutants show much weaker phenotypes than *ag* mutants in terms of floral meristem determinacy (Payne et al., 2004), which suggests that another pathway may exist in the *AG-WUS* regulatory loop.

Epigenetic control in development

Histone modifications are epigenetic controls used by eukaryotes to respond to external and internal signals. In Drosophila, It has been well established that histone modifications conferred by the polycomb group (PcG) and Trithorax (Trx) proteins play important roles in proper developmental patterning (reviewed in Muller and Kassis, 2006; Schwartz and Pirrotta, 2007). PcG genes were originally identified from genetic screens as regulators of homeotic gene expression. In loss-of-function PcG mutants, target genes are de-repressed, suggesting that PcG genes act as repressors at the transcriptional level. Further studies revealed that the PcG complex modifies chromatin structure by introducing histone H3 Lysine K27 trimethylation (H3K27me3) marks, which confer a transcriptionally repressive status onto target genes (Lachner et al., 2004). In plants, PcG genes were first identified on the basis of their role in development processes such as seed maturation, flower development and vernalization, and molecular genetic studies have demonstrated a role of these genes in the deposition of H3K27me3 onto target genes (reviewed in Pien and Grossniklaus, 2007).

Chromatin immunoprecipitation-microarray analysis (ChIP-on-Chip) was conducted using H3K27me3-specific antibodies in *Drosophila* and the results revealed

that PcG function is required at genes acting in all major developmental processes including the maintenance of stem cell identity (Schwartz and Pirrotta, 2007). ChIP-on-ChIP experiments with seedlings in *Arabidopsis* also showed that more than 4000 genes are direct targets of the PcG complex (Zhang et al., 2007). Interestingly, meristem identity genes such as *WUS* and *STM* were also targets of PcG. Moreover, it has been shown that PcG-mediated repression of *KNOX* genes is required to maintain SAM stability in *Arabidopsis* (Xu et al., 2008). These results suggest that there might be a connection between meristem activities such as floral meristem termination and PcG-mediated repression.

Functional mechanisms of the Polycomb Group in animals

The PcG is required to maintain the transcriptionally repressive status of target loci and is composed of at least three components: POLYCOMB REPRESSIVE COMPLEX1 (PRC1), POLYCOMB REPRESSIVE COMPLEX2 (PRC2) and Pleiohomeotic repressive complex (PhoRC). In *Drosophila*, PRC2 is composed of four subunits, which are Extra sex comb (ESC), Enhancer of zeste (E(Z)), Supressor of zeste (SU(Z)12) and p55. PRC2 sets up the H3K27me3 marks via *E*(*Z*) activity (Schwartz and Pirrotta, 2007). *E*(*Z*) encodes a SET domain that has methyltransferase activity. Although *E*(*Z*) itself is a methyltransferase, it is only functional when other proteins are assembled together with it in PRC2. PRC1 is composed of five subunits; Polyhomeotic (PH), chromodomain-containing Polycomb (Pc), dRING, Posterior sex combs (PSC) and Sex combs on midleg (SCM) (Cao and Zhang, 2004; Schwartz and Pirrotta, 2007). Pc is a

core component because the chromodomain of Pc can recognize and bind to H3K27me3. RING1b subunit has ubiquitin ligase activity. Consistently, this complex in mammals acts in the monoubiquitination of Histone H2 lysine 119, which plays a role in the further stable repression of target loci. Recently identified PhoRC contains two components: Pleiohomeotic (Pho), which encodes a DNA-binding domain, and a Scm-related gene containing four MBT (malignant brain tumour) domains (SFMBT) that is important for HOX gene silencing (Klymenko et al., 2006). Although it has been shown that PhoRC is involved in the recruitment of PRC1 and PRC2 through its DNA binding activity, its mechanism of action is still not clear.

Conserved function of the Polycomb Group in plants

Four components of PRC2 are conserved in plants: E(Z) – CURLY LEAF (CLF), SWINGER (SWN) and MEDEA (MEA), SU(Z)12 – EMBRYONIC FLOWER2 (EMF2), VERNALIZATION2 (VRN2) and FERTILIZATION INDEPENDENT SEED2 (FIS2), ESC – FERTILIZATION INDEPENDENT ENDOSPERM (FIE), and p55 – MULTICOPY SUPPRESSOR of IRA1 (MSI1). Genetic and biochemical studies proposed that at least three forms of PRC2 exist: FIS, VRN, and EMF, reflecting different SU(Z)12 paralogs, and each complex is involved in transcriptional gene repression at a specific developmental phase in *Arabidopsis* (Reviewed in Schtlowski et al., 2008).

The FIS complex, which is composed of *MEA, MSI1, FIE* and *FIS2,* controls seed development (Schtlowski et al., 2008). One target of the FIS complex, *PHERES1*

(*PHE1*), showed correlation between gene repression and the deposition of H3K27me3 marks, which *MEA* was partially responsible for. In the *mea* mutant, H3K27me3 marks were not completely abolished especially during the vegetative stage when *MEA* is not expressed (Makarevich et al., 2006). This suggests that two other SET domain proteins, *CLF* and *SWN* might have functional redundancy with MEA. *FUSCA3* (*FUS3*) and *Arabidopsis thaliana FORMIN HOMOLOGY PROTEIN5* (*AtFH5*) also have been identified as targets of FIS. In *fis complex* mutants, *FUS3* and *AtFH5* are ectopically expressed and MEA directly binds to the *FUS3* locus. *SWN* and *CLF* are also functionally redundant for *FUS* and *AtFH5* expression during the vegetative stage (Ingouff et al., 2005; Makarevich et al., 2006).

The VRN2 complex acts in the vernalization response (Schtlowski et al., 2008). It is composed of CLF/SWN, MSI, FIE and VRN2. The vernalization response has been well studied in *Arabidopsis*. Low temperature induces *VERNALIZATION INSENSITIVE 3* (*VIN3*), which recruits the *VRN2* complex to *Flowering Locus C* (*FLC*) to repress *FLC* transcription via H3H27me3 marks. *FLC* represses *Flowering Locus T* (*FT*) in leaves. Repression of *FLC* via low temperature results in transcriptional activation of *FT*, which physically interacts with FD in the apex to initiate flowering (Gendall et al., 2001; Levy et al., 2002). Although *VIN3* interacts with the *VRN2* complex, it is not considered as a component of the PCR2 complex as *VIN3* is only expressed during cold treatment (Wood et al., 2006).

The EMF complex is composed of CLF/SWN, MSI, FIE and EMF, and controls flowering time and flower development (Schtlowski et al., 2008). The floral homeotic

gene *AG* and the homeobox gene *STM* are direct targets of *CLF* (Schubert et al., 2006). *AG* and *STM* expression becomes ectopic and the H3K27me3 marks at the *AG* locus are almost deleted in *clf* mutants. Consistently, the phenotypes caused by ectopic expression of *AG* are very similar to those of *clf* mutants. The phenotypes include small plant size, curled up leaves and early flowering. The *emf* mutant flowers directly from the embryo stage without going through the vegetative stage. Similarly, H3K27me3 levels at *AG* are significantly decreased in *emf2* mutants.

There are no homologues of PRC1 and PhoRC in plants. However, a functional counterpart of PRC1 has been identified, which is *LIKE HETEROCHROMATIN PROTEIN1* (*LHP1*), also known as *TERMINAL FLOWER 2* (*TFL2*) (Gaudin et al., 2001). *LHP1/TFL2* was first identified as a homologue of *HP1,* which binds to methylated H3K9, a heterochromatic mark in animals. However, *LHP1/TFL2* is predominantly localized in euchromatin and also exhibits binding affinity to H3K27me3 in vitro. Further studies revealed that *LHP1/TFL2* is colocalized with H3K27me3 marks and consistently, *lhp1/tfl2* mutants show very similar phenotypes with PcG mutants, such as curled leaves and early flowering (Gaudin et al., 2001; Sung et al., 2006; Turck et al., 2007; Zhang et al., 2007). Because H3K27me3 marks still remain in *lhp1/tfl2* mutants, it is thought that *LHP1/TFL2* acts downstream of PRC2 as a PRC1-like protein (Turck et al., 2007; Zhang et al., 2007).

Recently, *AtRING1a* and *AtRING1b* were identified as homologues of *Drosophila* RING1 protein. The *Atring1a Atring1b* double mutant showed ectopic meristem activity, which was caused by ectopic expression of class I *KNOTTED-like homeobox* (*KNOX*)

genes (Xu et al., 2008). It was shown that transcriptional repression of *KNOX* was correlated with the presence of H3K27me3 marks. *AtRING1a* and *AtRING1b* physically interacted with *CLF* and *LHP1*. However, H3K27me3 levels did not change at *STM, KNAT2, KNAT6* and *AG* loci in the *Atring1a Atring1b* double mutant, which suggests that they act down stream of PRC2, probably as a PRC1-like function.

PcG recruitment to targets

Polycomb responsive elements (PREs) are cis-regulatory sequences that are essential to recruit the PcG complex to its target genes in animals (Wang et al., 2004; Grimaud et al., 2006). In *Drosophila*, PRC2, PRC1 and PhoRC bind to the *HOX* loci in a PRE-dependant manner. PhoRC is the only subunit that has a DNA-binding domain in the PcG complex and is therefore likely responsible for recruiting other PcG subunits to targets. Interestingly, it appears that PhoRC interacts with other PcG proteins transiently because biochemically purified PhoRC complex did not contain PRC1 or PRC2 proteins and vice versa (Muller et al., 2002; Klymenko et al., 2006). In addition, other transcription factors have been identified, which are involved in PcG recruitment such as *GAGA factor, Pipsqueak, Grainyhead, Zest* and *Dorsal switch protein 1*. However, loss of function mutants of these transcription factors do not show PcG mutant phenotypes (Muller et al., 2006).

In plants, there are no PREs or homologues of PhoRC. Therefore, it is not clear whether plant use the same mechanism for PcG recruitment. It is possible that unrelated transcription factors play roles in PcG recruitment in plants. Most recently, interesting

results in support of this hypothesis have been reported (Liu et al, 2009). *SHORT VEGETATIVE PHASE* (*SVP*) is a MADS box transcription factor that acts directly on *SEPALLATA 3* (*SEP3*) to repress *SEP3* expression. Interestingly, TFL2 was isolated as an interacting partner of SVP in a yeast two-hybrid screen and this interaction was further confirmed in vitro with purified proteins as well as extracts. Moreover, SVP and TFL2 bind to the same genomic region in the *SEP3* promoter that was identified as a TFL2 binding site through DNA adenine methyltransferase identification coupled with microarray (DamID-chip) (Liu et al, 2009). This implies that plants might use DNA binding domain-containing proteins or transcription factors to recruit the PcG to specific loci.

Here, we report that PcG-mediated suppression of *WUS* is required for floral meristem determinacy and *AG* directly recruits the PcG to result in *WUS* repression. We isolated a loss-of-function mutant, *clf-47*, in a subunit of the PcG complex, as an enhancer of *ag-10* in terms of floral meristem determinacy. Genetic studies showed that the PcG complex represses *WUS* expression in an *AG*-dependant manner for floral meristem determinacy. Therefore, we propose that *AG* represses *WUS* through PcG-mediated gene silencing to specify floral meristem determinacy.

RESULTS

Mutations in *CLF* enhance the floral determinacy defects of *ag-10*

Ethyl methanesulfonate (EMS) mutagenesis was performed to identify players that promote floral meristem determinacy. *ag-10* is a weak allele of *ag* (unpublished data)

whose floral phenotype is relatively normal except for the presence of occasional bulged siliques with additional floral organs inside (Fig. 1B, G). This phenotype indicates partial loss of floral determinacy. A recessive loss of function mutation in *CLF, clf-47,* which enhanced the *ag-10* phenotype in terms of floral determinacy, was isolated from the screen, which enhanced the *ag-10* phenotype in terms of floral determinacy.

The developmental defects caused by a loss of function mutation in *CLF* (*clf-2*) described in a previous study included overall smaller organ size, curled-up leaves and early flowering; no floral determinacy defects were observed (Fig. 1C; Goodrich et al., 1997). The *ag-10 clf-47* double mutant exhibited very similar phenotypes compared to *clf-47* and *clf-2* single mutants with regard to vegetative development and flowering time (data not shown). However, the *ag-10 clf-47* double mutant had much stronger floral determinacy defects as compared to the *ag-10* single mutant. While the *ag-10* plants had occasional bulged siliques, most siliques in the double mutant were smaller and bulged, especially those from the early-arising flowers on the primary inflorescence stem (Fig. 1C, D, G, H and M). Therefore, the *clf-47* mutation enhances the floral meristem determinacy defects of *ag-10*.

The timing of floral meristem termination was examined by histological sectioning of various stages of flowers of *ag-10* and *ag-10 clf-47* (Fig. 1I-L). In *ag-10*, as in wild type, the floral meristem is terminated by stage 6 when the carpel primordia are formed. In *ag-10 clf-47*, however, the dome-shaped meristem was still present between the two carpels at stages 6-7 (Fig. K) and additional organs were present in later stage

flowers (Fig. L), which indicated that floral meristem termination was delayed in *ag-10 clf-47*.

Cloning of *CLF*

Map-based cloning was conducted to clone the gene, the mutation in which enhanced the *ag-10* determinacy defect. The mutation was mapped closely to the F26B6 BAC and sequence analysis revealed that a G-to-A mutation at nucleotide 2381 in *CLF*, which resulted in the conversion of amino acid 794 in the SET domain from Arginine to Histidine (Fig. 2A). The SET domain is very conserved in E(Z) homologs and exhibits methyltransferase activity. The R794 residue is particularly highly conserved in the SET domain (Fig. 2B).

To confirm that the floral phenotype was caused by a mutation in *CLF,* we introduced another *clf* allele, *clf-2* into *ag-10.* Similarly, the *ag-10 clf*-2 double mutant also exhibited enhanced floral determinacy defects compared to the *ag-10* single mutant (Fig.1E, F and M). Interestingly, other phenotypes of *clf-2*, such as leaf curling and smaller plant size, were largely rescued by *ag-10* as by *ag-3* as reported by a previous study (Goodrich et al., 1997), however, the vegetative phenotypes of *clf-47* were not rescued by *ag-10* (see Discussion). These results suggest that *CLF* is involved in regulation of floral meristem determinacy.

***CLF* is necessary for temporal repression of *WUS* expression**

To investigate the molecular basis of the enhanced determinacy defects of the *ag-10 clf-47* double mutant, we first examined the expression of meristem-related genes such

as *WUS, STM*, *KNAT1, KNAT2, KNAT6* and *AP1* by real-time RT-PCR. Interestingly, *WUS* RNA levels were increased in *ag-10 clf-47* compared to wild type and the *clf-47* single mutant (Fig. 3). Since *WUS* promotes stem cell maintenance in meristems, the increased *WUS* expression could be responsible for floral determinacy defects of *ag-10 clf-47*.

We performed in situ hybridization to determine the temporal and spatial expression patterns of stem cell identitiy genes, *WUS* and *STM,* in floral meristems. In wild type, *WUS* is expressed in a small number of cells beneath the stem cells starting from newly formed floral meristems, but is shut off at stage 6 when carpel primordia are formed. In the *ag-10* single mutant, one out of ten inflorescences examined showed prolonged *WUS* expression until stage 7, the latest stage when *WUS* expression was observed in this genotype (Fig. 4A). In the *ag-10 clf-47* double mutant, nine out of ten inflorescences showed temporally prolonged *WUS* expression in much older flowers (Fig. 4B-D), which was never observed in the *ag-10* single mutant. *STM* expression also persisted much longer in the *ag-10 clf-47* double than the *ag-10* single mutant. While 20% of *ag-10* inflorescences exhibited prolonged *STM* expression until at most stage 8 (Fig. 4E), 70% of *ag-10 clf-47* inflorescences had *STM* expression in much older flowers (Fig.4F). As *STM* is a marker for meristematic cells, the results suggested that cells retained meristematic activity until a much later stage in the *ag-10 clf-47* double mutant.

To determine whether the prolonged *WUS* expression in the *ag-10 clf-47* floral meristems was the cause of the floral determinacy defects, we crossed the loss-of-function *wus-1* mutation into *ag-10 clf-47*. The *wus-1* mutation results in premature

termination of the floral meristem such that the flower terminates in a central stamen. *wus-1* was epistatic to *clf-47 ag-10* as the phenotypes of the *ag-10 clf-47 wus-1* triple mutant were identical to that of the *wus-1* single mutant in terms of floral determinacy (Fig. 5M-N). These results indicate that the floral determinacy defects of *ag-10 clf-47* was associated with persisted stem cell activity caused by prolonged *WUS* expression and *CLF* is required for *WUS* repression.

CLF and _AG_ confer floral meristem determinacy in the same genetic pathway

A number of genes are known to regulate stem cells in meristems. We evaluated the genetic relationship between *CLF* and the known genes by generating mutant combinations.

AG is a key factor in the temporal regulation of *WUS* expression. First, to test whether *AG* and *CLF* act in the same pathway, the *clf-47* mutation was introduced into the *ag* null mutant, *ag-1*. The floral phenotypes of the *ag-1 clf-47* double mutant were identical to that of the *ag-1* single mutant (Fig. 5O,P). This indicates that *CLF* and *AG* act in the same pathway in conferring floral meristem determinacy.

Next, we examined the genetic interaction between *clf-47* and mutations in other known regulators of stem cells or floral meristem determinacy, such as *SUP, AP2, CLV3,* and *STM*, by generating and analyzing genetic combinations.

The *sup-1* single mutant flowers exhibit numerous stamens and more than two carpels, which indicates more floral stem cell activity. However, the floral meristem eventually terminates in a few carpels. While the *clf-47 sup-1* double mutant resembled

the *sup-1* single mutant (Fig. 5B), the *ag-10 clf-47 sup-1* mutant exhibited dramatic enhancement of the determinacy phenotypes of either *ag-10 clf-47* or *sup-1* (Fig. 5C). The *ag-10 clf-47 sup-1* flower developed numerous stamens following a spiral phyllotaxy with an indeterminate floral meristem, a phenotype similar to that of flowers expressing the miR172-resistant *AP2* gene (*AP2m3*) (Fig. 5C). This indicates that *AG-CLF* and *SUP* act synergistically in floral meristem determinacy.

AP2 promotes stem cell fates in both the SAM and the floral meristems. By repressing *AP2* expression in floral meristems, miR172 promotes floral determinacy. *AP2m3* transgenic lines have indeterminate floral meristems that produce numerous stamens. When *AP2m3* was combined with *ag-1*, a stronger defect in floral determinacy such as enlarged and fasciated floral meristems were observed, suggesting that miR172/*AP2* and *AG* act in part in parallel. When *AP2m3* was introduced into *ag-10 clf-47*, it caused numerous stamens as in wild type. But old flowers of the *AP2m3 ag-10 clf-47* and *AP2m3 clf-47* genotypes developed floral meristem fasciation. These results indicate that *AG-CLF* and miR172 partially act in parallel in floral determinacy.

CLV1, 2, and 3 genes are also negative regulators of *WUS*. The *clv3-1* mutant shows increased floral organ numbers and enlarged floral meristems (Fig. 5J). The *clf-47 clv3-1* double mutants had essentially the same phenotypes as the *clv3-1* single mutants (Fig. 5K). Some but not all flowers of *ag-10 clf-47 clv3-1* plants showed fasciated floral meristems (Fig. 5L). This suggests that *AG-CLF* and *CLV3* act in parallel.

STM is required to maintain meristematic cells in an undifferentiated state. It is crucial for floral meristem maintenance because loss of function mutants of *STM* show

premature termination of the floral meristem such that the flowers have reduced numbers of floral organs (Fig. 5G). The *clf-47 stm-2* double mutant had the same phenotype as that of the *stm-2* single mutant with respect to floral meristem determinacy although homeotic changes were observed in the double mutant: all floral organs were transformed into sepal-like structures (Fig. 5H). In addition, *stm-2* was also epistatic to *ag-10 clf-47* in terms of floral meristem determinacy (Fig. 5I). It suggests that *STM* is required for the determinacy defects of *ag-10 clf-47* flowers.

The PcG is required for floral determinacy

The PcG establishes the H3K27me3 mark on target genes to maintain the transcriptionally repressive state. The PcG is composed of PRC1 and PRC2 in Arabidopsis. *CLF* is one component of the PRC2 complex, which introduces the H3K27me3 mark. *TFL2/LHP1*, a component of PRC1, recognizes the repressive H3K27me3 mark and maintains the repressive state. We investigated genetically whether the role of *CLF* in floral meristem determinacy reflects such as role for the PcG.

To evaluate whether the PRC1 component, *TFL2*, plays a role in floral determinacy, we generated the *ag-10 tfl2-2* double mutant, Since the *tfl2-2* allele was in the Col background, we crossed it to a line in which the *ag-10* mutation generated in the L*er* background was introgressed into Columbia by five backcrosses. This $ag\text{-}10^{Col}$ plant does not exhibit any floral determinacy defects, probably due to the presence of a suppressor/modifier in Columbia. The *tfl2-2* mutant also does not have any floral determinacy defects. However, the *tfl2-2* mutation enhanced the *ag-10* phenotype

although the phenotype was weaker than that of *ag-10 clf-47*. Some *ag-10 tfl2-2* gyneocia consisted of more than two carpels that were partially unfused (Fig. 6B). Overall, the double mutant siliques became shorter and deformed (Fig. 6C). These results imply that PcG function is involved in floral meristem determinacy.

***CLF* is required for shutting off *WUS* expression**

Although our results indicated that *CLF* is required for *WUS* repression in concert with *AG* function, it is not clear when *CLF* actually acts to repress *WUS* expression. Is *CLF* involved in the initial repression of *WUS* in which *AG* is required or in a later step after the initial repression to maintain the repressive state? To address this question, we examined the temporal dynamics of *WUS* expression in *ag-10 clf-47* by introducing the *pWUS::GUS* reporter that reflects endogenous *WUS* expression patterns (Grodd-Hardt et al., 2002). In wild type, this reporter is active in young floral meristems but is shut off by stage 6 (Fig. 4H). If *CLF* acts to maintain the repressed state initially set up by *AG*, one may expect the initial repression of *WUS* to still occur at stage 6 in *clf* but the repression cannot be maintained such that *WUS* is expressed again in older flowers. In *ag-10 clf-47,* continuous *GUS* expression was observed from early stages until stages 8-9 (Fig. 4I). In flowers of similar stages when *WUS* expression was visible in anthers (stages 8-9), prolonged *WUS* expression was clearly observed in the center of the flower in *ag-10 clf-47* but not wild type plants (Fig. 4H,I). In addition, examination of longitudinal sections of the samples confirmed prolonged *GUS* expression until late stages at the floral

meristem region (Fig. G). The fact that no initial shut off of *WUS* at stage 6 was observed in *ag-10 clf-47* suggests that *CLF* is required for the initial repression of *WUS*.

DISCUSSION

The floral meristems, unlike the SAM, are determinate. The expression of the stem cell promoting gene *WUS* is terminated at stage 6, resulting in floral meristem termination. *AG* is a key regulator that shuts down *WUS* expression at the right time to confer proper floral determinacy. Although the regulation of *WUS* by *AG* has been known for many years, the molecular mechanism underlying how *AG* represses *WUS* is unknown. Our studies revealed that *CLF*, a PcG gene, acts in the same genetic pathway as *AG* to confer floral determinacy and that the role of *CLF* reflects the function of the PcG complex. This finding uncovers a link between epigenetic regulation and the control of floral meristem determinacy.

Differences in two *clf* alleles, *clf-2* and *clf-47*

Mutations in *CLF* enhance the floral determinacy defects of *ag-10* as both *ag-10 clf-47* and *ag-10 clf-2* double mutants had much stronger floral determinacy defects as compared to the *ag-10* single mutant (Fig.1 D, F and M). *clf-47* is a point mutation in the SET domain while *clf-2* is a null allele. The vegetative phenotypes such as leaf curling and small plant size of *clf-47* were not rescued by *ag-10*, while those phenotypes of *clf-2* were largely rescued by *ag-10*. A previous study showed that the *clf-2* vegetative phenotypes were dependant on *AG* activity as the *clf* mutant phenotypes resembled those

of transgenic plants ectopically expressing *AG* and the *ag-3* mutation rescued the *clf-2* vegetative defects (leaf morphology and plant size) (Goodrich et al., 1997; Finnegan et al., 1996). Then, why aren't the vegetative phenotypes of *clf-47* mutants rescued by *ag-10*? We think it might be due to the nature of the *clf-47* allele, which behaves genetically as a recessive allele but may affect the function of the *CLF* homolog, *SWN*. In the null *clf-2* mutant, the PRC2 containing CLF (CLF-PRC2) is not expected to form properly. However, in the *clf-47* mutant, the full length of CLF protein is likely still generated and incorporated into the PRC2 complex, which is expected to be recruited to targets even though it is not functional. The non-functional CLF-PRC2 would compete with SWN-PRC2 and partially inhibit SWN activity. Therefore, *clf-47* is perhaps a more severe allele than *clf-2* in terms of H3K27me3 deposition on *AG* and perhaps other targets, which would explain why *ag-10* rescues the vegetative defects of *clf-2* but not *clf-47*.

Role of PcG genes in floral stem cell regulation

WUS expression persists much longer in *ag-10 clf-47* flowers (until stage 11) compared to *ag-10* flowers (until stage 7), which suggests that *CLF* is required for *WUS* repression in floral meristem determinacy (Fig. 4A-D). This result raises the question why no floral determinacy defects are observed in *clf* single mutants. One possible explanation is functional redundancy among PcG genes. CLF, SWN, and MEA are homologs of the Drosophila E(Z) protein that has H3K27 methyltransferase activity. Genetic studies have shown that *CLF* and *SWN* have partially functional redundancy in during vegetative development and floral transition (Chanvivattana et al., 2004).

Therefore, it is possible that the lack of floral meristem determinacy defects in *clf* single mutants is due to SWN activity. FIE is another subunit of the PRC2 complex, which has no other homologs in *Arabidopsis*. Indeed, plants in which *FIE* expression has been knocked down exhibit floral determinacy defects such as enlarged gynoecia with the multiple carpels (Katz et al., 2004)).

The role of *CLF* in floral meristem determinacy likely reflected that of PcG activity rather than that of CLF alone (Fig. 6). This was supported by the observation that a mutation in *TFL2*, a subunit of PRC1, also enhanced the floral determinacy defects of *ag-10*. How does the PcG affect floral meristem determinacy? The PcG is required to maintain the transcriptionally repressive status of target loci through H3K27 trimethylation. ChIP-on-ChIP experiments to examine H3K27me3 marks in *Arabidopsis* seedlings showed that more than 4000 genes are direct targets of the PcG complex (Zhang et al., 2007). Interestingly, the *WUS* locus has extensive H3K27me3. Moreover, a recent study shows that PcG-mediated repression of meristem identity genes, such as STM, KNAT1, 2, and 6, is required to maintain SAM stability in *Arabidopsis* (Xu et al., 2008). In the absence of PRC1-like activity, these genes are de-repressed, which causes ectopic meristem activity. Based on these observations, we propose that the PcG directly represses *WUS* expression in the floral meristem by depositing H3K27me3 marks at the *WUS* locus.

Functional relationship between *AG* and *CLF*

Our data indicate that *AG* and *CLF* act in the same genetic pathway to shut down *WUS* expression (Fig. 5O and P). What is the functional relationship between *AG* and *CLF*? In *Drosophila*, PhoRC, a subunit of PcG, and several other transcription factors are responsible for recruiting PRC1 and PRC2 to targets. In plants, there are no homologs of PhoRC, so transcription factors are likely candidates that are involved in PcG recruitment. In support of this view, a recent study showed that SVP, a MADS box transcription factor, directly guides TFL2 to the *SEP3* promoter, resulting in the repression of *SEP* expression. Therefore, it is possible that AG is required for PcG recruitment to targets in a direct or indirect manner.

The expression of *WUS* in the floral meristem starts to decrease from stage 3 when *AG* expression is initiated and is completely shut down after stage 6. The temporal and spatial expression of *CLF* overlaps with those of *AG* from stage3. This suggests that *CLF* possibly acts with *AG* from stage 3 to repress *WUS* expression. However, the *AG-CLF* pathway itself is necessary but not sufficient to shut down *WUS* expression by stage 6 because the phenotypes of PcG mutants are much weaker than strong *ag* mutants. Most recently, *KNU* was identified as a key intermediate in the *AG-WUS* regulatory loop (Sun et al., 2009). However, *KNU* is also necessary but not sufficient to terminate floral meristems because *knu* mutants show much weaker phenotypes than *ag* mutants in terms of floral meristem determinacy. Therefore, it is possible that the initial repression of *WUS* through the *AG-CLF* pathway needs a later synergistic mechanism such as *KNU* activity to precisely terminate the floral meristem.

MATERIALS AND METHODS

Plant Materials and Genetic Analysis

All mutants are in the L*er* background with the exception of *tfl2-2*, which is in the Col background, and *ag-10*^{col}, in which *ag-10* in L*er* was introgressed into Col through five backcrosses. *Arabidopsis* plants were grown at 24°C under continuous light.

To generate double or triple mutants involving *ag-10* or *ag-10 clf-47*, the *ag-10 clf-47* double mutant was crossed to *sup-1*, *clv3-1*, *stm-2/+*, *ag-1/+* and *wus-1/+*. In the F2 generation, plants resembling *clf* in vegetative phenotypes were screened for floral phenotypes characteristic of *sup-1*, *clv3-1*, *stm-2*, *ag-1* and *wus-1* flowers. Then the *ag-10* allele was genotyped by PCR and digestion with restriction enzyme. To identify *clf-47 AP2m3* or *ag-10 clf-47 AP2m3*, *AP2m3* was first crossed to *ag-10 clf-47*. Then F1 lines that exhibited *AP2m3* phenotypes were again crossed to *ag-10 clf-47* mutants. F1 lines of *AP2m3/+* × *AP2m3/+ ag-10/+ clf-47/+* were screened based on the *AP2m3* phenotypes and genotyped for *clf-47* and *ag-10*. For *ag-10* genotyping, the genomic DNA was amplified by PCR with JAGp75 (CAATGTCTCCCAAAGAGCCCAGGACTT) and JAGp76 (GCAACAAGGCATATAGATTTAATTTG) and PCR products from wild type could be digested by BstXI, whereas those from *ag-10* could not. For *clf-47* genotyping, PCR products amplified by CLFmuF (GAGTATGAACTTGCCTTAAGAACA) and CLFmuR (TTTTTGCGATCGTATATCTTCCCG) from *clf-47* were resistant to BstuI digestion.

EMS Mutagenesis

ag-10 seeds（1ml, 1000 seeds/100ul）were washed with 0.1% Tween-20 for 15 min followed by incubation with 0.2% EMS (30ul in 15ml water) for 12hr and three washes with 10 ml water each (1 hour for each wash on a rotator). *ag-10* enhancers were selected in the M2 based on the floral determinacy phenotype. The candidate lines were backcrossed at least two times to *ag-10* before further studies.

Map-based Cloning of *CLF*

ag-10 clf-47 (L*er*) was crossed to *ag-10*^{col} (Col). In the F2 population, plants showing *ag-10 clf-47* phenotypes were selected as the mapping population. Initially, 27 *ag-10 clf-47* plants were used for rough mapping, which showed that *clf-47* is linked to the marker nga1126 on chromosome 2. For the fine mapping, we designed new SSLP or CAPS markers in this region according to polymorphisms between L*er* and Col, using the Monsanto Arabidopsis polymorphism and Ler sequence database (http://www.arabidopsis.org/Cereon). Using these markers and 400 plants of known *clf-47* genotypes, we mapped *clf-47* to a 1,500 kb region between the BAC T16B14 and F3N11. Then sequencing analysis was conducted with candidate genes in this region.

Histochemical and Toluidine Blue Staining

GUS staining was performed as described (Jefferson et al., 1987; Rodrigues-Pousada et al., 1993). Inflorescences were fixed in 90% cold acetone for 15-20 min and rinsed with the rinse solution (50mM $NaPO_4$ pH7.2, 0.5mM $K_3Fe(CN)_6$, 0.5mM

$K_4Fe(CN)_6$). Then, they were vacuumed in the infiltration solution (50mM $NaPO_4$ pH7.2, 0.5mM $K_3Fe(CN)_6$, 0.5mM $K_4Fe(CN)_6$, 2mM X-Gluc) and incubated at 37°C.

For Toluidine Blue staining, the sectioned tissues on the slides were soaked in 0.1% Toluidine Blue in 0.1% sodium borate and rinsed in water. Then, they were dipped in an ethanol series and finally in xylene to dehydrate them.

Real-time RT-PCR

Total RNA from inflorescences was reverse-transcribed using SuperScriptII (Invitrogen) according to the manufacturers' instructions. Quantitative PCR was carried in triplicate on a Bio-Rad IQcycler apparatus with the Quantitech SYBR green kit (Bio-Rad). Primers used are listed in Table 1.

***In situ* Hybridization**

In situ hybridization was carried out as described (Chen et al., 2002). The *WUS* coding region was amplified by RT-PCR and cloned into pGEM-T-easy (Promega). This plasmid was digested with *Spe*I and transcribed with T7 RNA polymerase. The *STM* cDNA was subcloned into pCR2.1 (Invitrogen). This plasmid was digested with *BamH*I and transcribed with T7 RNA polymerase.

REFERENCES

Blazquez, M.A., Ferrandiz, C., Madueno, F., and Parcy, F. (2006). How floral meristems are built. Plant Mol Biol *60*, 855-870.

Bowman, J.L., Sakai, H., Jack, T., Weigel, D., Mayer, U., and Meyerowitz, E.M. (1992). *SUPERMAN*, a regulator of floral homeotic genes in Arabidopsis. Development *114*, 599-615.

Bowman, J.L., and Smyth, D.R. (1999). *CRABS CLAW*, a gene that regulates carpel and nectary development in Arabidopsis, encodes a novel protein with zinc finger and helix-loop-helix domains. Development *126*, 2387-2396.

Bowman, J.L., Smyth, D.R., and Meyerowitz, E.M. (1989). Gene directing flower development in Arabidopsis. Plant Cell *1*, 37-52.

Brand, U., Fletcher, J.C., Hobe, M., Meyerowitz, E.M., and Simon, R. (2000). Dependence of stem cell fate in Arabidopsis and a feedback loop regulated by *CLV3* activity. Science *289*, 617-619.

Cao, R., and Zhang, Y. (2004). The functions of E(Z)/EZH2-mediated methylation of lysine 27 in histone H3. Curr Opin Genet Dev *14*, 155-164.

Carles, C.C., and Fletcher, J.C. (2003). Shoot apical meristem maintenance: the art of a dynamic balance. Trends Plant Sci *8*, 394-401.

Carles, C.C., Lertpiriyapong, K., Reville, K., and Fletcher, J.C. (2004). The *ULTRAPETALA1* gene functions early in *Arabidopsis* development to restrict shoot apical meristem activity and acts through *WUSCHEL* to regulate floral meirstem determinacy. Genetics *167*, 1893-1903.

Chanvivattana, Y., Bishopp, A., Schubert, D., Stock, C., Moon, Y.H., Sung, Z.R., and Goodrich, J. (2004). Interaction of polycomb-group proteins controlling flowering in Arabidopsis. Development *131*, 5263-5276.

Chen, X. (2004). A microRNA as a translational repressor of *APETALA2* in *Arabidopsis* flower development. Science *303*, 2022-2025.

Chen, X., Liu, J., Cheng, Y.L., and Jia, D.X. (2002). *HEN1* functions plelotropically in Arabidopsis development and acts in C function in the flower. Development *129*, 1085-1094.

Clark, S.E., Running, M.P., and Meyerowitz, E.M. (1993). *CLAVATA1*, a regulator of meristem and flower development in Arabidopsis. Development *119*, 397-418.

Clark, S.E., Running, M.P., and Meyerowitz, E.M. (1995). *CLAVATA3* is a specific regulator of shoot and floral meristem development affecting the same processes as *CLAVATA1*. Development *121*, 2057-2067.

Clark, S.E., Williams, R.W., and Meyerowitz, E.M. (1997). The *CLAVATA1* gene encodes a putative receptor kinase that controls shoot and floral meristem size in Arabidopsis. Cell *89*, 575-585.

Das, P., Ito, T., Wellmer, F., Vernoux, T., Dedieu, A., Traas, J., and Meyerowitz, E.M. (2009). Floral stem cell termination involves the direct regulation of *AGAMOUS* by *PERIANTHIA*. Development *136*, 1605-1611.

Finnegan, E.J., Peacock, W.J., and Dennis, E.S. (1996). Reduced DNA methylation in Arabidopsis thaliana results in abnormal plant development. Proc Natl Acad Sci U S A *93*, 8449-8454.

Fletcher, J.C. (2001). The *ULTRAPETALA* gene controls shoot and floral meristem size in Arabidopsis. Development *128*, 1323-1333.

Fletcher, J.C., Brand, U., Running, M.P., Simon, R., and Meyerowitz, E.M. (1999). Signaling of cell fate decisions by *CLAVATA3* in Arabidopsis shoot meristems. Science *283*, 1911-1914.

Gallois, J.L., Nora, F.R., Mizukami, Y., and Sablowski, R. (2004). *WUSCHEL* induces shoot stem cell activity and developmental plasticity in the root meristem. Genes Dev *18*, 375-380.

Gaudin, V., Libault, M., Pouteau, S., Juul, T., Zhao, G.C., Lefebvre, D., and Grandjean, O. (2001). Mutations in *LIKE HETEROCHROMATIN PROTEIN 1* affect flowering time and plant architecture in Arabidopsis. Development *128*, 4847-4858.

Gendall, A.R., Levy, Y.Y., Wilson, A., and Dean, C. (2001). The *VERNALIZATION 2* gene mediates the epigenetic regulation of vernalization in Arabidopsis. Cell *107*, 525-535.

Goodrich, J., Puangsomlee, P., Martin, M., Long, D., Meyerowitz, E.M., and Coupland, G. (1997). A polycomb-group gene regulates homeotic gene expression in Arabidopsis. Nature *386*, 44-51.

Grimaud, C., Negre, N., and Cavalli, G. (2006). From genetics to epigenetics: the tale of Polycomb group and trithorax group genes. Chromosome Res *14*, 363-375.

Gross-Hardt, R., Lenhard, M., and Laux, T. (2002). *WUSCHEL* signaling functions in interregional communication during Arabidopsis ovule development. Genes Dev *16*, 1129-1138.

Ingouff, M., Gerald, J.N.F., Guerin, C., Robert, H., Sorensen, M.B., Van Damme, D., Geelen, D., Blanchoin, L., and Berger, F. (2005). Plant formin AtFH5 is an evolutionarily conserved actin nucleator involved in cytokinesis. Nat Cell Biol *7*, 374-U334.

Jefferson, R.A., Kavanagh, T.A., and Bevan, M.W. (1987). GUS fusions- *BETA-GLUCURONIDASE* as a sensitive and versatile fene fusion marker in higher-plants.. EMBO J *6*, 3901-3907.

Jeong, S., Trotochaud, A.E., and Clark, S.E. (1999). The Arabidopsis *CLAVATA2* gene encodes a receptor-like protein required for the stability of the CLAVATA1 receptor-like kinase. Plant Cell *11*, 1925-1933.

Klymenko, T., Papp, B., Fischle, W., Kocher, T., Schelder, M., Fritsch, C., Wild, B., Wilm, M., and Muller, J. (2006). A Polycomb group protein complex with sequence-specific DNA-binding and selective methyl-lysine-binding activities. Genes Dev *20*, 1110-1122.

Kondo, T., Sawa, S., Kinoshita, A., Mizuno, S., Kakimoto, T., Fukuda, H., and Sakagami, Y. (2006). A plant peptide encoded by *CLV3* identified by in situ MALDI-TOF MS analysis. Science *313*, 845-848.

Lachner, M., Sengupta, R., Schotta, G., and Jenuwein, T. (2004). Trilogies of histone lysine methylation as epigenetic landmarks of the eukaryotic genome (Cold Spring Harbor Lab Press, Publications Dept).

Laux, T., Mayer, K.F.X., Berger, J., and Jurgens, G. (1996). The *WUSCHEL* gene is required for shoot and floral meristem integrity in Arabidopsis. Development *122*, 87-96.

Lenhard, M., Jurgens, G., and Laux, T. (2002). The *WUSCHEL* and *SHOOTMERISTEMLESS* genes fulfil complementary roles in Arabidopsis shoot meristem regulation. Development *129*, 3195-3206.

Levy, Y.Y., Mesnage, S., Mylne, J.S., Gendall, A.R., and Dean, C. (2002). Multiple roles of Arabidopsis VRN1 in vernalization and flowering time control. Science *297*, 243-246.

Liu, C., Xi, W.Y., Shen, L.S., Tan, C.P., and Yu, H. (2009). Regulation of Floral Patterning by Flowering Time Genes. Dev Cell *16*, 711-722.

Lohmann, J.U., Hong, R.L., Hobe, M., Busch, M.A., Parcy, F., Simon, R., and Weigel, D. (2001). A molecular link between stem cell regulation and floral patterning in Arabidopsis. Cell *105*, 793-803.

Long, J.A., Moan, E.I., Medford, J.I., and Barton, M.K. (1996). A member of the *KNOTTED* class of homeodomain proteins encoded by the *STM* gene of Arabidopsis. Nature *379*, 66-69.

Lund, A.H., and van Lohuizen, M. (2004). Polycomb complexes and silencing mechansims. Curr Opin Cell Biol *16*, 239-246.

Makarevich, G., Leroy, O., Akinci, U., Schubert, D., Clarenz, O., Goodrich, J., Grossniklaus, U., and Kohler, C. (2006). Different Polycomb group complexes regulate common target genes in Arabidopsis. EMBO Rep *7*, 947-952.

Mayer, K.F.X., Schoof, H., Haecker, A., Lenhard, M., Jurgens, G., and Laux, T. (1998). Role of *WUSCHEL* in regulating stem cell fate in the Arabidopsis shoot meristem. Cell *95*, 805-815.

Muller, J., Hart, C.M., Francis, N.J., Vargas, M.L., Sengupta, A., Wild, B., Miller, E.L., O'Connor, M.B., Kingston, R.E., and Simon, J.A. (2002). Histone methyltransferase activity of a Drosophila polycomb group repressor complex. Cell *111*, 197-208.

Muller, J., and Kassis, J.A. (2006). Polycomb response elements and targeting of Polycomb group proteins in Drosophila. Curr Opin Genet Dev *16*, 476-484.

Ogawa, M., Shinohara, H., Sakagami, Y., and Matsubayashi, Y. (2008). Arabidopsis CLV3 peptide directly binds CLV1 ectodomain. Science *319*, 294-294.

Payne, T., Johnson, S.D., and Koltunow, A.M. (2004). *KNUCKLES* (*KNU*) encodes a C2H2 zinc-finger protein that regulates development of basal pattern elements of the Arabidopsis gynoecium. Development *131*, 3737-3749.

Pien, S., and Grossniklaus, U. (2007). Polycomb group and trithorax group proteins in Arabidopsis. Biochim Biophys Acta Gene Struct Expression *1769*, 375-382.

Prunet, N., Morel, P., Thierry, A.M., Eshed, Y., Bowman, J.L., Negrutiu, I., and Trehin, C. (2008). *REBELOTE, SQUINT*, and *ULTRAPETALA1* function redundantly in the temporal regulation of floral meristem termination in Arabidopsis thaliana. Plant Cell *20*, 901-919.

Rodriguespousada, R.A., Derycke, R., Dedonder, A., Vancaeneghem, W., Engler, G., Vanmontagu, M., and Vanderstraeten, D. (1993). The Arabidopsis *1-AMINOCYCLOPROPANE-1-CARBOXYLATE SYNTHASE GENE-1* is expressed during early development. Plant Cell *5*, 897-911.

Sablowski, R. (2007). Flowering and determinacy in Arabidopsis. J Exp Bot *58*, 899-907.

Sakai, H., Medrano, L.J., and Meyerowitz, E.M. (1995). Role of *SUPERMAN* in maintaining Arabidopsis floral whorl boundaries. Nature *378*, 199-203.

Sawa, S., Kinoshita, A., Nakanomyo, I., and Fukuda, H. (2006). CLV3/ESR-related (CLE) peptides as intercellular signaling molecules in plants. Chem Rec *6*, 303-310.

Schatlowski, N., Creasey, K., Goodrich, J., and Schubert, D. (2008). Keeping plants in shape: Polycomb-group genes and histone methylation. Semin Cell Dev Biol *19*, 547-553.

Schoof, H., Lenhard, M., Haecker, A., Mayer, K.F.X., Jurgens, G., and Laux, T. (2000). The stem cell population of Arabidopsis shoot meristems is maintained by a regulatory loop between the *CLAVATA* and *WUSCHEL* genes. Cell *100*, 635-644.

Schubert, D., Primavesi, L., Bishopp, A., Roberts, G., Doonan, J., Jenuwein, T., and Goodrich, J. (2006). Silencing by plant Polycomb-group genes requires dispersed trimethylation of histone H3 at lysine 27. EMBO J *25*, 4638-4649.

Schultz, E.A., Pickett, F.B., and Haughn, G.W. (1991). The *FLO10* gene-product regulates the expression domain of homeotic genes *AP3* and *PL* in Arabidopsis flowers. Plant Cell *3*, 1221-1237.

Schwartz, Y.B., and Pirrotta, V. (2007). Polycomb silencing mechanisms and the management of genomic programmes. Nat Rev Genet *8*, 9-22.

Scofield, S., and Murray, J.A.H. (2006). The evolving concept of the meristem. Plant Mol Biol *60*, V-vii.

Steeves, T.A., and Sussex, I.M. (1989). Patterns in plant development (Cambridge UK, Cambridge University Press).

Sun, B., Xu, Y.F., Ng, K.H., and Ito, T. (2009). A timing mechanism for stem cell maintenance and differentiation in the Arabidopsis floral meristem. Genes Dev *23*, 1791-1804.

Sung, S.B., He, Y.H., Eshoo, T.W., Tamada, Y., Johnson, L., Nakahigashi, K., Goto, K., Jacobsen, S.E., and Amasino, R.M. (2006). Epigenetic maintenance of the vernalized state in Arabidopsis thaliana requires *LIKE HETEROCHROMATIN PROTEIN 1*. Nat Genet *38*, 706-710.

Turck, F., Roudier, F., Farrona, S., Martin-Magniette, M.L., Guillaume, E., Buisine, N., Gagnot, S., Martienssen, R.A., Coupland, G., and Colot, V. (2007). Arabidopsis TFL2/LHP1 specifically associates with genes marked by trimethylation of histone H3 lysine 27. PLoS Genet *3*, 855-866.

Wang, L., Brown, J.L., Cao, R., Zhang, Y., Kassis, J.A., and Jones, R.S. (2004). Hierarchical recruitment of Polycomb group silencing complexes. Mol Cell *14*, 637-646.

Wood, C.C., Robertson, M., Tanner, G., Peacock, W.J., Dennis, E.S., and Helliwell, C.A. (2006). The Arabidopsis thaliana vernalization response requires a polycomb-like protein complex that also includes VERNALIZATION INSENSITIVE 3. Proc Natl Acad Sci U S A *103*, 14631-14636.

Xu, L., and Shen, W.H. (2008). Polycomb Silencing of *KNOX* Genes Confines Shoot Stem Cell Niches in Arabidopsis. Curr Biol *18*, 1966-1971.

Yanofsky, M.F., Ma, H., Bowman, J.L., Drews, G.N., Feldmann, K.A., and Meyerowitz, E.M. (1990). The protein encoded by the Arabidopsis homeotic gene *AGAMOUS* resembles transcription factors. Nature *346*, 35-39.

Zhang, X., Germann, S., Blus, B.J., Khorasanizadeh, S., Gaudin, V., and Jacobsen, S.E. (2007). The Arabidopsis LHP1 protein colocalizes with histone H3 Lys27 trimethylation. Nat Struct Mol Biol *14*, 869-871.

Zhang, X.Y., Clarenz, O., Cokus, S., Bernatavichute, Y.V., Pellegrini, M., Goodrich, J., and Jacobsen, S.E. (2007). Whole-genome analysis of histone H3 lysine 27 trimethylation in Arabidopsis. PLoS Biol *5*, 1026-1035.

Zhao, L., Kim, Y.J., Dinh, T.T., and Chen, X. (2007). miR172 regulates stem cell fate and defines the inner boundary of *APETALA3* and *PISTILLATA* expression domain in Arabidopsis floral meristems. Plant J *51*, 840-849.

Figure 1.1 Phenotypes of *ag* and *clf* single and double mutants

(A) A L*er* flower.

(B) An *ag-10* (weak allele) flower with a slightly enlarged gynoecium.

(C) A *clf-47* flower.

(D) An *ag-10 clf-47* flower with a much more enlarged gynoecium compared to *ag-10*.

(E) A *clf-2* flower.

(F) An *ag-10 clf-2* flower with similar phenotypes to those of *ag-10 clf-47*.

(G) Siliques from *ag-10* plants

(H) Siliques from *ag-10 clf-47* plants; the siliques are much more bulged and shorter compared to those from *ag-10* plants.

(I-L) Histological sections through stage 5 (I), stage 7 (J), stage 9 (K) and stage 11 (L) flowers of the *ag-10 clf-47* genotype, stained with toluidine blue. A dome-shaped structure is formed between two carpels (K, arrow). Additional organs are growing inside the carpels (L, arrow).

(M) Primary inflorescence stems from *ag-10*, *ag-10 clf-47* and *ag-10 clf-2* plants. Early-arising flowers of *ag-10 clf-47* and *ag-10 clf-2* double mutants show much more enhanced silique phenotypes compared to *ag-10*.

A
B
C
D
E
F
G
H
I
J
K
L
M
ag-10
ag-10 clf-47
ag-10 clf-2

Figure 1.2 Structure of the *CLF* gene and similarity between CLF and other E(Z) holomogs in eukaryotes in the SET domains

(A) A schematic diagram of the *CLF* gene showing the mutation in *clf-47* (G to A) in the 15th exon (asterisk).

(B) SET domain sequences are compared between CLF and other E(Z) homologs from mouse, human, drosophila and maize. The white letters on a black and dark gray background represent conserved and identical residues, respectively. The black letters on a white background represent different residues. The red box indicates the conserved R residue that is mutated to H in *clf-47*.

A

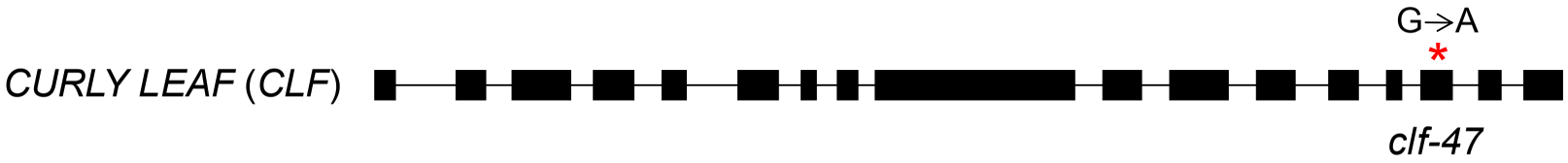
G→A
*
CURLY LEAF (CLF)
clf-47

B


H
CLF SDVSGWGAFLKNSVSKHEYLGEYTGELISHKEADKRGKIYDRCLFENCSFLFNLNDQFVL
Mouse_EZH1 SDVAGWGTFIKESVQKNEFISEYCGELISQDEADRRGKVYDKY---MSSFLFNLNNDFVV
Human_EZH2 SDVAGWGIFIKDPVQKNEFISEYCGEIISQDEADRRGKVYDKY---MCSFLFNLNNDFVV
Drosophia_EZ SDIAGWGIFLKEGAQKNEFISEYCGEIISQDEADRRGKVYDKY---MCSFLFNLNNDFVV
Maize_EZ1 SDVSGWGAFLKNSVSKHEYLGEYTGELISHKEADKRGKIYDR---ENSSFLFNLNNEYVL
CLF DAYRKGDKLKFANHSPEPNCYAKVIMVAGDHRVGICLFFAKERILAGEELFYDYRYEPDR
Mouse_EZH1 DATRKGNKIRFANHSVNPNCYAKVVMVNGDHRIG---IFAKRAIQAGEELFFDYRYSQAD
Human_EZH2 DATRKGNKIRFANHSVNPNCYAKVMMVNGDHRIG---IFAKRAIQTGEELFFDYRYSQAD
Drosophia_EZ DATRKGNKIRFANHSINPNCYAKVMMVTGDHRIG---IFAKRAIQPGEELFFDYRYGPTE
Maize_EZ1 DAYRMGDKLKFANHAPDPNCYAKVIMVTGDHRVG---IFAKERILAGEELFYDYRYEPDR

Figure 1.3 The expression of meristem identity genes in the several genotypes

mRNA levels of several meristem identity genes were determined by real-time RT-PCR analysis in L*er*, *ag-10*, *clf-47* and *ag-10 clf-47* inflorescences. The expression level of each gene was normalized to *UBIQUITIN 5* and compared to L*er*.

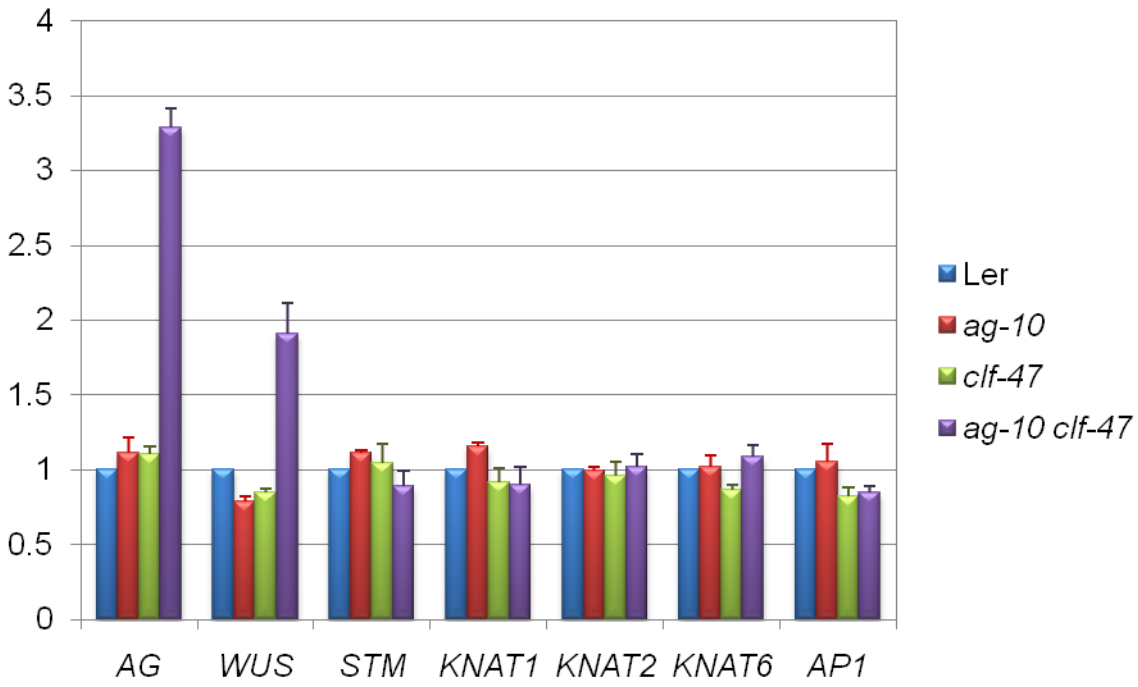
4
3.5
3
2.5
2
1.5
1
0.5
0
AG
WUS
STM
KNAT1
KNAT2
KNAT6
AP1
Ler
ag-10
clf-47
ag-10 clf-47

Figure 1.4 Expression patterns of *WUS* and *STM* in *ag-10* and *ag-10 clf-47* flowers

(A-F) *in situ* hybidization with *WUS* and *STM* antisense probes.

(A) *WUS* expression in an *ag-10* flower at stage 7.

(B-D) *WUS* expression in *ag-10 clf-47* flowers at stage 7 (B), stage 9 (C) and stage 11 (D).

(E, F) *STM* expression at stage 7 in an *ag-10* flower (E) and at stage 10 in an *ag-10 clf-47* flower (F).

(G) *pWUS::GUS* staining in an *ag-10 clf-47* flower at stages 8-9.

(H, I) *pWUS::GUS* staining in wild type (I) and *ag-10 clf-47* (J) inflorescences. Arrowheads indicates prolonged *GUS* expression until stages 8-9 in *ag-10 clf-47* flowers. The insets are stages 8-9 flowers.

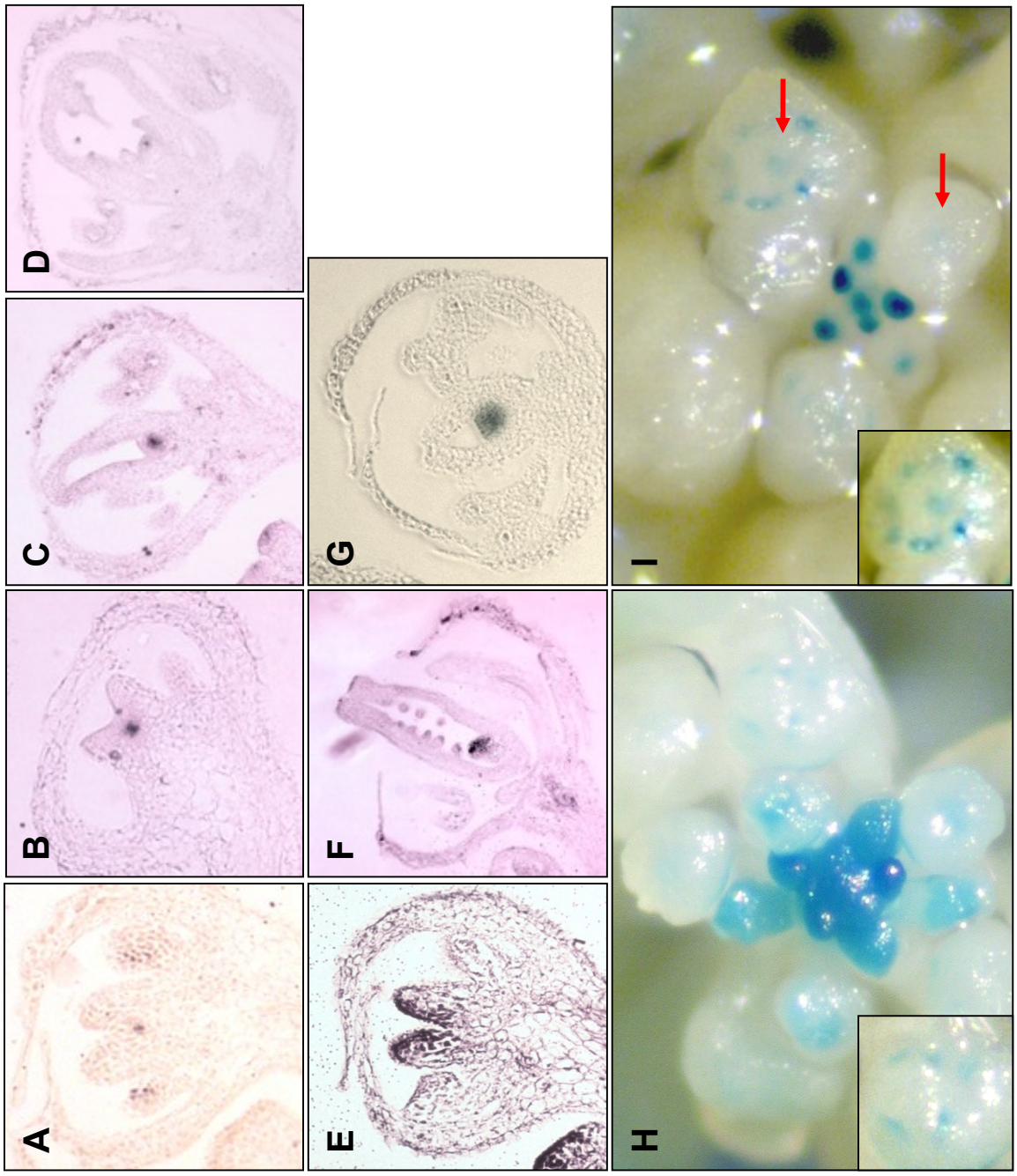
A
B
C
D
E
F
G
H
I

Figure 1.5 Phenotypes of *clf-47* and *ag-10 clf-47* in combination with loss of function mutations in other floral meristem regulators

(A) A *sup-1* flower with more stamens than wild type.

(B) A *clf-47 sup-1* flower. It resembles *sup-1* flowers.

(C) An *ag-10 clf-47 sup-1* flower. It develops an indeterminate floral meristem with numerous stamens.

(D) An *AP2m3* flower with an indeterminate floral meristem.

(E) A *clf-47 AP2m3* flower. The *clf-47* mutation seems to rescue the *AP2m3* defects in carpel formation but not in floral determinacy. The rescue of carpel formation could be due to increased *AG* expression in *clf-47*. The floral meristem is fasciated (arrowhead).

(F) An *ag-10 clf-47 AP2m3* flower. It shows almost the same phenotype to that of an *AP2m3* flower.

(G) An *stm-2* flower that lacks a full complement of floral organs.

(H) A *clf-47 stm-2* flower. It resembles *stm-2* flowers but also shows homeotic transformation of petals and stamens to sepal-like structures (arrowhead).

(I) An *ag-10 clf-47 stm-2* flower. It is identical to *stm-2* flowers especially in terms of floral meristem determinacy.

(J) A *clv3-1* flower with an enlarged gynoecium.

(K) A *clf-47 clv3-1* flower. It resembles *clv3-1* flowers.

(L) An *ag-10 clf-47 clv3-1* flower. Most of these flowers resemble *clv3-1* flowers but some flowers have further enlarged and unfused gynoecia (arrowhead).

(M) A *wus-1* flower that lacks a full complement of floral organs.

(N) An *ag-10 clf-47 wus-1* flower. It is identical to *wus-1* with respects to floral meristem determinacy.

(O) An *ag-1* (strong allele) flower.

(P) An *ag-1 clf-47* flower. It is identical to *ag-1* flowers.

A
B
C
D
E
F
G
H
I
J
K
L
M
N
O
P

Figure 1.6 Phenotypes of *tlf2-2* single mutants and *ag-10 tfl2-2* double mutants

(A) A *tfl2-2* flower.

(B) An *ag-10 tfl2-2* flower. The gynoecia consist of more than two carpels that are partially unfused.

(C) Siliques from *tfl2-2* and *ag-10 tfl2-2*. *ag-10 tfl2-2* siliques are shorter and deformed.

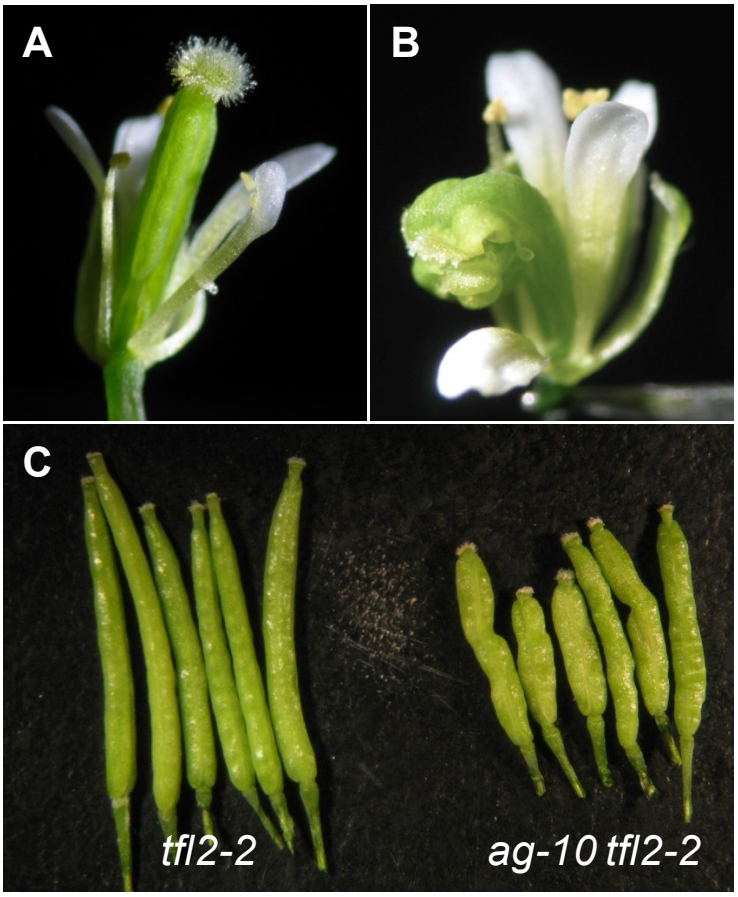
A
B
C
tfl2-2
ag-10 tfl2-2

Table 1.1 Primers used for real-time RT-PCR

	5' primer	3' primer
AG	ttctttgtgatgctgaagtc	atgctgattatttgttgacg
WUS	aaagattgagggcaagaac	cgtgatgatggtgaagtaga
STM	tagtaatggacgcaacacat	tagtaatggacgcaacacat
KNAT1	catcttacacccatcctttt	tgttatcgtttttgttggaa
KNAT2	tggatagaatgtgtggtttc	agtaagcgaggatacaaa
KNAT6	taagtcggttctgatgatgt	aggatacgaaggatgacaag
AP1	ttacccaaatctctccataaa	aaccaaacaaaacaaagacc

CHAPTER 2

Mediator promotes the transcription of microRNA genes in *Arabidopsis*

ABSTRACT

Small RNAs (microRNAs and small interfering RNAs) play important roles in biological processes such as developmental patterning, stress signaling and genome stability in plants. microRNAs are encoded by *MIR* genes, which are transcribed by RNA Polymerase II (Pol II). Here, we have identified a subunit of the Mediator complex as a modulator of microRNA biogenesis by promoting *MIR* gene transcription in *Arabidopsis*. Mediator is a conserved multiprotein complex that bridges sequence-specific transcriptional regulators to the Pol II transcriptional machinery to integrate regulatory information. We show that *MED20a* and two other subunits of Mediator, *MED17* and *MED18* are required for miRNA accumulation. In addition, *MIR* gene expression is affected at the transcriptional level and the expression of miRNA biogenesis genes is not affected in the *med20a* mutant. This indicates that Mediator is responsible for recruiting the Pol II machinery to *MIR* gene loci, probably in a direct manner in *Arabidopsis*. This study extends our understanding of the regulatory mechanisms underlying miRNA biogenesis.

INTRODUCTION

In recent years, the functional significance of small RNA (sRNA)-mediated gene silencing in biological processes in plants and animals has been increasingly recognized. Small RNAs of 20 - 30 nt in size are regulatory molecules that act as sequence-specific repressors of target gene expression. In plants, there are two types of small RNAs: microRNAs (miRNAs) and small interfering RNAs (siRNAs) (Reviewed in Chen, 2009). Most miRNA genes (*MIR*) are located in intergenic regions and have their own promoters. Many miRNAs target transcription factors that are involved in the processes of development and environmental stimulus signaling. Consequently, mutants of miRNA biogenesis genes show pleiotropic developmental defects, which are caused by overexpression of numerous transcription factors. Initially, siRNAs were identified as exogenous molecules from the events of transgene silencing or viral infection (Hamilton et al., 1999). Then, the existence of endogenous siRNAs was uncovered by direct cloning of small RNAs followed by sequencing (Ambros et al., 2003; Llave et al., 2002). Later, the application of high-throughput sequencing technology to small RNA discovery revealed that siRNAs make up the majority of endogenous small RNAs in plants and that most endogenous siRNAs are originated from tandem repeats or transposons (Lu et al., 2005). Endogenous siRNAs mostly act in genome stability, while some of them are involved in the developmental patterning and stress responses.

A common molecular framework underlies the biogenesis and function of most small RNAs in plants although they are derived from different genomic locations and have distinct biological functions. Small RNAs are derived from double stranded RNA

(dsRNA) formed through intramolecular base-pairing or by the activities of RNA-dependent RNA polymerases. Then, the dsRNA is processed into short sRNA/sRNA* duplexes by RNase III endonucleases, Dicer-like proteins (DCL). The sRNA duplex is methylated by the methyltransferase, HUA ENHANCER1 (HEN1). Finally, one sRNA strand is selectively incorporated into an ARGONAUTE (AGO) - containing effector complex. Although such a basic framework of small RNA biogenesis has been well established, additional factors, especially those that regulate small RNA biogenesis remain to be identified.

miRNA biogenesis in plants

Initially, It was believed that DNA-dependant RNA polymerase III (Pol III) mediates miRNA transcription because other small RNAs such as tRNAs and U6 snRNAs are transcribed by Pol III. However, several pieces of evidence in animal systems established that Pol II mediates the transcription of *MIR* genes into long pri-miRNAs, which have mRNA features such as a 5' cap structure and a 3' poly (A) tail (Lee et al., 2004; Cai et al., 2004). It is thought that Pol II is also responsible for *MIR* gene transcription in plants on the basis of common features between pri-miRNA and mRNAs as well as the presence of TATA boxes in the promoters of *MIR* genes (Xie et al., 2005), although direct evidence for Pol II transcription of *MIR* genes has yet to be obtained.

A pri-miRNA is cropped into pre-miRNA, which assumes a stem-loop structure, by DICER-LIKE1 (DCL1). The pre-miRNA is further processed by DCL1 into a 21 nt to

24 nt miRNA/miRNA* duplex (Park et al., 2002; Reinhart et al., 2002). In *Arabidopsis*, there are four DCL proteins that all act in small RNA biogenesis (Reviewed in Chen, 2009). DCL1 is the major RNase III enzyme acting in miRNA biogenesis, although a few miRNAs such as miR822 and miR839 are processed by DCL4 (Rajagopalan et al., 2006). There are two cofactors for DCL1 function, the dsRNA-binding protein HYPONASTIC LEAVES1 (HYL1) and the C2H2 Zn-finger protein SERRATE (SE) (Han et al., 2004; Lobbes et al., 2006; Vazquez et al., 2004; Yang et al., 2006). In mutants of *HYL1* and *SE*, mature miRNA accumulation is reduced, whereas pri-miRNA accumulation is increased, which suggests that the two proteins are involved in pri-miRNA processing. In addition, they were found to be colocalized in Dicing bodies with DCL1 in vivo (Fand and Spector 2007; Fujioka et al., 2007; Song et al., 2007). Recently, it has been shown that the accuracy of pri-miRNA processing to mature miRNA by DCL1 is increased in the presence of HYL1 and SE (Dong et al., 2008). Another nuclear RNA-binding protein, DAWDLE (DDL) also interacts with DCL1 (Yu et al., 2008). In *ddl* mutants, pri-miRNA accumulation is reduced despite no changes in miRNA gene transcription. Based on these results, it was proposed that DDL facilitates DCL1 to recognize its substrate. The nuclear heterodimeric cap-binding complex (*CBC*) is responsible for the accumulation of a subset of miRNAs (Gregory et al., 2008; Laubinger et al., 2008). The *CBC* is presumed to have similar functions as that of *HYL1* and *SE* because mutants in all these genes are similar in terms of pri-miRNA and mature miRNA accumulation.

The miRNA/miRNA* duplexes processed by DCL1 are methylated on the 2'OH of the 3'terminal ribose by the methyltransferase HEN1 (Yu et al., 2005). In vitro studies

showed that HEN1 preferentially methylates 21-24 nt RNA duplexes with 2 nt overhangs at their 3' end, which is a typical feature of DICER products. In the *hen1-1* mutant, mature miRNA accumulation was reduced and heterogeneity in miRNA size was observed (Li et al., 2005). The heterogeneity was revealed as a ladder of bands with a 1 nt interval. Based on the cloning of specific miRNAs in the *hen1-1* mutant, it was shown that U residues were added to the 3' end of unmethylated miRNAs. In addition, 3' truncated forms of miRNAs were also found. These results indicated that miRNA methylation protects miRNAs from uridylation or degradation. However, the functions of miRNA uridylation is not clear. Recently, a reverse genetic study identified the *SMALL RNA DEGRADING NUCLEASE* (*SDN*) gene family as involved in the control of miRNA stability (Ramachandran and Chen, 2008). SDN1 degrades single stranded small RNAs in vitro. In addition, knockdown of SDN family genes resulted in increased miRNA accumulation and pleiotropic developmental defects.

Methylated miRNA duplexes are exported from the nucleus to the cytoplasm via the exportin-5 homolog, HASTY and the miRNA strand is loaded onto an AGO1-containing RNA Induced Silencing Complex (RISC) (Park et al., 2005; Baumberger and Baulcombe 2005; Qi et al., 2005). Finally, a miRNA-RISC is recruited to its target mRNAs, resulting in mRNA cleavage or translational inhibition (Reviewed in Bartel et al., 2004).

Mechanism of miRNA function

First, a miRNA-RISC causes target mRNA cleavage. AGO1 is a major effector in a miRNA-RISC. *Arabidopsis* has ten AGO proteins. Until now, it has been shown that AGO1, AGO4, AGO6, AGO7 and AGO10 have apparent roles in small RNA function (Reviewed in Vaucheret, 2008). AGO proteins contain several functional domains: PAZ, MID and PIWI. The PIWI domain possesses RNase III-endonucleolytic activity. A miRNA-RISC recognizes a target mRNA in a sequence-specific manner and cleaves the mRNA at a defined position along the miRNA-mRNA duplex through the endonucleolytic activity of AGO1, which results in a reduction of target mRNA accumulation (Baumberger and Baulcombe, 2005; Fagard et al., 2000; Qi et al., 2005; Vaucheret et al., 2004). In *ago1* mutants, miRNA target gene expression is increased and 3' cleavage products of target mRNAs are reduced in abundance. AGO1 has slicer activity in vitro and most miRNAs are associated with AGO1 in vivo.

miRNAs also repress target gene expression via translational inhibition (Reviewed in Kim et al., 2009). Initially, It was thought that plant miRNAs predominantly act through mRNA cleavage unlike miRNAs in animals: animal miRNAs mostly work through translational inhibition. Recently, *miRNA-action deficient* (*mad*) mutants were isolated through a forward genetic screen (Brodersen et al., 2008). Characterization of these mutants suggested that plant miRNA-mediated translational inhibition is a widespread mechanism underlying miRNA function. Several factors have been identified, which are required for miRNA-mediated translational inhibition such as the microtubule-severing enzyme, KATANIN and the P-body component VARICOSE

(VCS). Interestingly, AGO10, a paralog of AGO1, is also involved in this pathway with AGO1 (Brodersen et al., 2008).

Mechanism of miRNA regulation

There may be many ways to control miRNA expression at the level of transcription, post-transcriptional processing, and stability. In addition, miRNA activities may also be regulated.

Pol II transcribes miRNA genes (Lee et al., 2004; Cai et al., 2004, Xie et al., 2005). Transcription factors, which act through cis-elements, are well-known modulators of Pol II activity as activators or repressors of protein-coding genes (Reviewed in Sikorski et al., 2009). Interestingly, several pieces of evidence also support the transcriptional regulation of miRNA gene expression via transcription factor activity. First, external stimulus response cis-elements, corresponding to binding site of known transcription factors, were found in miRNA gene promoters (Megraw et al., 2006). In addition, it was shown that some transcription factors were required for miRNA accumulation under stress conditions (Bari et al., 2006; Kawashima et al., 2009; Yamasaki et al., 2009). For example, *SQUAMOSA PROMOTER BINDING PROTEIN-LIKE 7* (*SPL7*) is required for miR398 gene expression through binding to cis-elements in the miR398 gene promoter under low-copper conditions (Yamasaki et al., 2009).

Regulation of miRNA gene expression can theoretically occur at the level of posttranscriptional processing. Although such regulation has been shown for the animal miRNA let-7 (Heo, et al., 2008; Viswanathan et al., 2008), no examples of

posttranscriptional regulation have been found in miRNA gene expression in plants. Recently, however, a mechanism to regulate miRNA action has been uncovered and named target mimicry. *INDUCED BY PHOSPHATE STARVATION1* (*IPS1*) is a non-coding RNA, which contains a motif with sequence complementarity to miR399. However, *IPS1* has a mismatch at the cleavage site within the miR399 base-pairing motif, which results in non-cleavable miR399-IPS1 pairs. *IPS1* appears to sequester miR399 from its real target. Indeed, overexpression of *IPS1* resulted in increased accumulation of the miR399 target gene (Fransco-Zorrilla et al., 2007). It is not clear yet whether target mimicry is a common mechanism to control the activities of miRNAs in general.

Biogenesis of endogenous siRNA in plants

There are three major types of endogenous siRNAs in *Arabidopsis*. They are natural antisense transcript-derived siRNAs (nat-siRNAs), trans-acting siRNAs (ta-siRNAs) and heterochromatic siRNAs (hc-siRNAs).

Natural antisense transcript-derived siRNAs (nat-siRNAs)

nat-siRNAs are inducible small RNAs in response to abiotic or biotic stresses. So far, two classes of nat-siRNAs have been reported. The first nat-siRNA was identified as a salt stress inducible small RNA from cis- natural antisense transcripts (NATs), Δ1-pyroline-5-carboxylate dehydrogenase (P5CDH) and SRO (Borsani et al., 2005). When two transcripts are present under the salt stress condition, they form dsRNA, which is processed by DCL2 to generate a 24 nt long nat-siRNA. Then, the 24 nt nat-siRNA causes an initial cleavage of the P5CHD mRNA, resulting in the generation of 21 nt nat-

siRNAs in a DCL1-, RDR6-, Suppressor of Gene silencing 3 (SGS3)- and Pol IV-dependant manner. In turn, 21 nt nat-siRNAs mediate further *P5CHD* mRNA cleavage to repress its expression, which results in increased salt tolerance. The second nat-siRNA is a pathogen-inducible nat-siRNA that acts with a similar mechanism as that of the salt-inducible nat-siRNA (Katiyar-Agarwal et al., 2006). Genome-wide analysis in *Arabidopsis* revealed the existence of many cis-NATs and siRNAs that match these cis-NATs (Yamada et al., 2003; Wang et al, 2005), which imply that nat-siRNA mediated-gene silencing is widespread and may be used in response to environmental cues.

trans-acting siRNAs (ta-siRNAs)

ta-siRNAs have a unique feature, which is that miRNA-mediated cleavage is required to initiate their biogenesis (Allen et al., 2005; Peragine et al., 2004; Rajagopalan et al., 2006; Vazquez et al., 2004; Yoshikawa et al., 2005). In *Arabidopsis*, there are four *TAS* loci. *TAS1*/2, *TAS3* and *TAS4* transcripts are initially cleaved by miR173, miR390 and miR828, respectively. In particular, miR390-mediated *TAS3* cleavage depends on AGO7 activity rather than AGO1. The cleavage somehow triggers the conversion of ssRNA to dsRNA by RDR6 and SGS3. Then, dsRNA is processed by DCL4 into small RNAs and methylated mature ta-siRNAs are loaded into AGO1-containing RISC complexes (Baumberger and Bualcombe, 2005). It is not clear yet, how miRNA-mediated cleavage of *TAS* transcripts leads to the production of ta-siRNAs, while similar cleavage of other miRNA target mRNAs does not.

heterochromatic siRNAs (hc-siRNAs)

hc-siRNAs are derived from heterochromatic loci and represent the great majority of endogenous siRNAs in plants. Plants have two specialized polymerases, Pol IV and Pol V, which are required for hc-siRNA biogenesis and function. Pol IV and Pol V are probably derived from Pol II because they are composed of 12 subunits that are paralogous or identical to those of Pol II (Huang et al., 2009; Lahmy et al., 2009; Ream et al., 2008). More than 90% of hc-siRNAs are Pol IV-dependant (Mosher et al., 2008; Zhang et al., 2007). Pol IV is presumed to transcribe transposable and repeated sequence elements (Herr et al., 2005; Kanno et al., 2005; Mosher et al., 2008; Onodera et al., 2005; Zhang et al., 2007). Pol IV-dependant transcripts are converted into dsRNA by RDR2 (Xie et al., 2004). The SNF2-like protein, CLASSY1, is also required for hc-siRNA biogenesis (Smith et al., 2007). Then, dsRNAs are diced into 24 nt small RNAs by DCL3 and the small RNAs are methylated by HEN1 (Xie et al., 2004; Yu et al., 2005). One strand of the hc-siRNA duplex is incorporated into an AGO4-containing RISC. AGO6 has partial functional redundancy with that of AGO4 (Zheng et al., 2007; Zilberman et al., 2003).

A recent study revealed the transcriptional activity of Pol V in vivo. Pol V generates transcripts (scaffold transcripts) that are adjacent to hc-siRNA target loci at heterochromatic regions (Wierzbicki et al., 2008). It is believed that Pol V transcripts recruit AGO4-RISC to the target loci through sequence specific interaction between Pol V transcripts and the hc-siRNA in the AGO4-RISC, which in turn recruits chromatin-modifying factors such as DNA methyltransferase, DRM2 and histone modifying

enzymes (El-Shami et al., 2007; Li et al., 2006; Wierzbicki et al., 2008). Intriguingly, the most recent study showed that Pol II is also required for endogenous siRNA mediated transcriptional gene silencing (TGS) at intergenic low-copy-number loci. Pol II generates noncoding scaffold transcripts, resulting in recruitment of AGO4/siRNAs to homologous loci similar to the mechanism of Pol V. In addition, Pol II transcription recruits Pol IV and Pol V to different locations at heterochromatic loci to promote siRNA biogenesis and siRNA-mediated TGS, respectively (Zheng et al., in press at Genes Dev.)

Biological function of endogenous siRNAs

Although nat-siRNAs, ta-siRNAs and hc-siRNAs are categorized into the same broad group of siRNAs on the basis of using dsRNA as the precursors in their biogenesis, their molecular and biological roles are quite distinct.

nat-siRNAs and ta-siRNAs act in environmental stress signaling and developmental processes, respectively, through post-transcriptional gene silencing (PTGS). The salt inducible *SRO5-P5CDH* nat-siRNAs guide *P5CDH* mRNA cleavage (Borsani et al., 2005). The reduced *P5CDH* expression results in increased proline accumulation, which increases salt stress tolerance. Target genes of ta-siRNAs have been identified based on computational analysis and some of them have been verified by experimental studies. ta-siRNAs from the *TAS3* locus target *AUXIN RESPONSE FACTOR* genes, *ARF3* and *ARF4* (Fahlgren et al., 2006). *ARF3* and *ARF4* are expressed on the abaxial side of leaf primorida and act to specify abaxial identity in leaf polarity. The *TAS3* gene is expressed on the adaxial side, and helps to reduce the expression of

ARF3 and *ARF4* on the adaxial side (Hunter et al., 2006; Garcia et al., 2006; Chitwood et al., 2009).

On the other hand, hc-siRNAs are mainly involved in the maintenance of genome stability through TGS. DNA and/or histone H3 in heterochromatic regions become methylated through hc-siRNA-AGO4 activity (Xie et al., 2004; Zilberman et al., 2003; Qi et al., 2006). This methylation suppresses transcriptional activity of the transposable elements and repetitive DNA, which is important to maintain genome stability. Indeed, in mutants of hc-siRNA biogenesis genes, DNA or H3K9 methylation level is decreased, which causes derepression of heterochromatic loci.

The Pol II transcriptional machinery

The dynamic changes in gene expression upon internal and external demands are first modulated at the transcriptional initiation step. Pol II, which is responsible for the transcription of a large portion of mRNA coding genes in eukaryotes, is recruited to promoters of genes (Sikorski and Buratowski, 2009). Biochemical studies show that Pol II alone is not sufficient to initiate transcription in vitro, which implies that it requires cofactors for transcriptional activity. One type of well-studied cofactor includes the basal initiation factors such as TFIIA, TFIIB, TFIID, TFIIE, TFIIF and TFIIH (Thomas et al., 2006; Reese, 2003). In the presence of these factors, which are so-called general transcription factors (GTFs), Pol II supports basal transcription in vitro. The assembly of the pre-initiation complex including Pol II and GTFs on the core promoter is a critical step for transcriptional initiation. Genetic and biochemical studies have revealed another

cofactor that plays an important role in Pol II recruitment: a multiple protein complex, Mediator. It is thought that Mediator bridges sequence-specific transcriptional regulators to the Pol II-containing pre-initiation complex to integrate regulatory information (Struhl, 1996; Yudkovsky et al., 2000; Kuras and Struhl, 1999; Li et al., 1999).

Structure of the Mediator complex

Mediator is a large protein complex, which is composed of 20-30 subunits. It is functionally and structurally conserved in all eukaryotes although species-specific subunits exist (Casamassimi and Napoli, 2007). Mediator was first identified in yeast, *Saccharomyces cerevisiae,* an organism in which it remains to be the best studied (Carlson et al., 1981; Neigeborn and Carlson, 1984; Simchen et al., 1984; Stern et al., 1984; Suzuki et al., 1988). Structural studies of the yeast Mediator complex revealed that it consists of three subdomains (Head, Middle and Tail) and a separable kinase module (Astrurias et al., 1999; Dotson et al., 2000; Sato et al., 2003; Guglielmi et al., 2004).

The head domain, composed of MED6, MED8, MED11, MED17, MED18, MED19, MED20 and MED22 subunits, mainly interacts with Pol II (Takagi et al., 2006). Disruption of the head domain results in dissociation of the Mediator complex from transcriptionally active promoters (Lariviere et al., 2006). The middle domain, which includes MED1, MED4, MED7, MED9, MED10, MED21 and MED31 subunits, directly interacts with the C-terminal domain (CTD) of the largest subunit in Pol II (Rbp1) (Kang et al., 2001). It is believed that the middle domain transmits input signal from transcriptional regulators to the head domain. The tail domain consists of MED2, MED3,

MED5, MED14, MED15 and MED16 subunits. It directly interacts with the DNA-bound transcriptional regulators (Park. et al., 2000; Lee et al., 1999; Han et al., 2001). The kinase module is detachable. It is composed of four proteins: MED12, MED13, cyclin-dependant kinase 8 (CDK8) and Cyclin C (CycC). The CDK8 module itself is a big complex (~600kDa). Therefore, Mediators containing the kinase module are referred as large mediators, whereas variants without this module are called small mediators (Sun et al., 1998; Malik et al., 2000; Mittler et al., 2001; Naar et al., 2002; Taatjes et al., 2004). The CDK8 module is mainly involved in transcriptional repression probably through its kinase activity, which can phosphorylate Rbp1 CTD heptads, some Mediator subunits, GTFs, and transcriptional regulators (Liu et al., 2004; Van de Peppel et al., 2005; Hengartner et al., 1998; Nelson et al., 2003; Chi et al., 2001; Vincent et al., 2001; Hallberg et al., 2004; Hirst et al., 1999).

Mediator is not a fixed complex. It has been noticed that several isoforms or alternative forms exist in cells (Casamassimi et al., 2007). Identification of large and small mediators based on the presence of the CDK8 module has uncovered the functional flexibility of Mediator, which acts as either an activator or a repressive factor (Sun et al., 1998; Malik et al., 2000; Mittler et al., 2001; Naar et al., 2002; Taatjes et al., 2004). In addition, new isoforms of several subunits have been identified and differences in the composition of complexes in the mammalian Mediator complex have been found (Mittler et al., 2001; wu et al., 2003). It is not clear how many alternative Mediator forms exist in organisms. However, it is thought that this structural arrangement probably makes it easier to integrate a multitude of regulatory inputs with limited integrators.

Molecular functions of Mediator

srb4 was isolated as a temperature sensitive mutant in yeast through a genetic screen aimed at the identification of regulators of gene transcription. Later, *SRB4* was found to be *MED17*, one of the head subunits. In the *srb4/med17* mutant, the expression of more than 90% of Pol II-dependant transcripts is decreased under the restrictive temperature (Holstege et al., 1998; Thompson CM et al., 1995). It suggests that Mediator might act as a general factor in Pol II transcription. Consistently, it has been shown that the head domain of the Mediator complex stimulates basal transcription in the absence of activators in vitro (Mittler et al., 2001; Wu et al., 2003; Baek et al., 2006). Based on these results, it is believed that Mediator acts as a general transcription factor.

However, this general view has been questioned by recent reports. A genome-wide analysis has shown that Mediator occupancy is not tightly correlated with Pol II occupancy within many highly active Pol II promoters in yeast (Fan et al., 2006). Moreover, another study suggests that Mediator is associated with promoters in an activator- rather than Pol II-dependent manner (Fan and Struhl, 2009). In contrast to these results, another most recent study argues that Mediator is associated with constitutively active genes and it is directly required for the recruitment of Pol II transcription machinery as a GTF (Ansari et al., 2009). Therefore, it appears that further investigations are needed to better understand the functions of the Mediator complex.

Mediator in plants

Recently, the Mediator complex was biochemically characterized in *Arabidopsis*. It contains 21 subunits conserved in eukaryotes and six plant-specific subunits (Backstrom et al., 2007). Although the CDK8 module was not co-purified with Mediator in the experiment, *Arabidopsis* has homologs to the *MED12*, *MED13*, *CDK8* and *CycC* genes. Prior to this purification of the *Arabidopsis* Mediator complex, several subunits have been studied genetically and have their own gene names.

PHYTOCHROME and FLOWERING TIME1 (PFT1), which is *MED25,* was isolated as a factor involved in the *Phytochrome B* (*phyB*)-dependant pathway to promote flowering time in response to shade (Cerdan and Chory et al., 2003). It was assumed to be a transcriptional coactivator on the basis of its nuclear localization, the presence of a glutamine-rich domain and its transcriptional activator activity in yeast when fused to the LexA DNA-binding domain. However, recently another report suggested that *PFT1* negatively regulates the phytochrome signaling pathway rather than acting as a component in that pathway (Wollenberg et al., 2008).

STRUWWELPETER (SWP)/*MED14* was reported as a nuclear protein playing a role in defining the duration of cell proliferation (Autran et al., 2002). An *swp* mutant exhibits dwarfism with an abnormal architecture such as fascinated stem and abnormal floral structures; some of the phenotypes were mainly due to reduced cell numbers. Consistently, ectopic expression of *SWP* caused increased cell numbers in clusters. It has since been reported that the repressive activity of LEUNIG (LUG), a transcriptional corepressor, involves interaction with SWP/MED14 and HUA ENHANCER3

(HEN3)/CDK8 (Gonzalez et al., 2007). *HEN3* was identified as a weak regulator of *AG*, which is a target of *LUG* (Liu, et al., 1995; Wang and Chen, 2004)). It is possible that *LUG* negatively regulates *AG* expression through a larger mediator complex containing the HEN3/CDK8 module that has repressive activity.

Recent studies have suggested that Mediator acts as an integrator in response to environmental cues in *Arabidopsis* (Kidd et al., 2009). Another function of *PFT1/MED25* is that it is required for Jasmonic Acid (JA)-dependant defense gene expression and resistance to leaf-infecting necrotrophic fungal pathogens (Dhawan et al., 2009). In addition, an *atmed8* mutant showed late flowering and delayed symptom development by infection of a root-infecting hemibiotrophic fungal pathogen (Dhawan et al., 2009). These results indicate that *MED8* is a regulator of disease resistance and flowering time. In another study, it was shown that *MED21* is also required for resistance to necrotrophic fungal pathogens. Interestingly, MED21 interacts with HISTONE MONOUBIQUITINATION1 (HUB1) that is also involved in defense against necrotrophic fungal pathogens. This result implied that *MED21* might integrate pathogen-infection signaling through chromatin modifications.

Here, we report that the plant Mediator complex promotes the transcription of miRNA genes. We isolated a mutant in *MED20a* that encodes a subunit of the head domain from a forward genetic screen as a mutant with pleiotropic developmental defects. In *med20a* and several mutants in other Mediator subunits, the levels of pri-miRNAs and mature miRNAs are reduced. We show that this reduction is due to decreased transcriptional activity. This study extends our understanding of the regulatory

mechanisms underlying miRNA biogenesis. Furthermore, we find that certain heterochromatic loci were derepressed in *med* mutants despite no changes of hc-siRNA levels. These results raise the possibility that the Mediator may act as a cofactor in the Pol V transcriptional machinery. Further studies are necessary to address the relationship between the Mediator and Pol V.

RESULTS

Isolation and characterization of a loss of function mutant of *AtMED20a*

A mutant with pleiotropic developmental phenotypes was isolated in a forward genetic screen. This mutant had light green cotyledons and some cotyledons had indentations to result in heart-shaped organs (Fig. 1F). The plant size of the mutant was smaller than that of wild type and some plants developed the three first true leaves instead of a pair of first true leaves, probably reflecting abnormal SAM activity (Fig. 1B). During the vegetative stage, the plant size was much smaller compared to wild type and leaves were curled down and shorter. The flowering time was delayed and the phyllotaxy of flowers was abnormal. In addition, floral organ size was smaller and some flowers had an increased number of petals. Fertility was dramatically reduced (Fig. 1I).

Genetic crosses indicated that the pleiotropic phenotypes were caused by a single, recessive mutation. The mutation was mapped to a 120 kb region covering the BAC T3B23 on Chromosome 2. Sequencing candidate genes in this region revealed a C-to-T mutation in At2g28230, which encodes a subunit of the head domain in the Mediator complex (Fig. 2A). The mutation is at the 58th nucleotide in the second exon and results

in a premature stop codon. A homology-based search identified two more homologs in *Arabidopsis*: At2g28020 and At4g09070. Therefore, we named the three genes At2g28230, At4g09070 and At2g28020 as *MED20a*, *MED20b* and *MED20c*, respectively (Fig. 2A). *Med20a* and *Med20b* have 85% identity at the nucleotide level. *MED20*c is shorter than *MED20a* and *MED20b*; there is 93% identity at the nucleotide level in exon 2 among the three genes.

Mediator is a large protein complex composed of three subdomains: head, middle and tail. To test whether the developmental phenotype of *med20a* mutants reflects its functions within the head domain of Mediator, we obtained two T-DNA mutant lines of genes encoding two other head domain subunits, MED17 and MED18, from the SALK collection and analyzed their phenotypes (Fig. 2B). The *med17* and *med18* mutants exhibited strikingly similar developmental defects as *med20a* (Fig. 1C, D, G and H). Therefore, Mediator is broadly involved in developmental processes in *Arabidopsis*.

Mediator is required for miRNA accumulation in *Arabidopsis*

miRNAs are a type of regulatory RNAs derived from the processing of longer transcripts from endogenous genes. Many miRNAs are involved in developmental patterning such that mutants in miRNA biogenesis genes exhibit pleiotropic developmental defects. *MIR* genes are likely to be transcribed by Pol II, but it is unknown whether Mediator plays a role in the expression of *MIR* genes. The developmental defects of *med* mutants suggest that the Mediator could be required for *MIR* gene expression. To

test this possibility, we first examined the accumulation of various mature miRNAs in the *med20a* mutant.

We determined the levels of 11 miRNAs and one ta-siRNA, the tasiR-ARF, which also functions in development, in wild-type and *med20a* inflorescences. Nine miRNAs and the tasiR-ARF were present at significantly reduced levels in *med20a* (Fig. 3A). This result implies that miRNA metabolism is generally affected in the *med20a* mutant. We also examined the levels of selected miRNAs in *med17* and *med18*. Consistently, all tested miRNAs were at reduced levels in *med17* and *med18* (Fig. 3B). Based on these results, we concluded that Mediator is generally involved in miRNA biogenesis in *Arabidopsis*.

Mediator regulates *MIR* gene expression at the transcriptional level

The reduced miRNA accumulation in the Mediator mutants may be due to reduced transcription of the genes, compromised post-transcriptional processing of the precursors, or decreased stability of the mature miRNAs. Since Pol II transcribes *MIR* genes, and the Mediator bridges transcription factors to the Pol II machinery to integrate transcriptional inputs or serves as a general transcription factor for Pol II, it is likely that the reduced miRNA accumulation in *med* mutants is attributable to reduced transcriptional activity of *MIR* genes. To test this hypothesis, pri-miRNA levels were determined in *med20a* by real-time RT-PCR.

We examined the levels of seven pri-miRNAs by real-time RT-PCR. Indeed, the levels of all pri-miRNAs were decreased in the *med20a* mutant to 20%-70% of the wild-

type levels (Fig. 4). This suggests that the Mediator is required for the transcription of *MIR* genes. To directly test that the mutation affects the activity of a *MIR* promoter, we introduced a *GUS* transgene under the control of the *MIR167a* endogenous promoter (*pMIR167a::GUS*) into the progeny of a *med20a/+* plant. *med20/+* transgenic lines in which the transgene was inserted into a single locus were obtained, and *med20a* and wild type plants containing the same transgene insertion were analyzed. GUS staining revealed decreased GUS expression in *med20a* compared to wild type plants (Fig. 4B), which suggests that the Mediator acts through the promoter of *MIR167a.*

The expression of miRNA biogenesis genes is not affected in *med20a* mutants

Since protein-coding genes are transcribed by Pol II and Mediator is possibly a GTF for Pol II, the reduced transcriptional activity of *MIR* genes in *med* mutants could be an indirect effect of reduced expression of certain protein-coding genes. We profiled changes in gene expression in the *med20a* mutant at the genomic level using Affymetrix ATH1 microarrays. We performed three biological replicates using inflorescences from wild type and the *med20a* mutant. A total of 754 genes were down-regulated and 140 genes were up-regulated in *med20a*. However, known miRNA biogenesis genes were not affected in *med20a*, which suggests that at least the reduced pri-miRNA and mature-miRNA levels in the *med20a* mutant was not due to reduced expression of miRNA biogenesis genes.

Some hc-siRNA target loci are de-repressed in *med* mutants

Plants have evolved two specialized polymerases, Pol IV and Pol V, from Pol II to act in hc-siRNA biogenesis and hc-siRNA-mediated DNA methylation, respectively. This raises the intriguing questions of whether the Mediator acts with Pol IV or Pol V as it does with Pol II in plants. In order to investigate this possibility, first we examined hc-siRNA accumulation levels in the *med20a* mutant. Northern blots on hc-siRNAs from 8 loci revealed that hc-siRNA accumulation was not affected in *med20a* mutants (Fig. 5). Since these hc-siRNAs are generated in a Pol IV-dependant manner, our results suggest that *Med20a* does not act with Pol IV.

Pol V acts downstream of siRNAs to recruit siRNAs to target loci to result in DNA methylation. It transcribes regions adjacent to the hc-siRNA target loci, to generate scaffold transcripts, which recruit the AGO4-siRNA complexes to chromatin. In a Pol V mutant, regardless of whether the hc-siRNAs are reduced in accumulation, the hc-siRNA loci are de-repressed due to a lack of DNA methylation or histone H3 lysine 9 (H3K9) methylation. To test whether Mediator in involved in the Pol V-dependant silencing of the hc-siRNA loci, we examined hc-siRNA target loci expression in the *med* mutants. Intriguingly, the AtSN1 locus was derepressed in *med20a*, *med17* and *med18* mutants, whereas other loci were not affected. This suggests that the Mediator may be involved in the Pol V pathway in a locus-specific manner.

Mediator acts as a GTF.

It is controversial whether the Mediator acts as GTF or not. In our studies of limited miRNAs, Mediator appears to act generally on *MIR* genes. To address the functional correlation between Mediator and Pol II in a genome-wide manner, we took advantage of a partial loss-of-function allele in the second largest subunit of Pol II isolated in our lab. We performed Affymetrix ATH1 microarray-based transcript profiling using inflorescence tissues from wild type, *med20a*, and the pol II allele, *nrpb2-3* (Zheng et al., in press at Genes Dev.). By comparing either mutant to the wild type, we found that a total of 754 genes were down-regulated and 140 genes were up-regulated in *med20a*, whereas a total of 448 genes were down regulated and 95 genes were up-regulated in *nrpb2-3.* The number of genes down regulated in *med20a* was almost twice that in *nrpb2-3*, which is not surprising given that *nrpb2-3* is a weak allele. Intriguingly, 84% (377 genes) of the down-regulated genes (448 genes) in *nrpb2-3* was also down-regulated in *med20a* (Fig. 7). This result indicates that the function of Pol II and Mediator are coordinated and supports the view of Mediator as a GTF. Based on the known functions of Pol II and Mediator, the up-regulated genes in *med20a* and *nrpb2-3* are likely outputs from the indirect effects. Interestingly, *NRPB1* encoding the largest subunit of Pol II, is two fold up-regulated in *med20a*, which suggests that there may be feed back regulation between the Mediator and Pol II.

DISCUSSION

Mediator and miRNA gene expression

med17, *med18* and *med20* mutants exhibit very similar and pleiotropic developmental defects (Fig. 1). One hypothesis is that the developmental defects in *med* mutants are caused by defects in miRNA gene expression because mutants in miRNA biogenesis genes also show pleiotropic developmental defects. Indeed, we showed that various miRNAs accumulate to lower levels in the *med20a* mutant and several selected miRNAs are at reduced levels in the *med17* and *med18* mutants. We focused on the reduced fertility phenotype that is observed in three *med* mutants to test whether it is caused by reduced miRNA levels. A previous study showed that the reduced fertility phenotype of *dcl1* mutants is due to over-expression of (AUXIN RESPONSE FACTOR8) *ARF8*, which is controlled by miR167; as such the phenotype is rescued by a loss-of-function mutant of *ARF8* (Goetz et al., 2007 and Vivian-Smith et al., 2007). However, the *arf8-6 med20a* double mutant has no obvious difference in the fertility defects compared to the *arf8-6* single mutant (data not shown). This suggests that the fertility defects of *med20a* mutants are unlikely caused by reduced levels of miR167. Alternatively, it might be more difficult to rescue the fertility defects in the Col background (from which the *med20a* mutant is derived) than the L*er* background (from which the *dcl1-9* mutant is derived).

There are three homologs of *MED20* in *Arabidopsis*, which are *MED20a*, *MED20b* and *MED20c*. Based on the analysis of the sequence homology and gene structure, *MED20a* and *MED20b* are very similar to each other, whereas *MED20c* is

much shorter (Fig. 2A). Our data showed that *MED20a* is required for *MIR* genes transcription. Do *MED20b* and *MED20c* also promote *MIR* expression? There is not a T-DNA insertion mutant in *MED20b*, and the T-DNA mutant of *MED20c* (the T-DNA is inserted in an exon) did not show any morphological defects, which implies that either *MED20c* is not necessary for *MIR* gene expression or that it functions partially redundantly with *MED20a*. In a previous study, the Mediator complex was biochemically purified in *Arabidopsis*. Intriguingly, MED20a but not MED20b was co-purified in the Mediator complex despite the two having such high sequence similarity. It suggests that either MED20b is not in the Mediator or the expression of *MED20b* is spatially or temporally different from that of *MED20a*. More molecular genetic and biochemical studies are necessary to determine the functions of *MED20b* and *MED20c*.

Our results show that 9 out of 11 miRNAs are at reduced levels in *med20a* and several selected miRNAs are also at reduced levels in *med17* and *med18* mutants (Fig. 3). In addition, Mediator regulates miRNA gene expression at the transcriptional level (Fig. 4). This indicates that Mediator generally promotes the transcription of *MIR* genes. However, the accumulation of two miRNAs, miR160 and miR158, is not affected in the *med20a* mutant. Why are these two miRNAs not affected? There are several possibilities. First, the two *MIR* genes do require *MED20a* for their transcription, but miR160 and miR158 levels are regulated at the posttranscriptional level. The AGO1-miR168 feed back loop has been proposed in *Arabidopsis* (Vaucheret et al., 2006). The levels of AGO1, a key effector protein in the miRNA action, need to be tightly regulated. miR168, which targets *AGO1*, is co-regulated with AGO1 at the posttranscriptional level to

precisely control AGO1 activity. However, so far, nothing is known about posttranscriptional control of miR160 and miR158. Second, *MED20a* may not be necessary for *MIR160* and *MIR158* gene expression. It is possible that a Mediator complex containing MED20b or c is responsible for the transcription of *MIR160* and *MIR158* genes. We need to examine the accumulation of miR160 and miR158 in other *med* mutants to determine whether Mediator is necessary for the transcription of these genes.

Mediator and endogenous siRNAs

Intriguingly, the *AtSN1* locus is de-repressed in *med20a*, *med17* and *med18* mutants (Fig. 6). This result raises the interesting hypothesis that Mediator is involved in the silencing of the hc-siRNA loci with Pol IV and/or Pol V, two polymerases that are derived from Pol II. Since the accumulation of endogenous hc-siRNAs is not affected in *med20a*, MED20a does not seem to act with Pol IV. Then, does the Mediator act with Pol V? At present, this is an open question. The next experiment would be to determine whether the accumulation of Pol V-dependant scaffold transcripts at the *AtSN1* locus is affected in *med* mutants. If the transcripts are at reduced levels in the *med* mutants, it indicates that Mediator is required for Pol V activity. On the other hand, it is also possible that Mediator acts in an hc-siRNA independent pathway to repress hc-siRNA loci. In addition, it is possible that a specific Mediator complex acts in a locus-specific manner, as not all hc-siRNA loci are de-repressed in *med20a*, *med17* and *med 18* mutants.

MATERIALS AND METHODS

Plant Materials

All mutants are in Col background. *Arabidopsis* plants were grown at 24°C under continuous light. T-DNA knock out lines of *MED17* and *MED18* were obtained from the Salk Institute Genomic Analysis Laboratory. *nrpb2-3* was isolated from our lab. *nrpe1-1* and the *pMIR167a::GUS* transgenic line were gifts form Dr. Thierry Lagrange and Dr. Wu, respectively.

Map-based Cloning of *MED20a*

med20a (Col) was crossed to L*er*. In the F2 population, plants showing *med20a* phenotypes were identified and used as the mapping population. Initially, 27 *med20a* plants were used in rough mapping, which showed that *MED20a* is linked to the marker NGA168 on chromosome 2. For the fine mapping, we designed new SSLP or CAPS markers in this region according to polymorphisms between L*er* and Col, using the Monsanto Arabidopsis polymorphism and L*er* sequence database (http://www.arabidopsis.org/Cereon). Using these markers and ~ 500 plants of known *med20a* genotypes, we mapped *MED20a* to a 120kb region covered by the BACs T3B23 and T1B3. In this region, 23 candidate genes were located and sequencing analysis was conducted with 4 candidate genes.

Genotyping

For *med20a* genotyping, genomic DNA was amplified by At2g28230-F (CATACCTCAATTTCGATTGGG) and At2g28230-R4 (GAAGAATCAGCTTCCAA-GAC) primers and PCR products from wild type could be digested by AluI, whereas those from *med20a* could not.

RT-PCR

Total RNA from inflorescence was reverse-transcribed using SuperScriptII (Invitrogen) and oligo-d(T) primers according to the manufacturers' instructions. For pri-miRNA detection, Quantitative PCR was carried in triplicate on a Bio-Rad IQcycler apparatus with the Quantitech SYBR green kit (Bio-Rad). To determine the expression levels of endogenous siRNA target loci, RT-PCR products were separated on agarose gel and stained with ethidium bromide. Primers used are listed in Table 2.1 and 2.3.

Small RNA Northern Blot Analysis

RNA isolation and hybridization for miRNAs and endogenous siRNAs were performed as described (Park et al., 2002). 10ug total RNA and 5ug small RNA-enriched RNA from inflorescence were used for miRNAs and endogenous siRNAs northern blots, respectively. 5′-End-labeled ^{32}P antisense DNA or RNA oligonucleotides were used to detect miRNAs and endogenous siRNAs. Oligo probes used are listed in Table 2.2.

Histochemical Staining

GUS staining was performed as described (Jefferson et al., 1987; Rodrigues-Pousada et al., 1993). Inflorescences were fixed in 90% cold acetone for 15-20 min and rinsed with the rinse solution (50mM $NaPO_4$ pH7.2, 0.5mM $K_3Fe(CN)_6$, 0.5mM $K_4Fe(CN)_6$). Then, they were vacuum-infiltrated in the staining solution (50mM $NaPO_4$ pH7.2, 0.5mM $K_3Fe(CN)_6$, 0.5mM $K_4Fe(CN)_6$, 2mM X-Gluc)) and incubated at 37°C.

ATH1 Affymetrix Microarray Analysis

GeneChip arrays were hybridized according to the manufacturer's instructions (Affymetrix). Data analysis was done according to Horanetal. (2008). Normalization of raw intensities across all probe sets was performed in R using RMA algorithms. To calculate P-values for increases or decreases in expression, the Wilcoxon signed-rank test was applied to each pair of chips after normalization using R&Bio Conductor (developed by Dr. Thomas Girke). A P-value of ≤ 0.05 in combination with a two-fold difference was used to define changes in gene expression.

REFERENCES

Adenot, X., Elmayan, T., Lauressergues, D., Boutet, S., Bouche, N., Gasciolli, V., and Vaucheret, H. (2006). *DRB4*-dependent TAS3 trans-acting siRNAs control leaf morphology through AGO7. Curr Biol *16*, 927-932.

Allen, E., Xie, Z.X., Gustafson, A.M., and Carrington, J.C. (2005). microRNA-directed phasing during trans-acting siRNA biogenesis in plants. Cell *121*, 207-221.

Ambros, V., Lee, R.C., Lavanway, A., Williams, P.T., and Jewell, D. (2003). MicroRNAs and other tiny endogenous RNAs in C-elegans. Curr Biol *13*, 807-818.

Ansari, S.A., He, Q.Y., and Morse, R.H. (2009). Mediator complex association with constitutively transcribed genes in yeast. Proc Natl Acad Sci U S A *106*, 16734-16739.

Asturias, F.J., Jiang, Y.W., Myers, L.C., Gustafsson, C.M., and Kornberg, R.D. (1999). Conserved structures of mediator and RNA polymerase II holoenzyme. Science *283*, 985-987.

Autran, D., Jonak, C., Belcram, K., Beemster, G.T.S., Kronenberger, J., Grandjean, O., Inze, D., and Traas, J. (2002). Cell numbers and leaf development in Arabidopsis: a functional analysis of the *STRUWWELPETER* gene. EMBO J *21*, 6036-6049.

Backstrom, S., Elfving, N., Nilsson, R., Wingsle, G., and Bjorklund, S. (2007). Purification of a plant mediator from Arabidopsis thaliana identifies PFT1 as the Med25 subunit. Mol Cell *26*, 717-729.

Baek, H.J., Kang, Y.K., and Roeder, R.G. (2006). Human mediator enhances basal transcription by facilitating recruitment of transcription factor IIB during preinitiation complex assembly. J Biol Chem *281*, 15172-15181.

Bari, R., Pant, B.D., Stitt, M., and Scheible, W.R. (2006). *PHO2*, microRNA399, and *PHR1* define a phosphate-signaling pathway in plants. Plant Physiol *141*, 988-999.

Baumberger, N., and Baulcombe, D.C. (2005). Arabidopsis *ARGONAUTE1* is an RNA slicer that selectively recruits rnicroRNAs and short interfering RNAs. Proc Natl Acad Sci U S A *102*, 11928-11933.

Borsani, O., Zhu, J.H., Verslues, P.E., Sunkar, R., and Zhu, J.K. (2005). Endogenous siRNAs derived from a pair of natural cis-antisense transcripts regulate salt tolerance in Arabidopsis. Cell *123*, 1279-1291.

Brodersen, P., Sakvarelidze-Achard, L., Bruun-Rasmussen, M., Dunoyer, P., Yamamoto, Y.Y., Sieburth, L., and Voinnet, O. (2008). Widespread translational inhibition by plant miRNAs and siRNAs. Science *320*, 1185-1190.

Cai, X.Z., Hagedorn, C.H., and Cullen, B.R. (2004). Human microRNAs are processed from capped, polyadenylated transcripts that can also function as mRNAs. RNA *10*, 1957-1966.

Carlson, M., Osmond, B.C., and Botstein, D. (1981). Mutations of yeast defective in sucrose utilization. Genetics *98*, 25-40.

Casamassimi, A., and Napoli, C. (2007). Mediator complexes and eukaryotic transcription regulation: An overview. Biochimie *89*, 1439-1446.

Cerdan, P.D., and Chory, J. (2003). Regulation of flowering time by light quality. Nature *423*, 881-885.

Chen, X. (2009). Small RNAs and Their Roles in Plant Development. Annu Rev Cell Dev Biol *25*, 21-44.

Chi, Y., Huddleston, M.J., Zhang, X.L., Young, R.A., Annan, R.S., Carr, S.A., and Deshaies, R.J. (2001). Negative regulation of Gcn4 and Msn2 transcription factors by Srb10 cyclin-dependent kinase. Genes Dev *15*, 1078-1092.

Chitwood, D.H., Nogueira, F.T.S., Howell, M.D., Montgomery, T.A., Carrington, J.C., and Timmermans, M.C.P. (2009). Pattern formation via small RNA mobility. Genes Dev *23*, 549-554.

Dhawan, R., Luo, H.L., Foerster, A.M., AbuQamar, S., Du, H.N., Briggs, S.D., Scheid, O.M., and Mengiste, T. (2009). HISTONE MONOUBIQUITINATION1 Interacts with a Subunit of the Mediator Complex and Regulates Defense against Necrotrophic Fungal Pathogens in Arabidopsis. Plant Cell *21*, 1000-1019.

Dong, Z., Han, M.H., and Fedoroff, N. (2008). The RNA-binding proteins HYL1 and SE promote accurate in vitro processing of pri-miRNA by DCL1. Proc Natl Acad Sci U S A *105*, 9970-9975.

Dotson, M.R., Yuan, C.X., Roeder, R.G., Myers, L.C., Gustafsson, C.M., Jiang, Y.W., Li, Y., Kornberg, R.D., and Asturias, F.J. (2000). Structural organization of yeast and mammalian mediator complexes. Proc Natl Acad Sci U S A *97*, 14307-14310.

El-Shami, M., Pontier, D., Lahmy, S., Braun, L., Picart, C., Vega, D., Hakimi, M.A., Jacobsen, S.E., Cooke, R., and Lagrange, T. (2007). Reiterated WG/GW motifs form functionally and evolutionarily conserved ARGONAUTE-binding platforms in RNAi-related components. Genes Dev *21*, 2539-2544.

Fagard, M., Boutet, S., Morel, J.B., Bellini, C., and Vaucheret, H. (2000). AGO1, QDE-2, and RDE-1 are related proteins required for post-transcriptional gene silencing in plants, quelling in fungi, and RNA interference in animals. Proc Natl Acad Sci U S A *97*, 11650-11654.

Fahlgren, N., Montgomery, T.A., Howell, M.D., Allen, E., Dvorak, S.K., Alexander, A.L., and Carrington, J.C. (2006). Regulation of *AUXIN RESPONSE FACTOR3* by TAS3 ta-siRNA affects developmental timing and patterning in Arabidopsis. Curr Biol *16*, 939-944.

Fan, X., and Struhl, K. (2009). Where Does Mediator Bind In Vivo? PLoS One *4*, Article No.: e5029.

Fan, X.C., Chou, D.M., and Struhl, K. (2006). Activator-specific recruitment of Mediator in vivo. Nat Struct Mol Biol *13*, 117-120.

Fang, Y.D., and Spector, D.L. (2007). Identification of nuclear dicing bodies containing proteins for microRNA biogenesis in living Arabidopsis plants. Curr Biol *17*, 818-823.

Franco-Zorrilla, J.M., Valli, A., Todesco, M., Mateos, I., Puga, M.I., Rubio-Somoza, I., Leyva, A., Weigel, D., Garcia, J.A., and Paz-Ares, J. (2007). Target mimicry provides a new mechanism for regulation of microRNA activity. Nat Genet *39*, 1033-1037.

Fujioka, Y., Utsumi, M., Ohba, Y., and Watanabe, Y. (2007). Location of a possible miRNA processing site in SmD3/SmB nuclear bodies in arabidopsis. Plant Cell Physiol *48*, 1243-1253.

Garcia, D., Collier, S.A., Byrne, M.E., and Martienssen, R.A. (2006). Specification of leaf polarity in Arabidopsis via the trans-acting siRNA pathway. Curr Biol *16*, 933-938.

Gonzalez, D., Bowen, A.J., Carroll, T.S., and Conlan, R.S. (2007). The transcription corepressor LEUNIG interacts with the histone deacetylase HDA19 and mediator components MED14 (SWP) and CDK8 (HEN3) to repress transcription. Mol Cell Biol *27*, 5306-5315.

Gregory, B.D., O'Malley, R.C., Lister, R., Urich, M.A., Tonti-Filippini, J., Chen, H., Millar, A.H., and Ecker, J.R. (2008). A link between RNA metabolism and silencing affecting Arabidopsis development. Dev Cell *14*, 854-866.

Guglielmi, B., van Berkum, N.L., Klapholz, B., Bijma, T., Boube, M., Boschiero, C., Bourbon, H.M., Holstege, F.C.P., and Werner, M. (2004). A high resolution protein interaction map of the yeast Mediator complex. Nucleic Acids Res *32*, 5379-5391.

Hallberg, M., Polozkov, G.V., Hu, G.Z., Beve, J., Gustafsson, C.M., Ronne, H., and Bjorklund, S. (2004). Site-specific Srb10-dependent phosphorylation of the yeast mediator subunit Med2 regulates gene expression from the 2-mu m plasmid. Proc Natl Acad Sci U S A *101*, 3370-3375.

Hamilton, A.J., and Baulcombe, D.C. (1999). A species of small antisense RNA in posttranscriptional gene silencing in plants. Science *286*, 950-952.

Han, M.H., Goud, S., Song, L., and Fedoroff, N. (2004). The Arabidopsis double-stranded RNA-binding protein HYL1 plays a role in microRNA-mediated gene regulation. Proc Natl Acad Sci U S A *101*, 1093-1098.

Han, S.J., Lee, J.S., Kang, J.S., and Kim, Y.J. (2001). Med9/Cse2 and Gal11 modules are required for transcriptional repression of distinct group of genes. J Biol Chem *276*, 37020-37026.

Hengartner, C.J., Myer, V.E., Liao, S.M., Wilson, C.J., Koh, S.S., and Young, R.A. (1998). Temporal regulation of RNA polymerase II by *Srb10* and *Kin28* cyclin-dependent kinases. Mol Cell *2*, 43-53.

Heo, I., Joo, C., Cho, J., Ha, M., Han, J.J., and Kim, V.N. (2008). *Lin28* Mediates the Terminal Uridylation of let-7 Precursor MicroRNA. Mol Cell *32*, 276-284.

Herr, A.J., Jensen, M.B., Dalmay, T., and Baulcombe, D.C. (2005). RNA polymerase IV directs silencing of endogenous DNA. Science *308*, 118-120.

Hirst, M., Kobor, M.S., Kuriakose, N., Greenblatt, J., and Sadowski, I. (1999). GAL4 is regulated by the RNA polymerase II holoenzyme-associated cyclin-dependent protein kinase SRB10/CDK8. Mol Cell *3*, 673-678.

Holstege, F.C.P., Jennings, E.G., Wyrick, J.J., Lee, T.I., Hengartner, C.J., Green, M.R., Golub, T.R., Lander, E.S., and Young, R.A. (1998). Dissecting the regulatory circuitry of a eukaryotic genome. Cell *95*, 717-728.

Horan, K., Jang, C., Bailey-Serres, J., Mittler, R., Shelton, C., Harper, J.F., Zhu, J.K., Cushman, J.C., Gollery, M., and Girke, T. (2008). Annotating genes of known and unknown function by large-scale coexpression analysis. Plant Physiol *147*, 41-57.

Huang, L.F., Jones, A.M.E., Searle, I., Patel, K., Vogler, H., Hubner, N.C., and Baulcombe, D.C. (2009). An atypical RNA polymerase involved in RNA silencing shares small subunits with RNA polymerase II. Nat Struct Mol Biol *16*, 91-93.

Hunter, C., Willmann, M.R., Wu, G., Yoshikawa, M., de la Luz Gutierrez-Nava, M., and Poethig, R.S. (2006). Trans-acting siRNA-mediated repression of *ETTIN* and *ARF4* regulates heteroblasty in Arabidopsis. Development *133*, 2973-2981.

Jefferson, R.A., Kavanagh, T.A., and Bevan, M.W. (1987). GUS fusions - *BETA-GLUCURONIDASE* as a sensitive and versatile gene fusion marker in higher-plants. EMBO J *6*, 3901-3907.

Kang, J.S., Kim, S.H., Hwang, M.S., Han, S.J., Lee, Y.C., and Kim, Y.J. (2001). The structural and functional organization of the yeast mediator complex. J Biol Chem *276*, 42003-42010.

Kanno, T., Huettel, B., Mette, M.F., Aufsatz, W., Jaligot, E., Daxinger, L., Kreil, D.P., Matzke, M., and Matzke, A.J.M. (2005). Atypical RNA polymerase subunits required for RNA-directed DNA methylation. Nat Genet *37*, 761-765.

Katiyar-Agarwal, S., Morgan, R., Dahlbeck, D., Borsani, O., Villegas, A., Zhu, J.K., Staskawicz, B.J., and Jin, H.L. (2006). A pathogen-inducible endogenous siRNA in plant immunity. Proc Natl Acad Sci USA *103*, 18002-18007.

Kawashima, C.G., Yoshimoto, N., Maruyama-Nakashita, A., Tsuchiya, Y.N., Saito, K., Takahashi, H., and Dalmay, T. (2009). Sulphur starvation induces the expression of microRNA-395 and one of its target genes but in different cell types. Plant J *57*, 313-321.

Kidd, B.N., Edgar, C.I., Kumar, K.K., Aitken, E.A., Schenk, P.M., Manners, J.M., and Kazan, K. (2009). The Mediator Complex Subunit PFT1 Is a Key Regulator of Jasmonate-Dependent Defense in Arabidopsis. Plant Cell *21*, 2237-2252.

Kim, V.N., Han, J., and Siomi, M.C. (2009). Biogenesis of small RNAs in animals. Nat Rev Mol Cell Biol *10*, 126-139.

Lahmy, S., Pontier, D., Cavel, E., Vega, D., El-Shami, M., Kanno, T., and Lagrange, T. (2009). PolV(PolIVb) function in RNA-directed DNA methylation requires the conserved active site and an additional plant-specific subunit. Proc Natl Acad Sci U S A *106*, 941-946.

Lariviere, L., Geiger, S., Hoeppner, S., Rother, S., Strasser, K., and Cramer, P. (2006). Structure and TBP binding of the Mediator head subcomplex Med8-Med18-Med20. Nat Struct Mol Biol *13*, 895-901.

Laubinger, S., Sachsenberg, T., Zeller, G., Busch, W., Lohmann, J.U., Rascht, G., and Weigel, D. (2008). Dual roles of the nuclear cap-binding complex and *SERRATE* in pre-mRNA splicing and microRNA processing in Arabidopsis thaliana. Proc Natl Acad Sci U S A *105*, 8795-8800.

Lee, Y., Kim, M., Han, J.J., Yeom, K.H., Lee, S., Baek, S.H., and Kim, V.N. (2004). MicroRNA genes are transcribed by RNA polymerase II. EMBO J *23*, 4051-4060.

Lee, Y.C., Park, J.M., Min, S., Han, S.J., and Kim, Y.J. (1999). An activator binding module of yeast RNA polymerase II holoenzyme. Mol Cell Biol *19*, 2967-2976.

Li, C.F., Pontes, O., El-Shami, M., Henderson, I.R., Bernatavichute, Y.V., Chan, S.W.L., Lagrange, T., Pikaard, C.S., and Jacobsen, S.E. (2006). An ARGONAUTE4-containing nuclear processing center colocalized with Cajal bodies in Arabidopsis thaliana. Cell *126*, 93-106.

Li, J.J., Yang, Z.Y., Yu, B., Liu, J., and Chen, X. (2005). Methylation protects miRNAs and siRNAs from a 3 '-end uridylation activity in Arabildopsis. Curr Biol *15*, 1501-1507.

Liu, Y., Kung, C., Fishburn, J., Ansari, A.Z., Shokat, K.M., and Hahn, S. (2004). Two cyclin-dependent kinases promote RNA polymerase II transcription and formation of the scaffold complex. Mol Cell Biol *24*, 1721-1735.

Liu, Z.C., and Meyerowitz, E.M. (1995). *LEUNIG* regulates *AGAMOUS* expression in Arabidopsis flowers. Development *121*, 975-991.

Llave, C., Kasschau, K.D., Rector, M.A., and Carrington, J.C. (2002). Endogenous and silencing-associated small RNAs in plants. Plant Cell *14*, 1605-1619.

Lobbes, D., Rallapalli, G., Schmidt, D.D., Martin, C., and Clarke, J. (2006). *SERRATE*: a new player on the plant microRNA scene. EMBO Rep *7*, 1052-1058.

Lu, C., Tej, S.S., Luo, S.J., Haudenschild, C.D., Meyers, B.C., and Green, P.J. (2005). Elucidation of the small RNA component of the transcriptome. Science *309*, 1567-1569.

Malik, S., and Roeder, R.G. (2000). Transcriptional regulation through Mediator-like coactivators in yeast and metazoan cells. Trends Biochem Sci *25*, 277-283.

Megraw, M., Baev, V., Rusinov, V., Jensen, S.T., Kalantidis, K., and Hatzigeorgiou, A.G. (2006). MicroRNA promoter element discovery in Arabidopsis. RNA *12*, 1612-1619.

Mittler, G., Kremmer, E., Timmers, H.T.M., and Meisterernst, M. (2001). Novel critical role of a human Mediator complex for basal RNA polymerase II transcription. EMBO Rep *2*, 808-813.

Mosher, R.A., Schwach, F., Studhollme, D., and Baulcombe, D.C. (2008). PolIVb influences RNA-directed DNA-methylation independently of its role in siRNA biogenesis. Proc Natl Acad Sci U S A *105*, 3145-3150.

Myers, L.C., Gustafsson, C.M., Hayashibara, K.C., Brown, P.O., and Kornberg, R.D. (1999). Mediator protein mutations that selectively abolish activated transcription. Proc Natl Acad Sci U S A *96*, 67-72.

Naar, A.M., Taatjes, D.J., Zhai, W.G., Nogales, E., and Tjian, R. (2002). Human CRSP interacts with RNA polymerase IICTD and adopts a specific CTD-bound conformation. Genes Dev *16*, 1339-1344.

Neigeborn, L., and Carlson, M. (1984). Genes affecting the regulation of *SUC2* gene-expression by glucose repression in Saccharomyces-cerevisiae. Genetics *108*, 845-858.

Nelson, C., Goto, S., Lund, K., Hung, W., and Sadowski, I. (2003). *Srb10/Cdk8* regulates yeast filamentous growth by phosphorylating the transcription factor Ste12. Nature *421*, 187-190.

Onodera, Y., Haag, J.R., Ream, T., Nunes, P.C., Pontes, O., and Pikaard, C.S. (2005). Plant nuclear RNA polymerase IV mediates siRNA and DNA methylation-dependent heterochromatin formation. Cell *120*, 613-622.

Park, J.M., Kim, H.S., Han, S.J., Hwang, M.S., Lee, Y.C., and Kim, Y.J. (2000). In vivo requirement of activator-specific binding targets of mediator. Mol Cell Biol *20*, 8709-8719.

Park, M.Y., Wu, G., Gonzalez-Sulser, A., Vaucheret, H., and Poethig, R.S. (2005). Nuclear processing and export of microRNAs in Arabidopsis. Proc Natl Acad Sci U S A *102*, 3691-3696.

Park, W., Li, J.J., Song, R.T., Messing, J., and Chen, X. (2002). CARPEL FACTORY, a Dicer homolog, and HEN1, a novel protein, act in microRNA metabolism in Arabidopsis thaliana. Curr Biol *12*, 1484-1495.

Peragine, A., Yoshikawa, M., Wu, G., Albrecht, H.L., and Poethig, R.S. (2004). *SGS3* and *SGS2/SDE1/RDR6* are required for juvenile development and the production of trans-acting siRNAs in Arabidopsis. Genes Dev *18*, 2368-2379.

Qi, Y., Denli, A.M., and Hannon, G.J. (2005). Biochemical specialization within Arabidopsis RNA silencing pathways. Mol Cell *19*, 421-428.

Qi, Y.J., He, X.Y., Wang, X.J., Kohany, O., Jurka, J., and Hannon, G.J. (2006). Distinct catalytic and non-catalytic roles of *ARGONAUTE4* in RNA-directed DNA methylation. Nature *443*, 1008-1012.

Rajagopalan, R., Vaucheret, H., Trejo, J., and Bartel, D.P. (2006). A diverse and evolutionarily fluid set of microRNAs in Arabidopsis thaliana. Genes Dev *20*, 3407-3425.

Ramachandran, V., and Chen, X. (2008). Degradation of microRNAs by a family of exoribonucleases in Arabidopsis. Science *321*, 1490-1492.

Ream, T.S., Haag, J.R., Wierzbicki, A.T., Nicora, C.D., Norbeck, A.D., Zhu, J.K., Hagen, G., Guilfoyle, T.J., Pasa-Tolic, L., and Pikaard, C.S. (2009). Subunit Compositions of the RNA-Silencing Enzymes Pol IV and Pol V Reveal Their Origins as Specialized Forms of RNA Polymerase II. Mol Cell *33*, 192-203.

Reese, J.C. (2003). Basal transcription factors. Curr Opin Genet Dev *13*, 114-118.

Reinhart, B.J., Weinstein, E.G., Rhoades, M.W., Bartel, B., and Bartel, D.P. (2002). MicroRNAs in plants. Genes Dev *16*, 1616-1626.

Rodriguespousada, R.A., Derycke, R., Dedonder, A., Vancaeneghem, W., Engler, G., Vanmontagu, M., and Vanderstraeten, D. (1993). The Arabidopsis *1-AMINOCYCLOPROPANE-1-CARBOXYLATE SYNTHASE GENE-1* is expressed during early development. Plant Cell *5*, 897-911.

Sato, S., Tomomori-Sato, C., Banks, C.A.S., Parmely, T.J., Sorokina, I., Brower, C.S., Conaway, R.C., and Conaway, J.W. (2003). A mammalian homolog of Drosophila melanogaster transcriptional coactivator intersex is a subunit of the mammalian mediator complex. J Biol Chem *278*, 49671-49674.

Sato, S., Tomomori-Sato, C., Banks, C.A.S., Sorokina, I., Parmely, T.J., Kong, S.E., Jin, J.J., Cai, Y., Lane, W.S., Brower, C.S.*, et al.* (2003). Identification of mammalian mediator subunits with similarities to yeast mediator subunits Srb5, Srb6, Med11, and Rox3. J Biol Chem *278*, 15123-15127.

Sikorski, T.W., and Buratowski, S. (2009). The basal initiation machinery: beyond the general transcription factors. Curr Opin Cell Biol *21*, 344-351.

Simchen, G., Winston, F., Styles, C.A., and Fink, G.R. (1984). *TY*-mediated gene-expression of the *LYS2* and *HIS4* genes of Saccharomyces-cerevisiae is controlled by the same *SPT* genes. Proc Natl Acad Sci U S A *81*, 2431-2434.

Smith, L.M., Pontes, O., Searle, L., Yelina, N., Yousafzai, F.K., Herr, A.J., Pikaard, C.S., and Baulcombe, D.C. (2007). An SNF2 protein associated with nuclear RNA silencing and the spread of a silencing signal between cells in Arabidopsis. Plant Cell *19*, 1507-1521.

Song, L., Han, M.H., Lesicka, J., and Fedoroff, N. (2007). Arabidopsis primary microRNA processing proteins HYL1 and DCL1 define a nuclear body distinct from the Cajal body. Proc Natl Acad Sci U S A *104*, 5437-5442.

Stern, M., Jensen, R., and Herskowitz, I. (1984). 5 *SWI* genes are required for expression of the *HO* gene in yeast.. J Mol Biol *178*, 853-868.

Sun, X.Q., Zhang, Y., Cho, H., Rickert, P., Lees, E., Lane, W., and Reinberg, D. (1998). NAT, a human complex containing Srb polypeptides that functions as a negative regulator of activated transcription. Mol Cell *2*, 213-222.

Suzuki, Y., Nogi, Y., Abe, A., and Fukasawa, T. (1988). GAL11 protein, an auxiliary transcription activator for genes encoding galactose-metabolizing enzymes in Saccharomyces-cerevisiae. Mol Cell Biol *8*, 4991-4999.

Taatjes, D.J., Marr, M.T., and Tjian, R. (2004). Opinion - Regulatory diversity among metazoan co-activator complexes. Nat Rev Mol Cell Biol *5*, 403-410.

Taatjes, D.J., Schneider-Poetsch, T., and Tjian, R. (2004). Distinct conformational states of nuclear receptor-bound CRSP-Med complexes. Nat Struct Mol Biol *11*, 664-671.

Takagi, Y., Calero, G., Komori, H., Brown, J.A., Ehrensberger, A.H., Hudmon, A., Asturias, F., and Kornberg, R.D. (2006). Head module control of mediator interactions. Mol Cell *23*, 355-364.

Thomas, M.C., and Chiang, C.M. (2006). The general transcription machinery and general cofactors. Crit Rev Biochem Mol Biol *41*, 105-178.

Thompson, C.M., and Young, R.A. (1995). General requirement for RNA-Polymerase-II holoenzymes in-vivo. Proc Natl Acad Sci U S A *92*, 4587-4590.

van de Peppel, J., Kettelarij, N., van Bakel, H., Kockelkorn, T., van Leenen, D., and Holstege, F.C.P. (2005). Mediator expression profiling epistasis reveals a signal transduction pathway with antagonistic submodules and highly specific downstream targets. Mol Cell *19*, 511-522.

Vaucheret, H. (2008). Plant *ARGONAUTES*. Trends Plant Sci *13*, 350-358.

Vaucheret, H., Mallory, A.C., and Bartel, D.P. (2006). *AGO1* homeostasis entails coexpression of MIR168 and *AGO1* and preferential stabilization of miR168 by *AGO1*. Mol Cell *22*, 129-136.

Vaucheret, H., Vazquez, F., Crete, P., and Bartel, D.P. (2004). The action of *ARGONAUTE1* in the miRNA pathway and its regulation by the miRNA pathway are crucial for plant development. Genes Dev *18*, 1187-1197.

Vazquez, F., Gasciolli, V., Crete, P., and Vaucheret, H. (2004). The nuclear dsRNA binding protein HYL1 is required for MicroRNA accumulation and plant development, but not posttranscriptional transgene silencing. Curr Biol *14*, 346-351.

Vazquez, F., Vaucheret, H., Rajagopalan, R., Lepers, C., Gasciolli, V., Mallory, A.C., Hilbert, J.L., Bartel, D.P., and Crete, P. (2004). Endogenous trans-acting siRNAs regulate the accumulation of Arabidopsis mRNAs. Mol Cell *16*, 69-79.

Vincent, O., Kuchin, S., Hong, S.P., Townley, R., Vyas, V.K., and Carlson, M. (2001). Interaction of the Srb10 kinase with Sip4, a transcriptional activator of gluconeogenic genes in Saccharomyces cerevisiae. Mol Cell Biol *21*, 5790-5796.

Viswanathan, S.R., Daley, G.Q., and Gregory, R.I. (2008). Selective blockade of MicroRNA processing by Lin28. Science *320*, 97-100.

Wang, H., Chua, N.H., and Wang, X.J. (2006). Prediction of trans-antisense transcripts in Arabidopsis thaliana. Genome Biol *7*, 11.

Wang, W.M., and Chen, X. (2004). *HUA ENHANCER3* reveals a role for a cyclin-dependent protein kinase in the specification of floral organ identity in Arabidopsis. Development *131*, 3147-3156.

Wang, X.J., Gaasterland, T., and Chua, N.H. (2005). Genome-wide prediction and identification of cis-natural antisense transcripts in Arabidopsis thaliana. Genome Biol *6*, 11.

Wierzbicki, A.T., Haag, J.R., and Pikaard, C.S. (2008). Noncoding Transcription by RNA Polymerase Pol IVb/Pol V Mediates Transcriptional Silencing of Overlapping and Adjacent Genes. Cell *135*, 635-648.

Wollenberg, A.C., Strasser, B., Cerdan, P.D., and Amasino, R.M. (2008). Acceleration of flowering during shade avoidance in Arabidopsis alters the aalance between *FLOWERING LOCUS C*-mediated repression and photoperiodic induction of flowering. Plant Physiol *148*, 1681-1694.

Wu, S.Y., Zhou, T.Y., and Chiang, C.M. (2003). Human mediator enhances activator-facilitated recruitment of RNA polymerase II and promoter recognition by TATA-binding protein (TBP) independently of TBP-associated factors. Mol Cell Biol *23*, 6229-6242.

Xie, Z.X., Allen, E., Fahlgren, N., Calamar, A., Givan, S.A., and Carrington, J.C. (2005). Expression of Arabidopsis *MIRNA* genes. Plant Physiol *138*, 2145-2154.

Xie, Z.X., Allen, E., Wilken, A., and Carrington, J.C. (2005). DICER-LIKE 4 functions in trans-acting small interfering RNA biogenesis and vegetative phase change in Arabidopsis thaliana. Proc Natl Acad Sci U S A *102*, 12984-12989.

Xie, Z.X., Johansen, L.K., Gustafson, A.M., Kasschau, K.D., Lellis, A.D., Zilberman, D., Jacobsen, S.E., and Carrington, J.C. (2004). Genetic and functional diversification of small RNA pathways in plants. PLoS Biol *2*, 642-652.

Yamada, K., Lim, J., Dale, J.M., Chen, H.M., Shinn, P., Palm, C.J., Southwick, A.M., Wu, H.C., Kim, C., Nguyen, M.*, et al.* (2003). Empirical analysis of transcriptional activity in the Arabidopsis genome. Science *302*, 842-846.

Yamasaki, H., Hayashi, M., Fukazawa, M., Kobayashi, Y., and Shikanai, T. (2009). *SQUAMOSA* Promoter Binding Protein-Like7 Is a Central Regulator for Copper Homeostasis in Arabidopsis. Plant Cell *21*, 347-361.

Yang, L., Liu, Z.Q., Lu, F., Dong, A.W., and Huang, H. (2006). *SERRATE* is a novel nuclear regulator in primary microRNA processing in Arabidopsis. Plant J *47*, 841-850.

Yoshikawa, M., Peragine, A., Park, M.Y., and Poethig, R.S. (2005). A pathway for the biogenesis of trans-acting siRNAs in Arabidopsis. Genes Dev *19*, 2164-2175.

Yu, B., Bi, L., Zheng, B.L., Ji, L.J., Chevalier, D., Agarwal, M., Ramachandran, V., Li, W.X., Lagrange, T., Walker, J.C.*, et al.* (2008). The *FHA* domain proteins DAWDLE in Arabidopsis and SNIP1 in humans act in small RNA biogenesis. Proc Natl Acad Sci U S A *105*, 10073-10078.

Yu, B., Yang, Z.Y., Li, J.J., Minakhina, S., Yang, M.C., Padgett, R.W., Steward, R., and Chen, X. (2005). Methylation as a crucial step in plant microRNA biogenesis. Science *307*, 932-935.

Zhang, X.Y., Henderson, I.R., Lu, C., Green, P.J., and Jacobsen, S.E. (2007). Role of RNA polymerase IV in plant small RNA metabolism. Proc Natl Acad Sci U S A *104*, 4536-4541.

Zheng, X.W., Zhu, J.H., Kapoor, A., and Zhu, J.K. (2007). Role of Arabidopsis *AGO6* in siRNA accumulation, DNA methylation and transcriptional gene silencing. EMBO J *26*, 1691-1701.

Zilberman, D., Cao, X.F., and Jacobsen, S.E. (2003). *ARGONAUTE4* control of locus-specific siRNA accumulation and DNA and histone methylation. Science *299*, 716-719.

Figure 2.1 Phenotypes of *med20a*, *med17* and *med18* mutants

(A-D) 8-day-old seedlings from Col (A), *med20a* (B), *med17* (C) and *med18* (D).

All Three *med* mutants have three cotyledons and three first true leaves as compared to Col with two cotyledons and a pair of first true leaves.

(E-H) 12-day-old seedlings from Col (E), *med20a* (F), *med17* (G) and *med18* (H).

The Overall plant size is smaller than that in Col in all three *med* mutants. Occasionally, split cotyledons are observed (arrowheads).

(I) Siliques from Col and *med20a*. *med20a* siliques are shorter and deformed.

A
B
C
D
E
F
G
H
I
Col
med20a

Figure 2.2 Structures of the Mediator genes

(A) A schematic diagram of *MED20* homologs: *MED20a*, *MED20d* and *MED20c*. The Star indicates the mutation causing a premature stop codon in the *med20a* mutant. Black rectangles represent exons. *MED20a* and *MED20b* are composed of 3 exons showing 93% identity at the nucleotide level. *MED20c* only encodes the conserved second exon compared to *MED20a* and *MED20b*.

(B) A schematic diagram of T-DNA insertion lines of *MED17* and *MED18*. Red triangles represent T-DNA insertions. The T-DNA lines SALK_102813 and SALK_027178 have T-DNA insertions in the seventh exon of *MED17* and the second intron of *MED18*, respectively.

A


med20a
*
MED20a
MED20b
MED20c

B

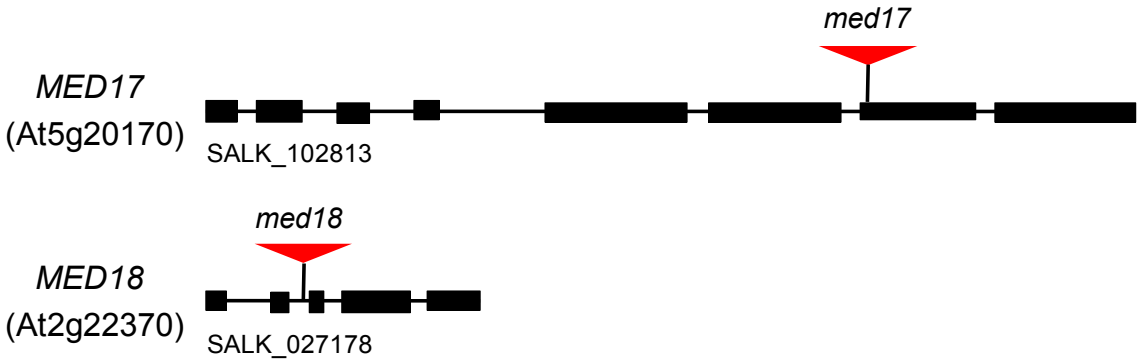
med17
MED17
(At5g20170)
SALK_102813
med18
MED18
(At2g22370)
SALK_027178

Figure 2.3 The accumulation of miRNAs and a ta-siRNA in *med* mutants

(A) The accumulation of miRNAs and a ta-siRNA was determined in Col and the *med20a* mutant by small RNA Northern blotting. Overall small RNA accumulation was reduced in *med20a*.

(B) The accumulation of several miRNAs was determined in Col, *med17* and *med18* by small RNA Northern blotting. miRNA accumulation was reduced in *med17* and *med18*.

(A, B) Total RNAs were extracted from inflorescences. The levels of each miRNA were normalized to those of U6 and compared to Col. The numbers indicate the relative abundance of small RNAs.

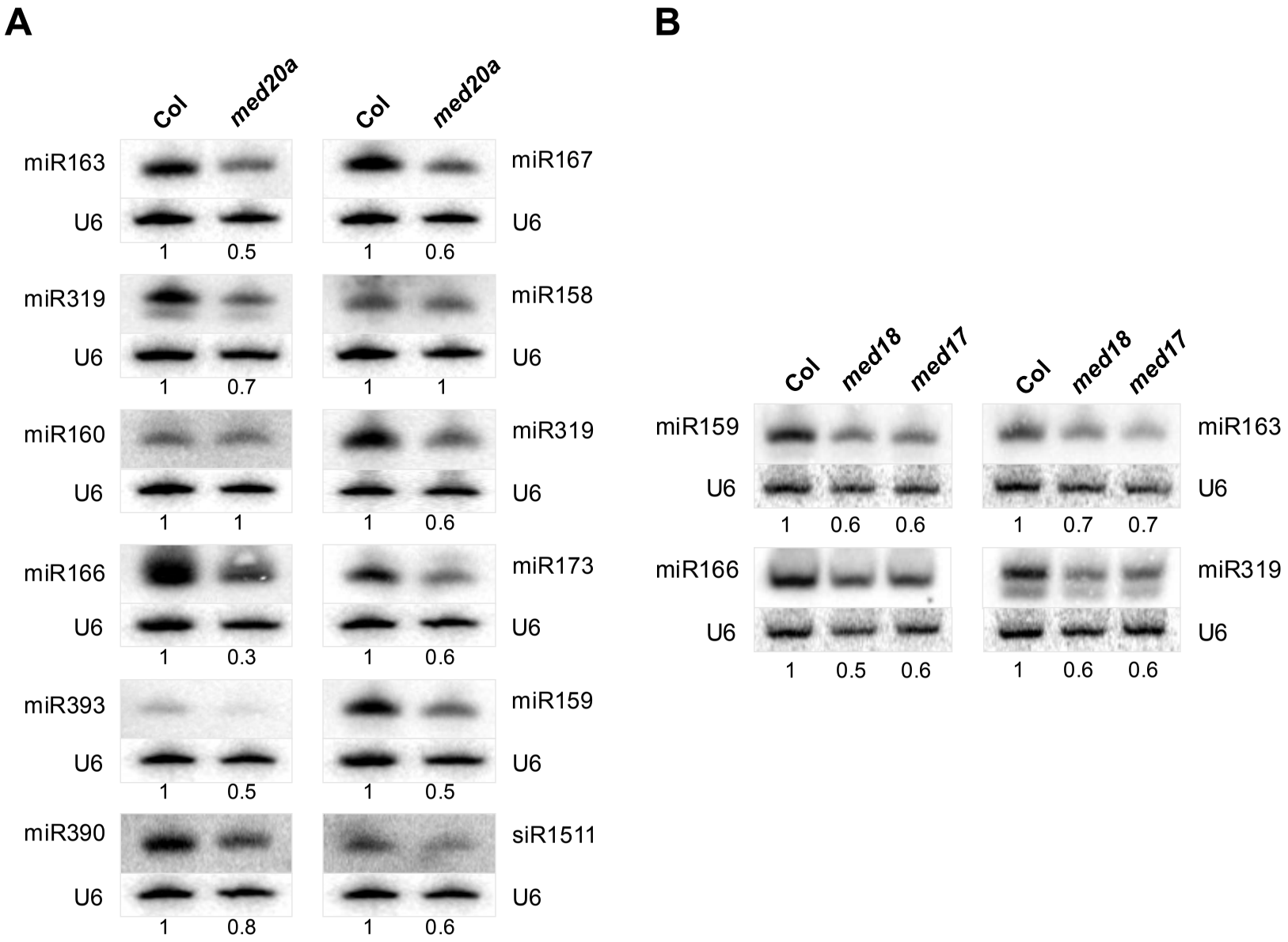
A
Col
med20a
Col
med20a
miR163
U6
1 0.5
miR167
U6
1 0.6
miR319
U6
1 0.7
miR158
U6
1 1
miR160
U6
1 1
miR319
U6
1 0.6
miR166
U6
1 0.3
miR173
U6
1 0.6
miR393
U6
1 0.5
miR159
U6
1 0.5
miR390
U6
1 0.8
siR1511
U6
1 0.6
B
Col
med18
med17
Col
med18
med17
miR159
U6
1 0.6 0.6
miR163
U6
1 0.7 0.7
miR166
U6
1 0.5 0.6
miR319
U6
1 0.6 0.6

Figure 2.4 The accumulation of pri-miRNAs in the *med20a* mutant

(A) The accumulation of several pri-miRNAs was determined by real-time RT-PCR in Col and the *med20a* mutant. The levels of pri-miRNAs were reduced in the *med20a* mutant. The RNAs were extracted from inflorescences. The pri-miRNA levels were normalized to those of *UBIQUITIN 5* and compared to Col.

(B) GUS expression driven by the *MIR167a* promoter was monitored in *med20a*. GUS expression in the sepals of the old flowers was reduced in *med20a* compared to Col (arrowheads).

A

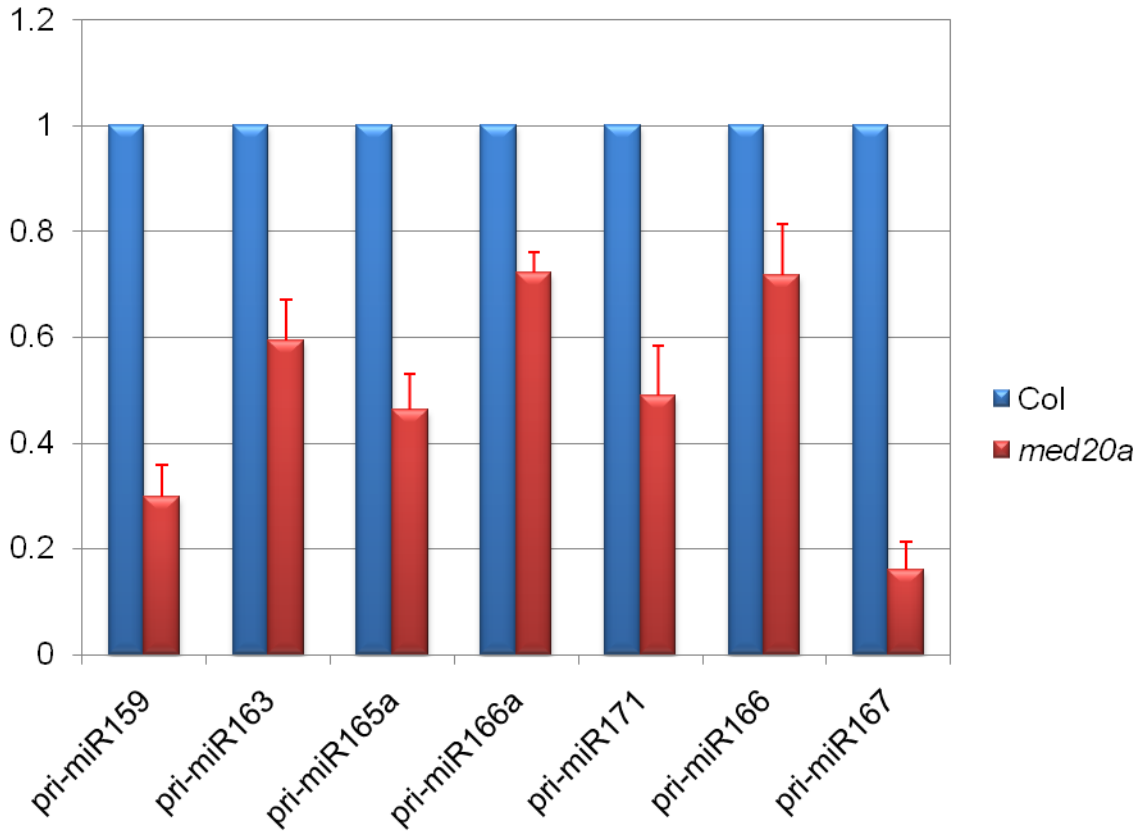

B

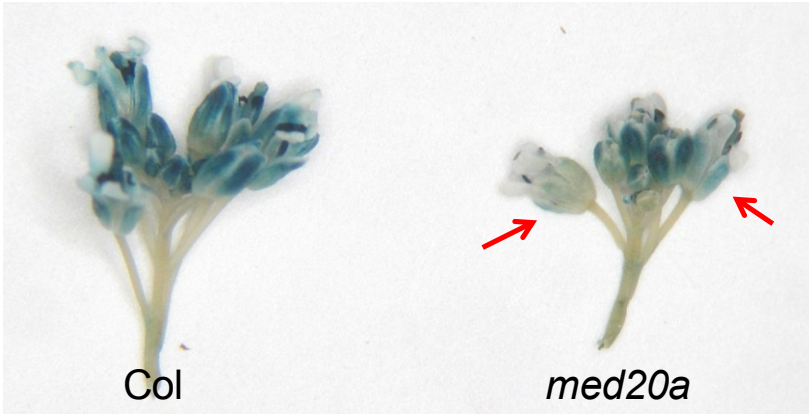

pMIR167a::GUS

Figure 2.5 The accumulation of endogenous hc-siRNAs in the *med20a* mutant

The accumulation of several endogenous hc-siRNAs was examined in the *med20a* mutant by small RNA Northern blotting. In general, the accumulation of endogenous hc-siRNAs was not affected in the *med20a* mutant. The RNAs were extracted from inflorescences.

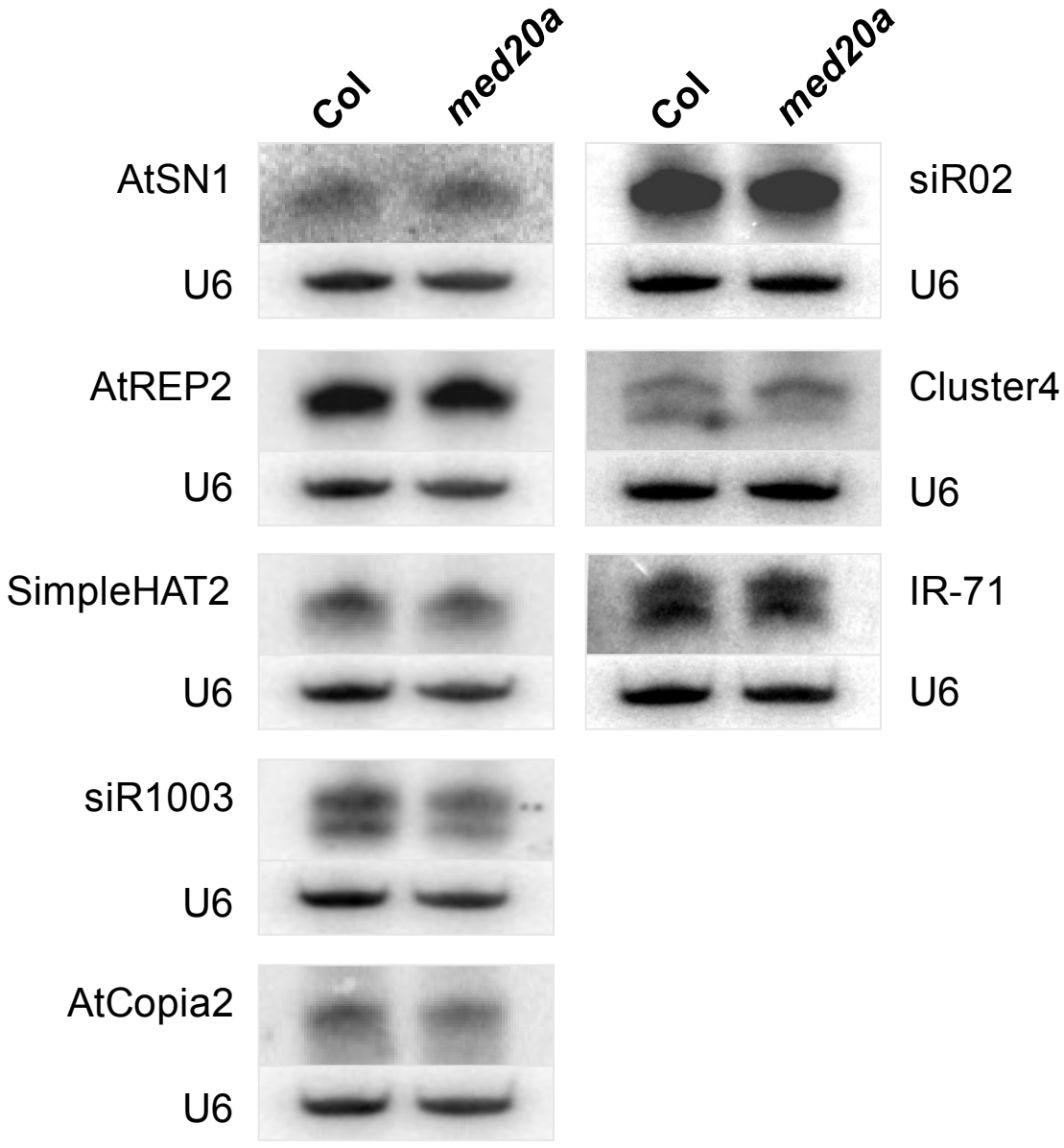
Col
med20a
Col
med20a
AtSN1
U6
siR02
U6
AtREP2
U6
Cluster4
U6
SimpleHAT2
U6
IR-71
U6
siR1003
U6
AtCopia2
U6

Figure 2.6 Transcript accumulation from endogenous hc-siRNA target loci in *med* mutants

Transcript accumulation from several endogenous hc-siRNA target loci was determined by RT-PCR in *med20a*, *med17* and *med18* mutants. The *AtSN1* region was derepressed in *med20a*, *med17* and *med18*, whereas no obvious difference was observed at other loci. *nrpe1-1* was used as a positive control, in which the hc-siRNA target loci are derepressed. RNAs were extracted from inflorescences and *UBIQUIN 5* was used as an internal control.

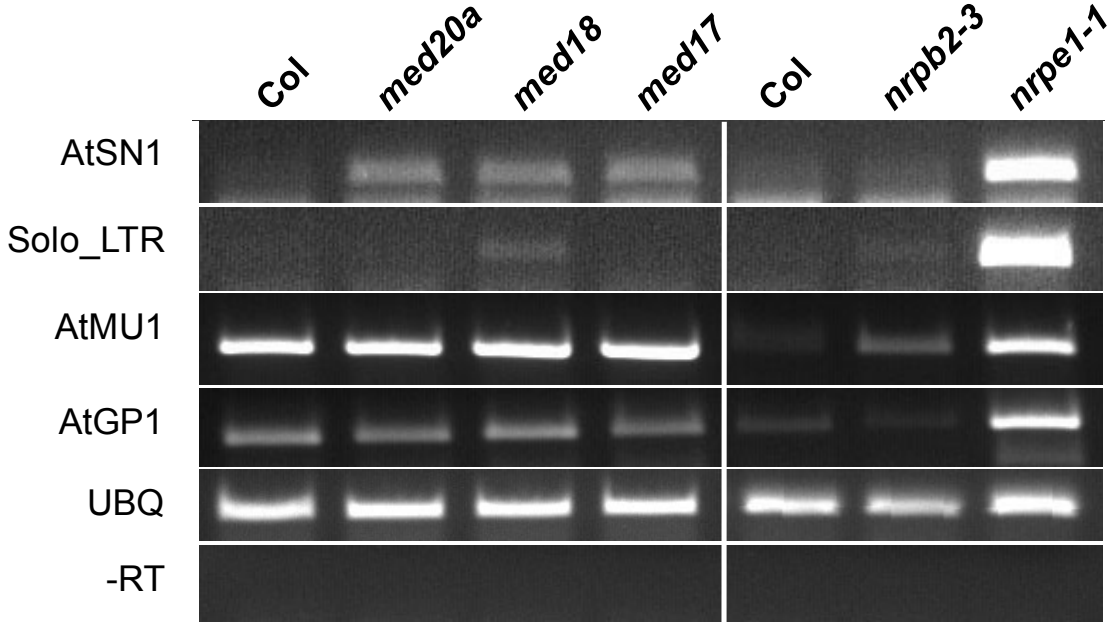
Col
med20a
med18
med17
Col
nrpb2-3
nrpe1-1
AtSN1
Solo_LTR
AtMU1
AtGP1
UBQ
-RT

Figure 2.7 A Venn diagram of genes affected by *med20a* and *nrpb2-3*

The blue oval represents the total number of down-regulated genes in the *med20a* mutant. The yellow oval represents the total number of down-regulated genes in the *nrpb2-3* mutant. The overlapping area of the blue and yellow ovals indicates the number of genes that are commonly down-regulated in the *med20a* and the *nrpb2-3* mutants.


med20a
377
377
71
nrpb2-3

Table 2.1 Primers used for real-time RT-PCR

	5’ primer	3’ primer
Pri-159	ggagctctacttccatcgtca	ccacgttctcatcaaaacttt
Pri-163	gcataggtcttgattggtgga	cgttgtcgttgaagaggttg
Pri-165a	attccctcatcataacacca	tcgatcttagcagattcaca
Pri-166a	gactctggctcgctctattca	tggtccgaagacgctaaac
Pri-171	ccgcgccaatatctcagta	tgtctccatttcaacacaca
Pri-167	gaagctgccagcatgatcta	gggtttatagaagggtgcga
UBQ5	ggtgctaagaagaggaagaat	ctccttctttctggtaaacgt

Table 2.2 Oligo probes used for small RNA Northern blot analysis

LNA-AtSN1	acca+acg+tgttg+ttgg+cccagtg+gtaaa+tctctca+gat
LNA-SiR02	g+ttg+acc+agt+ccg+cca+gcc+gat
LNA-AtREP2	g+cggg+acgg+gttt+ggca+ggac+gtta+ctt+aat
LNA-Cluster4	aa+gatc+aaac+atca+gca+gcgtc+ag+agg+ctt
LNA-SimpleHAT2	t+ggg+tta+ccc+attt+tgac+accc+cta
LNA-IR-71	g+gct+gca+act+ctt+gcg+gta+gaa+gcc+aat+atg+agg+aa
LNA-siR1003	a+tgc+caa+gtt+tgg+cct+cac+cgt+c
miR163	atccgaagttccaagtcctccttcaa
miR167	taggtcatgttggcagtttca
miR319	gggagcctcccttcagtccaa
miR158	tgctttgtctacatttggga
miR160	tggcataccagggagcccaggca
miR319	gggagctcccttcagtccaa
miR166	ccccaatgaatcctggtccgt
miR173	gtgatttctctctgtaagcgaa
miR393	gatcaatgcgatccctttgga
miR159	tagagctcccttcaatccaaa
miR390	ggcgctatccctcctgagctt
siR1511	aagtatcatcattcgccttgga
U6	aggggcccatgctaatccttcctc

Table 2.3 Primers used to detect endogenous siRNA target transcript

	5' primer	3' primer
AtSN1	accaacgtgctgttggcccagtggtaaatc	aaaataagtggtggttgtacaagc
soloLTR	aactaacgtcattacatacacatcttg	aattaggatcttgtttgccagcta
AtMu1	ccgagaactggttgtggttt	gctcttgctttggtgatggt
ATGP1	tggtttttcctgtccagtttg	aacaatcctaaccgggttcc
UBQ5	ggtgctaagaagaggaagaat	ctccttctttctggtaaacgt

Table 2.4 Genes down-regulated in *med20a*

Affimetrix code	Relative levels (wt/*med20a*)	AGI code	Description
248714_at	33.1498	AT5G48140	polygalacturonase, putative
249226_at	13.5886	AT5G42170	carboxylesterase
256307_at	10.1333	AT1G30350	pectate lyase family protein
258278_at	10.0925	AT3G26860	similar to unknown protein
251252_at	9.7081	AT3G62230	F-box family protein
251109_at	9.5035	AT5G01600	ATFER1 (FERRETIN 1)
265280_at	9.0098	AT2G28355	LCR5 (Low-molecular-weight cysteine-rich 5)
257121_at	8.6371	AT3G20220	auxin-responsive protein, putative
258639_at	8.6323	AT3G07820	polygalacturonase 3 (PGA3)
265405_at	8.6143	AT2G16750	protein kinase family protein
265080_at	8.1853	AT1G55570	SKS12 (SKU5 Similar 12)
256580_at	7.8375	AT3G28810	AT3G28810, similar to unknown protein
247424_at	7.7586	AT5G62850	ATVEX1 (VEGETATIVE CELL EXPRESSED1)
250631_at	7.5712	AT5G07430	pectinesterase family protein
259189_at	7.5458	AT3G01700	AGP11 (ARABINOGALACTAN PROTEIN 11)
256582_at	7.4316	AT3G28840	similar to unknown protein
246878_at	7.3074	AT5G26060	S1 self-incompatibility protein-related
265552_at	7.2928	AT2G07560	AHA6 (ARABIDOPSIS H(+)-ATPASE 6)
256833_at	7.0638	AT3G22910	calcium-transporting ATPase
261943_at	6.8314	AT1G80660	AHA9 (Arabidopsis H(+)-ATPase 9)
266558_at	6.6211	AT2G23900	glycoside hydrolase family 28 protein
250608_at	6.6057	AT5G07420	pectinesterase family protein
258561_at	6.5803	AT3G05960	sugar transporter, putative
262675_at	6.5639	AT1G75930	EXL6 (extracellular lipase 6)
257986_at	6.3667	AT3G20865	AGP40 (ARABINOGALACTAN-PROTEIN 40)
249046_at	6.3366	AT5G44400	FAD-binding domain-containing protein
257256_at	6.2877	AT3G21970	receptor-like protein kinase-related

Affimetrix code	Relative levels (wt/*med20a*)	AGI code	Description
254627_at	6.2871	AT4G18395	unknown protein
263753_at	6.2793	AT2G21490	LEA (DEHYDRIN LEA)
258058_at	6.1529	AT3G28980	similar to unknown protein
249429_at	6.1418	AT5G39880	similar to unknown protein
262282_at	6.0426	AT1G68610	similar to unknown protein
245376_at	5.9879	AT4G17690	peroxidase, putative
254123_at	5.9671	AT4G24640	APPB1
252733_at	5.9536	AT3G43120	auxin-responsive protein-related
246896_at	5.9019	AT5G25550	leucine-rich repeat family protein
256587_at	5.8220	AT3G28780	similar to unknown protein
255515_at	5.7225	AT4G02250	invertase/pectin methylesterase inhibitor family protein
253226_at	5.7055	AT4G35010	BGAL11 (beta-galactosidase 11)
256966_at	5.6825	AT3G13400	SKS13 (SKU5 Similar 13)
257102_at	5.5900	AT3G25050	XTH3 (XYLOGLUCAN ENDOTRANSGLUCOSYLASE/HYDROLASE 3)
248227_at	5.5832	AT5G53820	similar to unknown protein
261532_at	5.5730	AT1G71680	amino acid transmembrane transporter
253151_at	5.5373	AT4G35670	glycoside hydrolase family 28 protein
259269_at	5.5134	AT3G01270	pectate lyase family protein
266665_at	5.5078	AT2G29790	Encodes a Maternally expressed gene (MEG) family protein
265473_at	5.4981	AT2G15535	LCR10 (Low-molecular-weight cysteine-rich 10)
263950_at	5.4906	AT2G36020	HVA22J (HVA22-LIKE PROTEIN J)
253915_at	5.4604	AT4G27280	calcium-binding EF hand family protein
262156_at	5.4486	AT1G52680	late embryogenesis abundant protein-related
255101_at	5.4321	AT4G08670	protease inhibitor/seed storage/lipid transfer protein (LTP) family protein
262463_at	5.4312	AT1G50310	monosaccharide transporter (STP9)
249048_at	5.4184	AT5G44300	dormancy/auxin associated family protein
253660_at	5.3561	AT4G30140	GDSL-motif lipase/hydrolase family protein

Affimetrix code	Relative levels (wt/*med20a*)	AGI code	Description
263905_at	5.3348	AT2G36190	ATCWINV4 (ARABIDOPSIS THALIANA CELL WALL INVERTASE 4)
257392_at	5.3066	AT2G24450	FLA3 (FASCICLIN-LIKE ARABINOGALACTAN PROTEIN 3 PRECURSOR)
260001_at	5.3063	AT1G67990	caffeoyl-CoA 3-O-methyltransferase, putative
264187_at	5.3059	AT1G54860	similar to unknown protein
254001_at	5.2867	AT4G26260	MIOX4 (MYO-INOSITOL OXYGENASE 4)
267643_at	5.2679	AT2G32890	RALFL17 (RALF-LIKE 17)
262760_at	5.2648	AT1G10770	invertase/pectin methylesterase inhibitor family protein
264208_at	5.1911	AT1G22760	PAB3 (POLY(A) BINDING PROTEIN 3)
250174_at	5.1902	AT5G14380	AGP6 (ARABINOGALACTAN PROTEINS 6)
265331_at	5.1830	AT2G18420	Encodes a Gibberellin-regulated GASA/GAST/Snakin family protein
266918_at	5.1804	AT2G45800	LIM domain-containing protein
251228_at	5.1463	AT3G62710	glycosyl hydrolase family 3 protein
265127_at	5.1220	AT1G55560	SKS14 (SKU5 Similar 14)
261528_at	5.1210	AT1G14420	AT59 (Arabidopsis homolog of tomato LAT59)
254829_at	5.1026	AT4G12530	protease inhibitor/seed storage/lipid transfer protein (LTP) family protein
249536_at	5.0749	AT5G38760	similar to unknown protein
259266_at	5.0710	AT3G01240	similar to unknown protein
257691_at	5.0602	AT3G12660	FLA14 (FASCICLIN-LIKE ARABINOGALACTAN PROTEIN 14 PRECURSOR)
255952_at	5.0587	AT1G22130	AGL104
252710_at	5.0483	AT3G43860	ATGH9A4 (ARABIDOPSIS THALIANA GLYCOSYL HYDROLASE 9A4)
255276_at	5.0430	AT4G04930	DES-1-LIKE (fatty acid desaturase 1-like)
256955_at	5.0148	AT3G13390	SKS11 (SKU5 Similar 11)
261673_at	5.0073	AT1G18280	protease inhibitor/seed storage/lipid transfer protein (LTP) family protein
256588_at	4.9848	AT3G28790	similar to unknown protein

Affimetrix code	Relative levels (wt/*med20a*)	AGI code	Description
267322_at	4.9819	AT2G19330	leucine-rich repeat family protein
262987_at	4.9763	AT1G23240	caleosin-related family protein
267476_at	4.9719	AT2G02720	pectate lyase family protein
245946_at	4.9665	AT5G19580	glyoxal oxidase-related
245658_at	4.9514	AT1G28270	RALFL4 (RALF-LIKE 4)
257558_at	4.9424	AT3G22000	receptor-like protein kinase-related
246431_at	4.9196	AT5G17480	polcalcin, putative
254716_at	4.9096	AT4G13560	UNE15 (unfertilized embryo sac 15)
257821_at	4.8856	AT3G25170	RALFL26 (RALF-LIKE 26)
258685_at	4.8608	AT3G07830	polygalacturonase, putative
248872_at	4.8508	AT5G46795	MSP2 (MICROSPORE-SPECIFIC PROMOTER 2)
254158_at	4.8500	AT4G24380	hydrolase, acting on ester bonds
260022_at	4.8418	AT1G30020	similar to unknown protein
246841_at	4.8335	AT5G26700	germin-like protein, putative
248716_at	4.8087	AT5G48210	similar to unknown protein
251180_at	4.8070	AT3G62640	similar to unknown protein
257886_at	4.7907	AT3G17060	pectinesterase family protein
262817_at	4.7851	AT1G11770	electron carrier
256940_at	4.7609	AT3G30720	unknown protein
250904_at	4.7479	AT5G03620	subtilase family protein
250638_at	4.7373	AT5G07540	GRP16 (Glycine rich protein 16)
249503_at	4.7153	AT5G39310	ATEXPA24 (ARABIDOPSIS THALIANA EXPANSIN A24)
256584_at	4.7010	AT3G28750	similar to unknown protein
256638_at	4.6818	AT3G19090	RNA-binding protein, putative
265672_at	4.6328	AT2G31980	cysteine proteinase inhibitor-related
261244_at	4.6131	AT1G20150	subtilase family protein
251250_at	4.5942	AT3G62180	invertase/pectin methylesterase inhibitor family protein
250635_at	4.5868	AT5G07510	GRP14 (Glycine rich protein 14)

Affimetrix code	Relative levels (wt/*med20a*)	AGI code	Description
251358_at	4.5786	AT3G61160	shaggy-related protein kinase beta
258077_at	4.5550	AT3G26110	similar to BCP1 (Brassica campestris pollen protein 1)
252052_at	4.5357	AT3G52600	ARABIDOPSIS THALIANA CELL WALL INVERTASE 2
266697_at	4.5350	AT2G19770	PRF5 (PROFILIN5)
265133_at	4.5331	AT1G51240	similar to unknown protein
258408_at	4.5245	AT3G17630	ATCHX19 (CATION/H+ EXCHANGER 19)
260233_at	4.5207	AT1G74550	CYP98A9 (cytochrome P450, family 98, subfamily A, polypeptide 9)
267449_at	4.5156	AT2G33690	late embryogenesis abundant protein, putative
267443_at	4.5014	AT2G19000	similar to glycine-rich protein
250091_at	4.4888	AT5G17340	similar to unknown protein
258968_at	4.4885	AT3G10460	self-incompatibility protein-related
251854_at	4.4829	AT3G54800	pleckstrin homology (PH) domain-containing protein
251339_at	4.4759	AT3G60780	similar to unknown protein
251258_at	4.4210	AT3G62170	VGDH2 (VANGUARD 1 HOMOLOG 2)
253831_at	4.4116	AT4G27580	unknown protein
249584_at	4.4075	AT5G37810	NIP4
251397_at	4.3902	AT3G60570	ATEXPB5 (ARABIDOPSIS THALIANA EXPANSIN B5)
263363_at	4.3821	AT2G03850	late embryogenesis abundant domain-containing protein
266764_at	4.3789	AT2G47050	invertase/pectin methylesterase inhibitor family protein
252300_at	4.3765	AT3G49160	pyruvate kinase family protein
262683_at	4.3724	AT1G75920	family II extracellular lipase 5 (EXL5)
247546_at	4.3675	AT5G61605	similar to unknown protein
255530_at	4.3465	AT4G02140	similar to unknown protein
247402_at	4.3409	AT5G62750	unknown protein
257637_at	4.3365	AT3G25810	myrcene/ocimene synthase, putative
254886_at	4.3228	AT4G11760	LCR17 (Low-molecular-weight cysteine-rich 17)
250639_at	4.3119	AT5G07560	GRP20 (Glycine rich protein 20)

Affimetrix code	Relative levels (wt/*med20a*)	AGI code	Description
250637_at	4.3070	AT5G07530	GRP17 (Glycine rich protein 17)
250514_at	4.3026	AT5G09550	RAB GDP-dissociation inhibitor
248926_at	4.3020	AT5G45880	pollen Ole e 1 allergen and extensin family protein
266494_at	4.2944	AT2G07040	ATPRK2A
261245_at	4.2845	AT1G20135	hydrolase, acting on ester bonds
254762_at	4.2785	AT4G13230	late embryogenesis abundant domain-containing protein
261072_at	4.2747	AT1G07340	ATSTP2 (SUGAR TRANSPORTER 2)
250204_at	4.2560	AT5G13990	ATEXO70C2 (exocyst subunit EXO70 family protein C2)
247253_at	4.2527	AT5G64790	glycosyl hydrolase family 17 protein
264993_at	4.2321	AT1G67290	glyoxal oxidase-related
259265_at	4.2262	AT3G01250	unknown protein
255806_at	4.1949	AT4G10260	pfkB-type carbohydrate kinase family protein
266115_at	4.1792	AT2G02140	LCR72/PDF2.6 (Low-molecular-weight cysteine-rich 72)
250121_at	4.1735	AT5G16500	protein kinase family protein
256766_at	4.1632	AT3G22231	PCC1 (PATHOGEN AND CIRCADIAN CONTROLLED 1)
252440_at	4.1549	AT3G47440	TIP5
257255_at	4.1452	AT3G21960	receptor-like protein kinase-related
245577_at	4.1430	AT4G14780	protein kinase, putative
250239_at	4.1175	AT5G13580	ABC transporter family protein
265022_at	4.1164	AT1G24520	BCP1 (Brassica campestris pollen protein 1)
246545_at	4.0902	AT5G15110	pectate lyase family protein
248761_at	4.0849	AT5G47635	similar to unknown protein
264603_at	4.0649	AT1G04670	similar to pollen-preferential protein
252005_at	4.0575	AT3G52810	ATPAP21/PAP21 (purple acid phosphatase 21)
263450_at	4.0531	AT2G31500	CPK24 (calcium-dependent protein kinase 24)
246416_at	4.0475	AT5G16920	similar to unknown protein

Affimetrix code	Relative levels (wt/*med20a*)	AGI code	Description
259063_at	4.0457	AT3G07450	protease inhibitor/seed storage/lipid transfer protein (LTP) family protein
264235_at	4.0389	AT1G54560	XIE (Myosin-like protein XIE)
259693_at	4.0371	AT1G63060	similar to unknown protein
257082_at	4.0341	AT3G20580	COBL10 (COBRA-LIKE PROTEIN 10 PRECURSOR)
252090_at	4.0143	AT3G52130	protease inhibitor/seed storage/lipid transfer protein (LTP) family protein
261623_at	4.0072	AT1G01980	ATSEC1A
267440_at	3.9895	AT2G19070	transferase family protein
260757_at	3.9792	AT1G48940	plastocyanin-like domain-containing protein
260888_at	3.9733	AT1G29140	pollen Ole e 1 allergen and extensin family protein
258671_at	3.9686	AT3G08560	VHA-E2 (VACUOLAR H+-ATPASE SUBUNIT E ISOFORM 2)
254024_at	3.9542	AT4G25780	pathogenesis-related protein, putative
252908_at	3.9509	AT4G39670	glycolipid binding
253012_at	3.9413	AT4G37900	glycine-rich protein
258748_at	3.9337	AT3G05930	GLP8 (GERMIN-LIKE PROTEIN 8)
245468_at	3.9329	AT4G15980	pectinesterase family protein
258392_at	3.9305	AT3G15400	ATA20 (Arabidopsis thaliana anther 20)
263043_at	3.9198	AT1G23350	invertase/pectin methylesterase inhibitor family protein
262764_at	3.9170	AT1G13140	CYP86C3 (cytochrome P450, family 86, subfamily C, polypeptide 3)
249852_at	3.9031	AT5G23270	STP11 (SUGAR TRANSPORTER 11)
258605_at	3.9005	AT3G02970	phosphate-responsive 1 family protein
252085_at	3.8935	AT3G52000	SCPL36 (serine carboxypeptidase-like 36)
247639_at	3.8929	AT5G60500	undecaprenyl pyrophosphate synthetase family protein
246761_at	3.8820	AT5G27980	seed maturation family protein
255822_at	3.8691	AT2G40610	ATEXPA8 (ARABIDOPSIS THALIANA EXPANSIN A8)
265923_at	3.8672	AT2G18470	protein kinase family protein

Affimetrix code	Relative levels (wt/*med20a*)	AGI code	Description
258889_at	3.8595	AT3G05610	pectinesterase family protein
246208_at	3.8592	AT4G36490	SEC14 cytosolic factor, putative
256381_at	3.8583	AT1G66850	protease inhibitor/seed storage/lipid transfer protein (LTP) family protein
256581_at	3.8518	AT3G28830	similar to unknown protein
265002_at	3.8448	AT1G24400	LHT2 (LYSINE HISTIDINE TRANSPORTER 2)
263166_at	3.8425	AT1G03050	epsin N-terminal homology (ENTH) domain-containing protein
252035_at	3.8223	AT3G52160	beta-ketoacyl-CoA synthase family protein
260788_at	3.8174	AT1G06260	cysteine proteinase, putative
245700_at	3.8093	AT5G04180	carbonic anhydrase family protein
257951_at	3.8055	AT3G21700	GTP binding
257405_at	3.8054	AT1G24620	polcalcin, putative
248073_at	3.7863	AT5G55720	pectate lyase family protein
250957_at	3.7761	AT5G03250	phototropic-responsive NPH3 family protein
259221_at	3.7751	AT3G03530	NPC4 (NONSPECIFIC PHOSPHOLIPASE C4)
266750_at	3.7583	AT2G47040	VGD1 (VANGUARD1)
257532_at	3.7563	AT3G04700	similar to unknown protein
249527_at	3.7518	AT5G38710	proline oxidase, putative
257469_at	3.7489	AT1G49290	similar to unknown protein
257862_at	3.7426	AT3G17760	GAD5 (GLUTAMATE DECARBOXYLASE 5)
263084_at	3.7400	AT2G27180	unknown protein
253725_at	3.7366	AT4G29340	PRF4 (PROFILIN 4)
257925_at	3.7323	AT3G23170	similar to unknown protein
258767_at	3.7261	AT3G10890	(1-4)-beta-mannan endohydrolase, putative
262022_at	3.7184	AT1G35490	bZIP family transcription factor
252881_at	3.7090	AT4G39610	similar to unknown protein
253240_at	3.6931	AT4G34510	KCS2 (3-ketoacyl-CoA synthase 2)
253590_at	3.6920	no_match	no_match

Affimetrix code	Relative levels (wt/*med20a*)	AGI code	Description
249375_at	3.6783	AT5G40730	AGP24 (ARABINOGALACTAN PROTEIN 24)
265401_at	3.6768	AT2G10970	invertase/pectin methylesterase inhibitor family protein
255580_at	3.6718	AT4G01470	GAMMA-TIP3/TIP1
266259_at	3.6716	AT2G27830	similar to pentatricopeptide (PPR) repeat-containing protein
248484_at	3.6707	AT5G51030	short-chain dehydrogenase/reductase (SDR) family protein
261045_at	3.6637	AT1G01310	allergen V5/Tpx-1-related family protein
247512_at	3.6450	AT5G61720	similar to unknown protein
251590_at	3.6434	AT3G57690	AGP23/ATAGP23 (ARABINOGALACTAN-PROTEIN 23)
267178_at	3.6425	AT2G37750	unknown protein
261687_at	3.6382	AT1G47280	unknown protein
259044_at	3.6377	AT3G03430	polcalcin, putative
249950_at	3.6324	AT5G18910	protein kinase family protein
248470_at	3.6311	AT5G50830	unknown protein
266708_at	3.6245	AT2G03200	aspartyl protease family protein
254338_at	3.6158	AT4G22080	pectate lyase family protein
258216_at	3.6007	AT3G17980	C2 domain-containing protein
266654_at	3.5919	AT2G25890	glycine-rich protein
266799_at	3.5888	AT2G22860	ATPSK2 (PHYTOSULFOKINE 2 PRECURSOR)
262122_at	3.5853	AT1G02790	PGA4 (POLYGALACTURONASE 4)
252933_at	3.5788	AT4G39110	protein kinase family protein
265176_at	3.5717	AT1G23520	similar to unknown protein
250606_at	3.5677	AT1G69940	ATPPME1
260228_at	3.5670	AT1G74540	CYP98A8 (cytochrome P450, family 98, subfamily A, polypeptide 8)
263144_at	3.5647	AT1G54070	dormancy/auxin associated protein-related
257119_at	3.5596	AT3G20190	leucine-rich repeat transmembrane protein kinase, putative

Affimetrix code	Relative levels (wt/*med20a*)	AGI code	Description
246377_at	3.5569	AT1G57550	hydrophobic protein, putative
247804_at	3.5420	AT5G58170	glycerophosphoryl diester phosphodiesterase family protein
250636_at	3.5416	AT5G07520	GRP18 (Glycine rich protein 18)
247981_at	3.5166	AT5G56640	MIOX5 (MYO-INOSITOL OXYGENASE 5)
248367_at	3.5115	AT5G52360	actin-depolymerizing factor, putative
245232_at	3.4940	AT4G25590	ADF7 (ACTIN DEPOLYMERIZING FACTOR 7)
258168_at	3.4931	AT3G21570	unknown protein
245036_at	3.4838	AT2G26410	IQD4 (IQ-domain 4)
245151_at	3.4805	AT2G47550	pectinesterase family protein
262115_at	3.4777	AT1G02813	similar to unknown protein
252061_at	3.4527	AT3G52620	unknown protein
259615_at	3.4498	AT1G47980	similar to unknown protein
265263_at	3.4488	AT2G42940	DNA-binding family protein
248822_at	3.4455	AT5G47000	peroxidase, putative
250662_at	3.4409	AT5G07010	sulfotransferase family protein
266143_at	3.4389	AT2G38905	hydrophobic protein, putative
265007_at	3.4333	AT1G61563	RALFL8 (RALF-LIKE 8)
257819_at	3.4318	AT3G25165	RALFL25 (RALF-LIKE 25)
264601_at	3.4301	AT1G04540	C2 domain-containing protein
254494_at	3.4247	AT4G20050	QRT3 (QUARTET 3)
265368_at	3.4233	AT2G13350	C2 domain-containing protein
246418_at	3.4232	AT5G16960	NADP-dependent oxidoreductase, putative
247925_at	3.4198	AT5G57560	TCH4 (TOUCH 4)
259975_at	3.4188	AT1G76470	cinnamoyl-CoA reductase
265186_at	3.4160	AT1G23560	similar to unknown protein
256297_at	3.4141	AT1G69500	oxygen binding
252063_at	3.4037	AT3G51590	LTP12 (LIPID TRANSFER PROTEIN 12)
258516_at	3.3974	AT3G06490	MYB108 (MYB DOMAIN PROTEIN 108)

Affimetrix code	Relative levels (wt/*med20a*)	AGI code	Description
247462_at	3.3925	AT5G62080	protease inhibitor/seed storage/lipid transfer protein (LTP) family protein
265404_at	3.3917	AT2G16730	BGAL13 (beta-galactosidase 13)
258523_at	3.3899	AT3G06830	pectinesterase family protein
260941_at	3.3861	AT1G44970	peroxidase, putative
260997_at	3.3832	AT1G26610	zinc finger (C2H2 type) family protein
252820_at	3.3772	AT3G42640	AHA8 (ARABIDOPSIS H(+)-ATPASE 8)
259886_at	3.3739	AT1G76370	protein kinase, putative
255423_at	3.3738	AT4G03290	calcium-binding protein, putative
262949_at	3.3706	AT1G75790	SKS18 (SKU5 Similar 18)
247293_at	3.3463	AT5G64510	similar to unnamed protein product [Vitis vinifera]
256059_at	3.3447	AT1G06990	GDSL-motif lipase/hydrolase family protein
257059_at	3.3361	AT3G15280	similar to unnamed protein product [Vitis vinifera]
251595_at	3.3293	AT3G57620	glyoxal oxidase-related
260143_at	3.3277	AT1G71880	SUC1 (SUCROSE-PROTON SYMPORTER 1)
258753_at	3.3266	AT3G09530	ATEXO70H3 (exocyst subunit EXO70 family protein H3)
260661_at	3.3265	AT1G19500	similar to unknown protein
250561_at	3.3167	AT5G08030	glycerophosphoryl diester phosphodiesterase family protein
260076_at	3.3116	AT1G73630	calcium-binding protein, putative
245777_at	3.3081	AT1G73540	ATNUDT21 (Arabidopsis thaliana Nudix hydrolase homolog 21)
267466_at	3.2988	AT2G19010	GDSL-motif lipase/hydrolase family protein
266850_at	3.2951	AT2G26850	F-box family protein
261511_at	3.2916	AT1G71770	PAB5 (POLY(A)-BINDING PROTEIN)
258732_at	3.2897	AT3G05820	beta-fructofuranosidase, putative
255703_at	3.2819	AT4G00040	chalcone and stilbene synthase family protein
256589_at	3.2747	AT3G28740	cytochrome P450 family protein
245820_at	3.2694	AT1G26320	NADP-dependent oxidoreductase, putative

Affimetrix code	Relative levels (wt/*med20a*)	AGI code	Description
262585_at	3.2692	AT1G15460	ATBOR4/BOR4
261670_at	3.2688	AT1G18520	TET11 (TETRASPANIN11)
253772_at	3.2537	AT4G28395	ATA7 (Arabidopsis thaliana anther 7)
267398_at	3.2497	AT2G44560	ATGH9B11 (ARABIDOPSIS THALIANA GLYCOSYL HYDROLASE 9B11)
257065_at	3.2483	AT3G18220	phosphatidic acid phosphatase family protein
265024_at	3.2431	AT1G24600	similar to unknown protein
262765_at	3.2417	AT1G13150	CYP86C4 (cytochrome P450, family 86, subfamily C, polypeptide 4)
263106_at	3.2395	AT2G05160	zinc finger (CCCH-type) family protein
257261_at	3.2380	AT3G21920	pollen coat receptor kinase, putative
260518_at	3.2140	AT1G51410	cinnamyl-alcohol dehydrogenase, putative (CAD)
258498_at	3.2101	AT3G02480	ABA-responsive protein-related
262917_at	3.2064	AT1G64800	unknown protein
259346_at	3.2054	AT3G03910	glutamate dehydrogenase, putative
258035_at	3.2053	AT3G21180	ACA9 (autoinhibited Ca2+ -ATPase 9)
257076_at	3.2042	AT3G19680	similar to unknown protein
262179_at	3.2035	AT1G77980	AGL66
257402_at	3.1994	AT1G23570	similar to unknown protein
263087_at	3.1991	AT2G16130	mannitol transporter, putative
253153_at	3.1980	AT4G35700	zinc finger (C2H2 type) family protein
257107_at	3.1919	AT3G29070	protein transmembrane transporter
264923_at	3.1912	AT1G65970	TPX2 (THIOREDOXIN-DEPENDENT PEROXIDASE 2
259464_at	3.1895	AT1G18990	similar to unknown protein
261448_at	3.1894	AT1G21140	nodulin, putative
266548_at	3.1860	AT2G35210	AGD10/MEE28/RPA (MATERNAL EFFECT EMBRYO ARREST 28)
267295_at	3.1779	AT2G23800	GGPS2 (GERANYLGERANYL PYROPHOSPHATE SYNTHASE 2)

Affimetrix code	Relative levels (wt/*med20a*)	AGI code	Description
253643_at	3.1717	AT4G29780	similar to unknown protein
248880_at	3.1625	AT5G46200	similar to unknown protein
265164_at	3.1622	AT1G23600	similar to unknown protein
255345_at	3.1508	AT4G04460	aspartyl protease family protein
247122_at	3.1461	AT5G66020	ATSAC1B/IBS2 (IMPAIRED IN BABA-INDUCED STERILITY 2)
259820_at	3.1447	AT1G66210	subtilase family protein
259635_at	3.1259	AT1G56360	ATPAP6/PAP6 (purple acid phosphatase 6)
263126_at	3.1208	AT1G78460	SOUL heme-binding family protein
266743_at	3.1198	AT2G02990	RNS1 (RIBONUCLEASE 1)
264529_at	3.1156	AT1G30820	CTP synthase, putative
260621_at	3.1154	AT1G08065	carbonate dehydratase/ zinc ion binding
255175_at	3.1017	AT4G07960	ATCSLC12 (Cellulose synthase-like C12)
261222_at	3.0989	AT1G20120	family II extracellular lipase, putative
245674_at	3.0949	AT1G56680	glycoside hydrolase family 19 protein
254104_at	3.0920	AT4G25040	integral membrane family protein
255815_at	3.0802	AT1G19890	ATMGH3/MGH3 (MALE-GAMETE-SPECIFIC HISTONE H3)
261559_at	3.0796	AT1G01780	LIM domain-containing protein
254453_at	3.0787	AT4G21120	AAT1 (CATIONIC AMINO ACID TRANSPORTER 1)
251825_at	3.0774	AT3G55100	ABC transporter family protein
261015_at	3.0767	AT1G26480	GRF12 (GENERAL REGULATORY FACTOR 12)
260335_at	3.0757	AT1G74000	SS3 (STRICTOSIDINE SYNTHASE 3)
252531_at	3.0753	AT3G46520	ACT12 (ACTIN-12)
264039_at	3.0649	AT2G03740	late embryogenesis abundant domain-containing protein
262801_at	3.0638	AT1G21010	similar to unknown protein
251697_at	3.0600	AT3G56600	inositol or phosphatidylinositol kinase
257442_at	3.0565	AT2G28680	cupin family protein
256354_at	3.0541	AT1G54870	oxidoreductase

Affimetrix code	Relative levels (wt/*med20a*)	AGI code	Description
255835_at	3.0507	AT2G33420	similar to unknown protein
267255_at	3.0450	AT2G22950	calcium-transporting ATPase, plasma membrane-type, putative
247736_at	3.0406	AT5G59370	ACT4 (ACTIN 4)
254972_at	3.0373	AT4G10440	dehydration-responsive family protein
251039_at	3.0365	AT5G02020	similar to unknown protein
254607_at	3.0358	AT4G18920	similar to unknown protein
250294_at	3.0301	AT5G13380	auxin-responsive GH3 family protein
258727_at	3.0261	AT3G11930	universal stress protein (USP) family protein
251298_at	3.0260	AT3G62040	hydrolase
254090_at	3.0259	AT4G25010	nodulin MtN3 family protein
266901_at	3.0241	AT2G34600	JAZ7/TIFY5B (JASMONATE-ZIM-DOMAIN PROTEIN 7)
264112_at	3.0138	AT2G13680	CALS5 (CALLOSE SYNTHASE 5)
257726_at	3.0127	AT3G18360	VQ motif-containing protein
247758_at	3.0072	AT5G59120	ATSBT4.13
247178_at	3.0055	AT5G65205	short-chain dehydrogenase/reductase (SDR) family protein
246392_at	3.0054	AT1G58120	similar to unnamed protein product [Vitis vinifera]
248274_at	3.0052	AT5G53510	ATOPT9 (oligopeptide transporter 9)
260011_at	3.0050	AT1G68110	epsin N-terminal homology (ENTH) domain-containing protein
254347_at	3.0027	AT4G22070	WRKY31 (WRKY DNA-binding protein 31)
252107_at	3.0026	AT3G51490	TMT3 (TONOPLAST MONOSACCHARIDE TRANSPORTER3)
266530_at	2.9994	AT2G16910	AMS (ABORTED MICROSPORES)
253087_at	2.9984	AT4G36350	ATPAP25/PAP25 (purple acid phosphatase 25)
246099_at	2.9977	AT5G20230	ATBCB (ARABIDOPSIS BLUE-COPPER-BINDING PROTEIN)
251361_at	2.9915	AT3G61230	LIM domain-containing protein

Affimetrix code	Relative levels (wt/*med20a*)	AGI code	Description
250619_at	2.9913	AT5G07230	protease inhibitor/seed storage/lipid transfer protein (LTP) family protein
257543_at	2.9886	AT3G28960	amino acid transporter family protein
245970_at	2.9845	AT5G20710	BGAL7 (beta-galactosidase 7)
246592_at	2.9741	AT5G14890	NHL repeat-containing protein
260097_at	2.9716	AT1G73220	ARABIDOPSIS THALIANA ORGANIC CATION/CARNITINE TRANSPORTER1
245622_at	2.9691	AT4G14080	MEE48 (maternal effect embryo arrest 48)
250648_at	2.9664	AT5G06760	late embryogenesis abundant group 1 domain-containing protein
254468_at	2.9663	AT4G20460	NAD-dependent epimerase/dehydratase family protein
252160_at	2.9656	AT3G50570	hydroxyproline-rich glycoprotein family protein
265179_at	2.9642	AT1G23650	unknown protein
245057_at	2.9641	AT2G26490	transducin family protein
263360_at	2.9627	AT2G03830	unknown protein
266765_at	2.9612	AT2G46860	ATPPA3
255064_at	2.9593	AT4G08950	phosphate-responsive protein, putative (EXO)
254809_at	2.9592	AT4G12410	auxin-responsive family protein
263453_at	2.9582	AT2G22180	hydroxyproline-rich glycoprotein family protein
245335_at	2.9550	AT4G16160	ATOEP16-2/ATOEP16-S
256392_at	2.9505	AT3G06260	GATL4 (Galacturonosyltransferase-like 4)
247897_at	2.9491	AT5G57810	TET15 (TETRASPANIN15)
248194_at	2.9405	AT5G54095	similar to unknown protein
263195_at	2.9391	AT1G36150	protease inhibitor/seed storage/lipid transfer protein (LTP) family protein
260032_at	2.9339	AT1G68750	ATPPC4 (Arabidopsis thaliana phosphoenolpyruvate carboxylase 4)
259282_at	2.9333	AT3G11430	ATGPAT5/GPAT5 (GLYCEROL-3-PHOSPHATE ACYLTRANSFERASE 5)
245636_at	2.9312	AT1G25240	epsin N-terminal homology (ENTH) domain-containing protein

Affimetrix code	Relative levels (wt/*med20a*)	AGI code	Description
265185_at	2.9255	AT1G23670	similar to unknown protein
253222_at	2.9202	AT4G34850	chalcone and stilbene synthase family protein
246582_at	2.9201	AT1G31750	proline-rich family protein
260306_at	2.9172	AT1G70540	EDA24 (embryo sac development arrest 24)
245246_at	2.9102	AT1G44224	Encodes a ECA1 gametogenesis related family protein
259852_at	2.9052	AT1G72280	AERO1 (ARABIDOPSIS ENDOPLASMIC RETICULUM OXIDOREDUCTINS 1)
252780_at	2.9008	AT3G42960	ATA1 (ARABIDOPSIS TAPETUM 1)
262664_at	2.8980	AT1G13970	similar to unknown protein
260038_at	2.8967	AT1G68875	unknown protein
252493_at	2.8960	AT3G46750	similar to hypothetical protein [Vitis vinifera]
260386_at	2.8901	AT1G74010	strictosidine synthase family protein
246136_at	2.8891	AT5G28470	transporter
251944_at	2.8879	AT3G53510	ABC transporter family protein
252415_at	2.8876	AT3G47340	ASN1 (DARK INDUCIBLE 6)
257800_at	2.8843	AT3G15900	similar to unknown [Populus trichocarpa]
255717_at	2.8766	AT4G00350	MATE efflux family protein
258337_at	2.8749	AT3G16040	similar to unknown protein
249447_at	2.8723	AT5G39400	pollen specific phosphatase, putative
265903_at	2.8676	AT2G25600	SPIK (SHAKER POLLEN INWARD K+ CHANNEL)
258840_at	2.8564	AT3G04620	nucleic acid binding
246915_at	2.8536	AT5G25880	ATNADP-ME3 (NADP-MALIC ENZYME 3)
248534_at	2.8532	AT5G50030	invertase/pectin methylesterase inhibitor family protein
260737_at	2.8495	AT1G17540	kinase
252679_at	2.8484	AT3G44260	CCR4-NOT transcription complex protein, putative
259399_at	2.8482	AT1G17710	phosphoric monoester hydrolase
253863_at	2.8417	AT4G27420	ABC transporter family protein
253880_at	2.8399	AT4G27590	copper-binding protein-related
260438_at	2.8391	AT1G68290	ENDO 2 (ENDONUCLEASE 2)

Affimetrix code	Relative levels (wt/*med20a*)	AGI code	Description
248964_at	2.8379	AT5G45340	CYP707A3 (cytochrome P450, family 707, subfamily A, polypeptide 3)
263011_at	2.8320	AT1G23250	caleosin-related
257633_at	2.8238	AT3G26125	CYP86C2 (cytochrome P450, family 86, subfamily C, polypeptide 2)
251981_at	2.8237	AT3G53080	galactose-binding lectin family protein
266201_at	2.8215	AT2G39060	nodulin MtN3 family protein
251558_at	2.8153	AT3G57810	OTU-like cysteine protease family protein
248638_at	2.8119	AT5G49070	beta-ketoacyl-CoA synthase family protein
256860_at	2.8101	AT3G23840	transferase family protein
256481_at	2.8100	AT1G33430	galactosyltransferase family protein
250349_at	2.8087	AT5G12000	kinase
266488_at	2.8072	AT2G47670	invertase/pectin methylesterase inhibitor family protein
261305_at	2.8067	AT1G48470	GLN1
258078_at	2.8066	AT3G25870	similar to unknown protein
246751_at	2.8028	AT5G27870	pectinesterase family protein
250158_at	2.8001	AT5G15190	unknown protein
250308_at	2.7999	AT5G12180	CPK17 (calcium-dependent protein kinase 17)
249337_at	2.7951	AT5G41080	glycerophosphoryl diester phosphodiesterase family protein
262674_at	2.7941	AT1G75910	EXL4 (extracellular lipase 4)
245314_at	2.7929	AT4G16745	exostosin family protein
257154_at	2.7924	AT3G27210	Identical to Uncharacterized protein At3g27210 (Y-2)
266462_at	2.7882	AT2G47770	benzodiazepine receptor-related
265571_at	2.7844	AT2G28020	similar to unknown protein
266029_at	2.7821	AT2G05850	SCPL38 (serine carboxypeptidase-like 38)
252623_at	2.7814	AT3G45320	similar to unknown protein
247451_at	2.7793	AT5G62320	MYB99 (myb domain protein 99)
253934_at	2.7776	AT4G26830	hydrolase, hydrolyzing O-glycosyl compounds
264175_at	2.7716	AT1G02050	chalcone and stilbene synthase family protein

Affimetrix code	Relative levels (wt/*med20a*)	AGI code	Description
254490_at	2.7700	AT4G20320	CTP synthase
259744_at	2.7689	AT1G71160	beta-ketoacyl-CoA synthase family protein
262697_at	2.7679	AT1G75940	ATA27 (Arabidopsis thaliana anther 27)
255976_at	2.7646	AT1G22010	unknown protein
249150_at	2.7539	AT5G43340	PHT6 (phosphate transporter 6)
245053_at	2.7488	AT2G26450	pectinesterase family protein
250917_at	2.7433	AT5G03690	fructose-bisphosphate aldolase, putative
247055_at	2.7390	AT5G66740	similar to unknown protein
257170_at	2.7324	AT3G23770	glycosyl hydrolase family 17 protein
257869_at	2.7206	AT3G25160	ER lumen protein retaining receptor family protein
259987_at	2.7053	AT1G75030	ATLP-3 (Arabidopsis thaumatin-like protein 3)
253807_at	2.7042	AT4G28280	similar to unknown protein
253262_at	2.7036	AT4G34440	protein kinase family protein
260158_at	2.7033	AT1G79910	similar to unknown protein
248888_at	2.6870	AT5G46240	KAT1 (K+ ATPASE 1)
259262_at	2.6843	AT3G01020	ATISU2/ISU2 (IscU-like 2)
258005_at	2.6833	AT3G19390	cysteine proteinase, putative
262723_at	2.6758	AT1G43630	similar to unknown protein
264395_at	2.6732	AT1G12070	Rho GDP-dissociation inhibitor family protein
263718_at	2.6731	AT2G13570	CCAAT-box binding transcription factor, putative
248448_at	2.6702	AT5G51190	AP2 domain-containing transcription factor, putative
262742_at	2.6691	AT1G28550	AtRABA1i (Arabidopsis Rab GTPase homolog A1i)
249381_at	2.6671	AT5G40040	60S acidic ribosomal protein P2 (RPP2E)
253181_at	2.6607	AT4G35180	LHT7 (LYS/HIS TRANSPORTER 7)
245159_at	2.6602	AT2G33100	ATCSLD1 (Cellulose synthase-like D1)
255479_at	2.6496	AT4G02380	SAG21 (SENESCENCE-ASSOCIATED GENE 21)
246616_at	2.6493	AT5G36260	aspartyl protease family protein
260773_at	2.6452	AT1G78440	ATGA2OX1 (GIBBERELLIN 2-OXIDASE 1)
250576_at	2.6448	AT5G08250	cytochrome P450 family protein

Affimetrix code	Relative levels (wt/*med20a*)	AGI code	Description
262147_at	2.6443	AT1G52570	PLDALPHA2 (PHOSPHLIPASE D ALPHA 2)
265188_at	2.6417	AT1G23800	ALDH2B7 (Aldehyde dehydrogenase 2B7)
264882_at	2.6407	AT1G61110	ANAC025 (Arabidopsis NAC domain containing protein 25)
261462_at	2.6277	AT1G07850	fringe-related protein
251297_at	2.6225	AT3G62020	GLP10 (GERMIN-LIKE PROTEIN 10)
258940_at	2.6160	AT3G09930	GDSL-motif lipase/hydrolase family protein
254009_at	2.6132	AT4G26390	pyruvate kinase, putative
261051_at	2.6125	AT1G01280	CYP703/CYP703A2
248840_at	2.6089	AT5G46770	unknown protein
265031_at	2.6017	AT1G61590	protein kinase, putative
259338_at	2.6010	AT3G03800	SYP131 (syntaxin 131)
263046_at	2.5907	AT2G05380	GRP3S (GLYCINE-RICH PROTEIN 3 SHORT ISOFORM)
263215_at	2.5891	AT1G30710	FAD-binding domain-containing protein
258645_at	2.5834	AT3G07850	exopolygalacturonase
257939_at	2.5809	AT3G19930	STP4 (SUGAR TRANSPORTER 4)
248804_at	2.5759	AT5G47470	nodulin MtN21 family protein
263627_at	2.5749	AT2G04675	unknown protein
257349_at	2.5747	AT2G30630	similar to unknown protein
258465_at	2.5738	AT3G17220	invertase/pectin methylesterase inhibitor family protein
252606_at	2.5680	AT3G45010	SCPL48 (serine carboxypeptidase-like 48)
251491_at	2.5676	AT3G59480	pfkB-type carbohydrate kinase family protein
246106_at	2.5520	AT5G28680	protein kinase family protein
256416_at	2.5472	AT3G11050	ATFER2 (FERRITIN 2)
263927_at	2.5460	AT2G21890	mannitol dehydrogenase, putative
262385_at	2.5456	AT1G72960	root hair defective 3 GTP-binding (RHD3) family protein
258600_at	2.5442	AT3G02810	protein kinase family protein
253031_at	2.5415	AT4G38190	ATCSLD4 (Cellulose synthase-like D4)

Affimetrix code	Relative levels (wt/*med20a*)	AGI code	Description
246123_at	2.5383	AT5G20390	beta-1,3-glucanase, putative
267081_at	2.5382	AT2G41210	phosphatidylinositol-4-phosphate 5-kinase family protein
253781_at	2.5378	AT4G28580	magnesium transporter CorA-like family protein (MRS2-6)
261648_at	2.5334	AT1G27730	STZ (SALT TOLERANCE ZINC FINGER)
263981_at	2.5330	AT2G42870	HLH1/PAR1 (PHY RAPIDLY REGULATED 1)
256743_at	2.5318	AT3G29370	similar to unknown protein
261264_at	2.5308	AT1G26710	similar to unknown protein
257090_at	2.5304	AT3G20530	protein kinase family protein
253034_at	2.5289	AT4G38230	CPK26 (calcium-dependent protein kinase 26)
248350_at	2.5260	AT5G52160	protease inhibitor/seed storage/lipid transfer protein (LTP) family protein
261221_at	2.5247	AT1G19960	similar to transmembrane receptor
253721_at	2.5237	AT4G29250	transferase family protein
248932_at	2.5189	AT5G46050	ATPTR3/PTR3 (PEPTIDE TRANSPORTER PROTEIN 3)
250903_at	2.5159	AT5G03600	GDSL-motif lipase/hydrolase family protein
251197_at	2.5150	AT3G62960	glutaredoxin family protein
245883_at	2.5112	AT5G09500	40S ribosomal protein S15 (RPS15C)
249194_at	2.5104	AT5G42490	kinesin motor family protein
263320_at	2.5080	AT2G47180	ATGOLS1 (ARABIDOPSIS THALIANA GALACTINOL SYNTHASE 1)
245912_at	2.5075	AT5G19600	SULTR3
262696_at	2.5049	AT1G75870	unknown protein
266592_at	2.5011	AT2G46210	delta-8 sphingolipid desaturase, putative
254230_at	2.4965	AT4G23660	ATPPT1 (ARABIDOPSIS THALIANA POLYPRENYLTRANSFERASE 1)
261442_at	2.4936	AT1G28375	unknown protein
260693_at	2.4915	AT1G32450	proton-dependent oligopeptide transport (POT) family protein

Affimetrix code	Relative levels (wt/*med20a*)	AGI code	Description
245029_at	2.4881	AT2G26580	YAB5 (YABBY5)
261875_at	2.4852	AT1G50610	leucine-rich repeat transmembrane protein kinase, putative
263831_at	2.4797	AT2G40300	ATFER4 (FERRITIN 4)
256662_at	2.4784	AT3G11980	MS2 (MALE STERILITY 2)
251569_at	2.4707	AT3G58290	meprin and TRAF homology domain-containing protein
255295_at	2.4682	AT4G04760	sugar transporter family protein
258344_at	2.4681	AT3G22650	F-box family protein
249283_at	2.4670	AT5G41800	amino acid transporter family protein
252571_at	2.4653	AT3G45280	SYP72 (SYNTAXIN OF PLANTS 72)
258012_at	2.4623	AT3G19310	phospholipase C
265761_at	2.4586	AT2G01330	transducin family protein
261396_at	2.4580	AT1G79800	plastocyanin-like domain-containing protein
246918_at	2.4565	AT5G25340	similar to unknown protein
252131_at	2.4559	AT3G50930	AAA-type ATPase family protein
267087_at	2.4548	AT2G32460	AtM1/AtMYB101/MYB101 (myb domain protein 101)
247759_at	2.4548	AT5G59040	COPT3 (Copper transporter 3)
250154_at	2.4511	AT5G15140	aldose 1-epimerase family protein
256647_at	2.4467	AT3G13610	oxidoreductase, 2OG-Fe(II) oxygenase family protein
262146_at	2.4315	AT1G52580	rhomboid family protein
264710_at	2.4295	AT1G09790	COBL6 (COBRA-LIKE PROTEIN 6 PRECURSOR)
251743_at	2.4245	AT3G55890	yippee family protein
246913_at	2.4239	AT5G25830	zinc finger (GATA type) family protein
248211_at	2.4233	AT5G54010	glycosyltransferase family protein
247843_at	2.4228	AT5G58050	glycerophosphoryl diester phosphodiesterase family protein
256827_at	2.4220	AT3G18570	glycine-rich protein
250143_at	2.4184	AT5G14670	ATARFA1B (ADP-RIBOSYLATION FACTOR A1B)
258870_at	2.4163	AT3G03080	NADP-dependent oxidoreductase, putative

Affimetrix code	Relative levels (wt/*med20a*)	AGI code	Description
266078_at	2.4160	AT2G40670	ARR16 (response regulator 16)
253195_at	2.4132	AT4G35420	dihydroflavonol 4-reductase family
263233_at	2.4110	AT1G05577	similar to unknown protein
251235_at	2.4095	AT3G62860	esterase/lipase/thioesterase family protein
266866_at	2.4050	AT2G29940	ATPDR3/PDR3 (PLEIOTROPIC DRUG RESISTANCE 3)
261392_at	2.3972	AT1G79780	Identical to UPF0497 membrane protein At1g79780
254193_at	2.3948	AT4G23870	similar to unknown protein
262912_at	2.3902	AT1G59740	proton-dependent oligopeptide transport (POT) family protein
262558_at	2.3892	AT1G31335	unknown protein
262755_at	2.3863	AT1G16360	LEM3 (ligand-effect modulator 3) family protein
258686_at	2.3831	AT3G07840	polygalacturonase, putative
252102_at	2.3811	AT3G50970	LTI30 (LOW TEMPERATURE-INDUCED 30)
250610_at	2.3790	AT5G07550	GRP19 (Glycine rich protein 19)
259116_at	2.3783	AT3G01350	proton-dependent oligopeptide transport (POT) family protein
255861_at	2.3783	AT2G30290	vacuolar sorting receptor, putative
245997_at	2.3773	AT5G20810	auxin-responsive protein, putative
246646_at	2.3762	AT5G35090	unknown protein
262707_at	2.3712	AT1G16290	similar to predicted protein [Physcomitrella patens subsp. patens]
246242_at	2.3684	AT4G36600	late embryogenesis abundant domain-containing protein
245345_at	2.3679	AT4G16640	matrix metalloproteinase, putative
260791_at	2.3671	AT1G06250	lipase class 3 family protein
254685_at	2.3630	AT4G13790	auxin-responsive protein, putative
255958_at	2.3616	AT1G22150	SULTR1
254956_at	2.3580	AT4G10850	nodulin MtN3 family protein
257850_at	2.3579	AT3G13065	SRF4 (STRUBBELIG-RECEPTOR FAMILY 4)

Affimetrix code	Relative levels (wt/*med20a*)	AGI code	Description
245979_at	2.3552	AT5G13150	ATEXO70C1 (exocyst subunit EXO70 family protein C1)
264659_at	2.3512	AT1G09930	ATOPT2 (oligopeptide transporter 2)
249401_at	2.3507	AT5G40260	nodulin MtN3 family protein
260080_at	2.3492	AT1G78160	APUM7 (ARABIDOPSIS PUMILIO 7)
252914_at	2.3442	AT4G39130	dehydrin family protein
252140_at	2.3350	AT3G51070	dehydration-responsive protein-related
265115_at	2.3346	AT1G62450	Rho GDP-dissociation inhibitor family protein
255386_at	2.3345	AT4G03620	myosin heavy chain-related
253846_at	2.3327	AT4G28000	AAA-type ATPase family protein
263231_at	2.3322	AT1G05680	UDP-glucoronosyl/UDP-glucosyl transferase family protein
250479_at	2.3282	AT5G10260	AtRABH1e (Arabidopsis Rab GTPase homolog H1e)
265012_at	2.3263	AT1G24470	short-chain dehydrogenase/reductase (SDR) family protein
251745_at	2.3217	AT3G55980	zinc finger (CCCH-type) family protein
260702_at	2.3181	AT1G32250	calmodulin, putative
266371_at	2.3171	AT2G41410	calmodulin, putative
260943_at	2.3169	AT1G45145	ATTRX5 (thioredoxin H-type 5)
247519_at	2.3165	AT5G61430	ANAC100/ATNAC5 (Arabidopsis NAC domain containing protein 100)
258114_at	2.3142	AT3G14660	CYP72A13 (cytochrome P450, family 72, subfamily A, polypeptide 13)
254287_at	2.3121	AT4G22960	similar to unknown protein
258239_at	2.3115	AT3G27690	LHCB2:4 (Photosystem II light harvesting complex gene 2.3)
263659_at	2.3087	no_match	no_match
264210_at	2.3050	AT1G22640	MYB3 (myb domain protein 3)
245076_at	2.3038	AT2G23170	GH3.3
261712_at	2.3022	AT1G32780	alcohol dehydrogenase, putative
254961_at	2.2988	AT4G11030	long-chain-fatty-acid--CoA ligase, putative

Affimetrix code	Relative levels (wt/*med20a*)	AGI code	Description
262615_at	2.2987	AT1G13950	EIF-5A (eukaryotic translation initiation factor 5A-1)
266184_at	2.2982	AT3G54700	carbohydrate transmembrane transporter
263062_at	2.2871	AT2G18180	SEC14 cytosolic factor, putative
263133_at	2.2856	AT1G78450	SOUL heme-binding family protein
261061_at	2.2856	AT1G07540	TRFL2 (TRF-LIKE 2)
248377_at	2.2829	AT5G51720	similar to Os07g0467200 [Oryza sativa]
267158_at	2.2826	AT2G37640	ATEXPA3 (ARABIDOPSIS THALIANA EXPANSIN A3)
257183_at	2.2818	AT3G13220	ABC transporter family protein
260260_at	2.2802	AT1G68540	oxidoreductase family protein
252101_at	2.2754	AT3G51300	ARAC11/ATRAC11/ATROP1/ROP1/ROP1AT (RHO-RELATED PROTEIN FROM PLANTS 1)
265560_at	2.2754	AT2G05520	GRP-3 (GLYCINE-RICH PROTEIN 3)
247723_at	2.2743	AT5G59220	protein phosphatase 2C, putative
257523_at	2.2742	AT3G01620	glycosyl transferase family 17 protein
267147_at	2.2714	AT2G38240	oxidoreductase, 2OG-Fe(II) oxygenase family protein
265387_at	2.2675	AT2G20670	similar to unknown protein
252095_at	2.2643	AT3G51000	epoxide hydrolase, putative
263754_at	2.2638	AT2G21510	DNAJ heat shock N-terminal domain-containing protein
252663_at	2.2592	AT3G44070	beta-galactosidase
249878_at	2.2568	AT5G23090	TATA-binding protein-associated phosphoprotein Dr1 protein, putative (DR1)
247255_at	2.2544	AT5G64780	similar to unknown protein
256433_at	2.2536	AT3G10985	SAG20 (WOUND-INDUCED PROTEIN 12)
255956_at	2.2511	AT1G22015	DD46
254550_at	2.2488	AT4G19690	IRT1 (IRON-REGULATED TRANSPORTER 1)
264284_at	2.2478	AT1G61860	protein kinase, putative
259986_at	2.2477	AT1G75050	similar to ATLP-3 (Arabidopsis thaumatin-like protein 3)

Affimetrix code	Relative levels (wt/*med20a*)	AGI code	Description
259719_at	2.2446	AT1G61070	LCR66/PDF2.4 (Low-molecular-weight cysteine-rich 66)
252781_at	2.2438	AT3G42950	glycoside hydrolase family 28 protein
255950_at	2.2421	AT1G22110	structural constituent of ribosome
254120_at	2.2354	AT4G24570	mitochondrial substrate carrier family protein
254926_at	2.2346	AT4G11280	ACS6 (1-AMINOCYCLOPROPANE-1-CARBOXYLIC ACID (ACC) SYNTHASE 6)
252698_at	2.2334	AT3G43670	copper amine oxidase, putative
254033_at	2.2327	AT4G25950	VATG3 (VACUOLAR ATP SYNTHASE G3)
251874_at	2.2271	AT3G54240	hydrolase, alpha/beta fold family protein
248525_at	2.2236	AT5G50610	similar to unknown protein
261499_at	2.2231	AT1G28430	CYP705A24 (cytochrome P450, family 705, subfamily A, polypeptide 24)
259516_at	2.2188	AT1G20450	ERD10/LTI45 (EARLY RESPONSIVE TO DEHYDRATION 10)
262643_at	2.2187	AT1G62770	invertase/pectin methylesterase inhibitor family protein
258249_at	2.2177	AT3G15830	phosphatidic acid phosphatase-related
261341_at	2.2108	AT1G52940	ATPAP5/PAP5 (purple acid phosphatase 5)
266453_at	2.2107	AT2G43230	serine/threonine protein kinase, putative
248824_at	2.2104	AT5G46940	invertase/pectin methylesterase inhibitor family protein
264007_at	2.2057	AT2G21140	ATPRP2 (PROLINE-RICH PROTEIN 2)
253149_at	2.2047	AT4G35650	isocitrate dehydrogenase, putative
258848_at	2.2016	AT3G03300	DCL2 (DICER-LIKE 2)
260577_at	2.2007	AT2G47340	invertase/pectin methylesterase inhibitor family protein
259982_at	2.1993	AT1G76410	ATL8
256497_at	2.1991	AT1G31580	ECS1
253850_at	2.1984	AT4G28090	SKS10 (SKU5 Similar 10)
253641_at	2.1979	AT4G29980	similar to unknown protein
264827_at	2.1952	AT1G03390	transferase family protein
259351_at	2.1919	AT3G05150	sugar transporter family protein

Affimetrix code	Relative levels (wt/*med20a*)	AGI code	Description
248968_at	2.1881	AT5G45280	pectinacetylesterase, putative
255837_at	2.1853	AT2G33460	RIC1
264320_at	2.1832	AT1G04090	similar to unknown protein
264127_at	2.1810	AT1G79250	protein kinase, putative
263788_at	2.1784	AT2G24580	sarcosine oxidase family protein
251835_at	2.1755	AT3G55180	esterase/lipase/thioesterase family protein
256398_at	2.1738	AT3G06100	NIP7
250437_at	2.1643	AT5G10430	AGP4 (ARABINOGALACTAN-PROTEIN 4)
260367_at	2.1621	AT1G69760	similar to unknown protein
256506_at	2.1576	AT1G75160	similar to unknown protein
247193_at	2.1571	AT5G65380	ripening-responsive protein, putative
265261_at	2.1560	AT2G42990	GDSL-motif lipase/hydrolase family protein
247280_at	2.1491	AT5G64260	phosphate-responsive protein, putative
264482_at	2.1440	AT1G77210	sugar transporter, putative
264891_at	2.1407	AT1G23200	pectinesterase family protein
255847_at	2.1393	AT2G33270	thioredoxin family protein
265680_at	2.1315	AT2G32150	haloacid dehalogenase-like hydrolase family protein
253525_at	2.1274	AT4G31330	similar to unknown protein
261576_at	2.1254	AT1G01070	nodulin MtN21 family protein
246491_at	2.1238	AT5G16100	similar to hypothetical protein
263368_at	2.1201	no_match	no_match
245193_at	2.1199	AT1G67810	Fe-S metabolism associated domain-containing protein
258451_at	2.1196	AT3G22360	AOX1B (alternative oxidase 1B)
249783_at	2.1182	AT5G24270	SOS3 (SALT OVERLY SENSITIVE 3)
248040_at	2.1143	AT5G55970	zinc finger (C3HC4-type RING finger) family protein
259570_at	2.1140	AT1G20440	COR47 (cold regulated 47)
254173_at	2.1101	AT4G24580	pleckstrin homology (PH) domain-containing protein-related
252930_at	2.1065	AT4G39010	ATGH9B18

Affimetrix code	Relative levels (wt/*med20a*)	AGI code	Description
249767_at	2.1039	AT5G24090	acidic endochitinase (CHIB1)
246569_at	2.1030	AT5G14980	esterase/lipase/thioesterase family protein
251455_at	2.1024	AT3G60100	CSY5 (CITRATE SYNTHASE 5)
247170_at	2.0981	AT5G65530	protein kinase, putative
257737_at	2.0948	AT3G27440	uracil phosphoribosyltransferase, putative
246425_at	2.0938	AT5G17420	IRX3 (IRREGULAR XYLEM 3, MURUS 10)
267527_at	2.0927	AT2G45610	hydrolase
250541_at	2.0920	AT5G09520	hydroxyproline-rich glycoprotein family protein
260178_at	2.0917	AT1G70720	invertase/pectin methylesterase inhibitor family protein
256586_at	2.0902	AT3G28770	similar to unknown protein
261335_at	2.0898	AT1G44800	nodulin MtN21 family protein
245423_at	2.0891	AT4G17483	palmitoyl protein thioesterase family protein
265064_at	2.0887	AT1G61630	equilibrative nucleoside transporter, putative (ENT7)
246963_at	2.0883	AT5G24820	aspartyl protease family protein
248191_at	2.0868	AT5G54130	calcium-binding EF hand family protein
250745_at	2.0861	AT5G05850	leucine-rich repeat family protein
245322_at	2.0828	AT4G14815	protease inhibitor/seed storage/lipid transfer protein (LTP) family protein
258984_at	2.0819	AT3G08970	DNAJ heat shock N-terminal domain-containing protein
264798_at	2.0805	AT1G08730	XIC (Myosin-like protein XIC)
254792_at	2.0796	AT4G12920	aspartyl protease family protein
267458_at	2.0793	AT2G33670	MLO5 (MILDEW RESISTANCE LOCUS O 5)
265681_at	2.0784	AT2G24370	kinase
267035_at	2.0777	AT2G38400	AGT3 (ALANINE:GLYOXYLATE AMINOTRANSFERASE 3)
254111_at	2.0727	AT4G24890	ATPAP24/PAP24 (purple acid phosphatase 24)
260424_at	2.0721	AT1G72460	leucine-rich repeat transmembrane protein kinase, putative
262936_at	2.0716	AT1G79400	ATCHX2 (CATION/H+ EXCHANGER 2)
258919_at	2.0715	AT3G10525	similar to SIM (SIAMESE)

Affimetrix code	Relative levels (wt/*med20a*)	AGI code	Description
247941_at	2.0715	AT5G57200	epsin N-terminal homology (ENTH) domain-containing protein
265180_at	2.0711	AT1G23590	similar to unknown protein
250366_at	2.0705	AT5G11420	similar to unknown protein
267488_at	2.0672	AT2G19110	HMA4 (Heavy metal ATPase 4)
251723_at	2.0663	AT3G56230	speckle-type POZ protein-related
248467_at	2.0652	AT5G50800	nodulin MtN3 family protein
254917_at	2.0613	AT4G11350	transferase, transferring glycosyl groups
267066_at	2.0548	AT2G41040	methyltransferase-related
258967_at	2.0510	AT3G10470	zinc finger (C2H2 type) family protein
257896_at	2.0509	AT3G16920	chitinase
262651_at	2.0501	AT1G14100	FUT8 (FUCOSYLTRANSFERASE 8)
248168_at	2.0491	AT5G54570	glycosyl hydrolase family 1 protein
258322_at	2.0483	AT3G22740	HMT3 (Homocysteine S-methyltransferase 3)
267094_at	2.0422	AT2G38080	IRX12/LAC4 (laccase 4)
261069_at	2.0416	AT1G07410	AtRABA2b (Arabidopsis Rab GTPase homolog A2b)
264758_at	2.0409	AT1G61340	F-box family protein
257397_at	2.0402	AT2G20430	RIC6 (ROP-INTERACTIVE CRIB MOTIF-CONTAINING PROTEIN 6)
254487_at	2.0394	AT4G20780	calcium-binding protein, putative
252363_at	2.0393	AT3G48460	GDSL-motif lipase/hydrolase family protein
245959_at	2.0383	AT5G19640	proton-dependent oligopeptide transport (POT) family protein
265821_at	2.0361	AT2G17950	WUS (WUSCHEL)
259429_at	2.0342	AT1G01600	CYP86A4 (cytochrome P450, family 86, subfamily A, polypeptide 4)
252769_at	2.0311	AT3G42850	galactokinase, putative
256200_at	2.0278	AT1G58210	EMB1674 (EMBRYO DEFECTIVE 1674)
266824_at	2.0277	AT2G22800	HAT9 (homeobox-leucine zipper protein 9)
263566_at	2.0274	AT2G15340	glycine-rich protein

Affimetrix code	Relative levels (wt/*med20a*)	AGI code	Description
246540_at	2.0267	AT5G15600	SP1L4 (SPIRAL1-LIKE4)
250199_at	2.0258	AT5G14180	MPL1 (MYZUS PERSICAE-INDUCED LIPASE 1)
258719_at	2.0256	AT3G09540	pectate lyase family protein
246075_at	2.0240	AT5G20410	MGD2 (monogalactosyldiacylglycerol synthase 2)
264342_at	2.0209	AT1G12080	contains domain PTHR22683 (PTHR22683)
263720_at	2.0197	AT2G13620	ATCHX15 (cation/hydrogen exchanger 15)
250241_at	2.0196	AT5G13600	phototropic-responsive NPH3 family protein
250532_at	2.0190	AT5G08540	similar to unnamed protein product [Vitis vinifera]
258385_at	2.0181	AT3G15510	ATNAC2 (Arabidopsis thaliana NAC domain containing protein 2)
252167_at	2.0155	AT3G50560	short-chain dehydrogenase/reductase (SDR) family protein
264124_at	2.0152	AT1G79360	ATOCT2 (ARABIDOPSIS THALIANA ORGANIC CATION/CARNITINE TRANSPORTER2)
245353_at	2.0126	AT4G16000	similar to unknown protein
262393_at	2.0117	AT1G49490	leucine-rich repeat family protein
256914_at	2.0106	AT3G23880	F-box family protein
250806_at	2.0103	AT5G05070	zinc ion binding
251654_at	2.0090	AT3G57140	SDP1-LIKE (SDP1-LIKE)
253652_at	2.0064	AT4G30040	aspartyl protease family
262942_at	2.0057	AT1G79450	LEM3 (ligand-effect modulator 3) family protein
263889_at	2.0047	AT2G37010	ATNAP12 (Arabidopsis thaliana non-intrinsic ABC protein 12)
249718_at	2.0024	AT5G35740	glycosyl hydrolase family protein 17

Table 2.5 Genes up-regulated in *med20a*

Affimetrix code	Relative levels (wt/*med20a*)	AGI code	Description
258809_at	2.0005	AT3G04070	ANAC047 (Arabidopsis NAC domain containing protein 47)
264527_at	2.0017	AT1G30760	FAD-binding domain-containing protein
245816_at	2.0027	AT1G26210	similar to unknown protein
249332_at	2.0044	AT5G40980	similar to unknown protein
260549_at	2.0089	AT2G43535	trypsin inhibitor, putative
250633_at	2.0093	AT5G07460	PMSR2 (PEPTIDEMETHIONINE SULFOXIDE REDUCTASE 2)
257066_at	2.0179	AT3G18280	protease inhibitor
249975_at	2.0249	AT3G06320	ribosomal protein L33 family protein
253133_at	2.0257	AT4G35800	NRPB1 (RNA POLYMERASE II LARGE SUBUNIT)
261080_at	2.0313	AT1G07370	PCNA1 (PROLIFERATING CELLULAR NUCLEAR ANTIGEN)
259785_at	2.0343	AT1G29490	auxin-responsive family protein
255557_at	2.0348	AT4G01990	pentatricopeptide (PPR) repeat-containing protein
262499_at	2.0360	AT1G21770	similar to unknown protein
256335_at	2.0476	AT1G72110	similar to unknown protein
258888_at	2.0491	AT3G05620	pectinesterase family protein
253101_at	2.0491	AT4G37430	CYP91A2 (CYTOCHROME P450 MONOOXYGENASE 91A2)
258235_at	2.0590	AT3G27620	AOX1C (alternative oxidase 1C)
257130_at	2.0629	AT3G20210	DELTA-VPE (delta vacuolar processing enzyme)
254309_at	2.0629	AT4G22420	Identical to Putative F-box protein At4g22420
260528_at	2.0746	AT2G47260	WRKY23 (WRKY DNA-binding protein 23)
254431_at	2.0865	AT4G20840	FAD-binding domain-containing protein
262238_at	2.0890	AT1G48300	similar to hypothetical protein [Vitis vinifera]
259142_at	2.0968	AT3G10200	dehydration-responsive protein-related
257487_at	2.0970	AT1G71850	similar to unknown protein
258548_at	2.1023	AT3G06910	Ulp1 protease family protein

Affimetrix code	Relative levels (wt/*med20a*)	AGI code	Description
253697_at	2.1028	AT4G29700	type I phosphodiesterase/nucleotide pyrophosphatase family protein
250660_at	2.1080	AT5G07060	zinc finger (CCCH-type) family protein
257517_at	2.1087	AT3G16330	similar to unknown protein
247615_at	2.1087	AT5G60250	zinc finger (C3HC4-type RING finger) family protein
254288_at	2.1094	AT4G22970	AESP (ARABIDOPSIS HOMOLOG OF SEPARASE)
250528_at	2.1223	AT5G08600	U3 ribonucleoprotein (Utp) family protein
264363_at	2.1254	AT1G03170	similar to unknown protein
252478_at	2.1308	AT3G46540	epsin N-terminal homology (ENTH) domain-containing protein
252965_at	2.1392	AT4G38860	auxin-responsive protein, putative
258255_at	2.1407	AT3G26800	similar to unknown protein
259520_at	2.1483	AT1G12320	similar to unknown protein
263153_at	2.1512	AT1G54000	myrosinase-associated protein, putative
252827_at	2.1546	AT4G39950	CYP79B2 (cytochrome P450, family 79, subfamily B, polypeptide 2)
254964_at	2.1550	AT4G11080	high mobility group (HMG1/2) family protein
257207_at	2.1650	AT3G14900	similar to unnamed protein product [Vitis vinifera]
257062_at	2.1661	AT3G18290	EMB2454 (EMBRYO DEFECTIVE 2454)
257167_at	2.1683	AT3G24340	CHR40 (chromatin remodeling 40)
260869_at	2.1697	AT1G43800	acyl-(acyl-carrier-protein) desaturase, putative
266098_at	2.1718	AT2G37870	protease inhibitor/seed storage/lipid transfer protein (LTP) family protein
263200_at	2.1744	AT1G05600	pentatricopeptide (PPR) repeat-containing protein
252563_at	2.1824	AT3G45970	ATEXLA1 (ARABIDOPSIS THALIANA EXPANSIN-LIKE A1)
260461_at	2.1839	AT1G10980	similar to unknown protein
253943_at	2.1884	AT4G27030	small conjugating protein ligase
247515_at	2.1984	AT5G61740	ATATH14 (ABC2 homolog 14)
249955_at	2.2008	AT5G18840	sugar transporter, putative

Affimetrix code	Relative levels (wt/*med20a*)	AGI code	Description
266968_at	2.2241	AT2G39360	protein kinase family protein
251476_at	2.2276	AT3G59670	similar to unknown protein
252330_at	2.2344	AT3G48770	ATP binding / DNA binding
265121_at	2.2449	AT1G62560	flavin-containing monooxygenase family protein
249515_at	2.2479	AT5G38530	tryptophan synthase-related
265053_at	2.2481	AT1G52000	jacalin lectin family protein
249426_at	2.2761	AT5G39840	ATP-dependent RNA helicase, mitochondrial, putative
259489_at	2.2935	AT1G15790	similar to protein binding / transcription cofactor
252269_at	2.2939	AT3G49580	similar to unknown protein
251704_at	2.3571	AT3G56360	similar to unknown protein
254862_at	2.3574	AT4G12030	bile acid:sodium symporter family protein
260805_at	2.3698	AT1G78320	ATGSTU23
245537_at	2.3777	no_match	no_match
259793_at	2.3778	AT1G64380	AP2 domain-containing transcription factor, putative
266989_at	2.4080	AT2G39330	jacalin lectin family protein
247167_at	2.4118	AT5G65850	F-box family protein
245743_at	2.4263	AT1G51080	similar to unnamed protein product [Vitis vinifera]
261951_at	2.4286	AT1G64490	similar to unknown protein
265233_at	2.4291	AT2G07718	hypothetical protein
264830_at	2.4366	AT1G03710	cysteine protease inhibitor
256175_at	2.4385	AT1G51670	similar to unknown protein
259937_at	2.4412	AT3G13080	ATMRP3 (Arabidopsis thaliana multidrug resistance-associated protein 3)
246750_at	2.4429	no_match	no_match
252199_at	2.4470	AT3G50270	transferase family protein
252972_at	2.4607	AT4G38840	auxin-responsive protein, putative
260553_at	2.4649	AT2G41800	similar to unknown protein
261460_at	2.4650	AT1G07880	ATMPK13 (ARABIDOPSIS THALIANA MAP KINASE 13)

Affimetrix code	Relative levels (wt/*med20a*)	AGI code	Description
251065_at	2.4702	AT5G01870	lipid transfer protein, putative
247878_at	2.4921	AT5G57760	unknown protein
257641_at	2.4966	AT3G25760	AOC1 (ALLENE OXIDE CYCLASE 1)
254375_at	2.4986	AT4G21800	QQT2 (QUATRE-QUART2)
254786_at	2.5048	AT4G12890	gamma interferon responsive lysosomal thiol reductase family protein
263883_at	2.5265	AT2G21830	DC1 domain-containing protein
247317_at	2.5408	AT5G64060	ANAC103 (Arabidopsis NAC domain containing protein 103)
248015_at	2.5421	AT5G56370	F-box family protein
260112_at	2.5502	AT1G63310	similar to oxidoreductase, acting on NADH or NADPH
246145_at	2.5517	AT5G19880	peroxidase, putative
258121_at	2.5533	AT3G14530	geranylgeranyl pyrophosphate synthase, putative
249616_at	2.5560	AT5G37750	heat shock protein binding
257008_at	2.5713	AT3G14210	ESM1 (EPITHIOSPECIFIER MODIFIER 1)
247679_at	2.5994	AT5G59540	oxidoreductase, 2OG-Fe(II) oxygenase family protein
260745_at	2.6166	AT1G78370	ATGSTU20 (Arabidopsis thaliana Glutathione S-transferase (class tau) 20)
257021_at	2.6261	AT3G19710	BCAT4 (BRANCHED-CHAIN AMINOTRANSFERASE4)
251576_at	2.6309	AT3G58200	meprin and TRAF homology domain-containing protein
251181_at	2.6654	AT3G62820	invertase/pectin methylesterase inhibitor family protein
252897_at	2.6818	AT4G39490	CYP96A10 (cytochrome P450, family 96, subfamily A, polypeptide 10)
257763_at	2.6921	AT3G23120	leucine-rich repeat family protein
258380_at	2.7153	AT3G16650	PP1/PP2A phosphatases pleiotropic regulator 2 (PRL2)
255302_at	2.7473	AT4G04830	methionine sulfoxide reductase domain-containing protein
258108_at	2.7474	AT3G23570	dienelactone hydrolase family protein
258414_at	2.7644	AT3G17380	meprin and TRAF homology domain-containing protein
245385_at	2.7802	AT4G14020	rapid alkalinization factor (RALF) family protein

Affimetrix code	Relative levels (wt/*med20a*)	AGI code	Description
256976_at	2.7814	AT3G21020	transposable element gene
250646_at	2.7971	AT5G06720	peroxidase, putative
259925_at	2.8132	AT1G75040	PR5 (PATHOGENESIS-RELATED GENE 5)
251017_at	2.8359	AT5G02760	protein phosphatase 2C family protein
245989_at	2.8731	AT5G20620	UBQ4 (ubiquitin 4)
267500_at	2.8969	AT2G45510	CYP704A2 (cytochrome P450, family 704, subfamily A, polypeptide 2)
251026_at	2.9044	AT5G02200	FHL (FAR-RED-ELONGATED HYPOCOTYL1-LIKE)
267567_at	2.9609	AT2G30770	CYP71A13 (CYTOCHROME P450, FAMILY 71, SUBFAMILY A, POLYPEPTIDE 13)
257247_at	3.0197	AT3G24140	FMA (FAMA)
250485_at	3.0432	AT5G09990	PROPEP5 (Elicitor peptide 5 precursor)
261913_at	3.0536	AT1G65860	flavin-containing monooxygenase family protein
247549_at	3.0582	AT5G61420	MYB28 (MYB DOMAIN PROTEIN 28)
254546_at	3.0751	AT4G19850	ATPP2-A2 (Arabidopsis thaliana phloem protein 2-A2)
248270_at	3.0969	AT5G53450	ORG1 (OBP3-RESPONSIVE GENE 1)
259711_at	3.1351	AT1G77570	DNA binding / transcription factor
267317_at	3.2016	AT2G34700	pollen Ole e 1 allergen and extensin family protein
245275_at	3.2520	AT4G15210	ATBETA-AMY (BETA-AMYLASE)
248777_at	3.3457	AT5G47920	similar to unknown protein
259766_at	3.5153	AT1G64360	unknown protein
245296_at	3.5158	AT4G16370	ATOPT3 (OLIGOPEPTIDE TRANSPORTER)
262357_at	3.5936	AT1G73040	jacalin lectin family protein
256459_at	3.7282	AT1G36180	ATP binding / biotin binding / catalytic/ ligase
258370_at	4.0312	AT3G14395	unknown protein
264400_at	4.0809	AT1G61800	GPT2 (glucose-6-phosphate/phosphate translocator 2)
258707_at	4.1212	AT3G09480	histone H2B, putative
250476_at	4.2695	AT5G10140	FLC (FLOWERING LOCUS C)
251524_at	4.5066	AT3G58990	aconitase C-terminal domain-containing protein

Affimetrix code	Relative levels (wt/*med20a*)	AGI code	Description
266395_at	4.6573	AT2G43100	aconitase C-terminal domain-containing protein
256977_at	4.8141	AT3G21040	transposable element gene
251677_at	5.0754	AT3G56980	BHLH039/ORG3 (OBP3-RESPONSIVE GENE 3)
250828_at	5.0916	AT5G05250	similar to unknown protein
264761_at	5.1905	AT1G61280	Identical to Probable phosphatidylinositol N-acetylglucosaminyltransferase subunit P
249866_at	6.0798	AT5G23010	MAM1 (2-isopropylmalate synthase 3)
264751_at	7.2730	AT1G23020	ATFRO3/FRO3 (FERRIC REDUCTION OXIDASE 3)
254907_at	9.6005	AT4G11190	disease resistance-responsive family protein / dirigent family protein
251952_at	10.3627	AT3G53650	histone H2B, putative
254909_at	24.8558	AT4G11210	disease resistance-responsive family protein / dirigent family protein
261684_at	52.6078	AT1G47400	similar to unknown protein

CHAPTER 3

SAP negatively modulates the activities of a subset of miRNAs in *Arabidopsis*

ABSTRACT

Small RNAs (miRNAs and siRNAs) are regulatory molecules that act in a sequence specific manner. Small RNA-mediated gene silencing governs many biological processes such as developmental patterning, stress signaling and genome stability in plants. Here we report that *STERILE APETALA* (*SAP*), which was first identified as a negative regulator of *AGAMOUS*, acts as a negative regulator of the activities of a subset of miRNAs in *Arabidopsis*. Although miRNA accumulation is not changed in *sap* mutants, the mRNA and protein levels of several miRNA target genes were reduced. In addition, we show that some miRNAs are more active in *sap* mutants on the basis of the accumulation level of the 3' cleavage products of their target mRNAs. These results indicate that *SAP* negatively modulates miRNA activity at the posttranscriptional level. Moreover, certain endogenous siRNA loci are over-repressed in *sap* mutants despite no changes in siRNA accumulation, raising the possibility that *SAP* also acts as a negative factor in siRNA-mediated gene silencing. This study extends our knowledge of the regulatory mechanisms underlying small RNA-mediated gene scilecing by showing that the activities of miRNAs can be modulated.

INTRODUCTION

Small RNAs of 20 - 30 nt in size are regulatory molecules that act as sequence-specific repressors of target gene expression. In plants, there are two types of small RNAs: microRNAs (miRNAs) and small interfering RNAs (siRNAs) (Reviewed in Chen, 2009). Many miRNAs target transcription factors that are involved in the processes of development and environmental stimulus signaling. Endogenous siRNAs mostly act in genome stability, while some of them are involved in developmental patterning and stress responses. Despite differences in genomic origins and functions of the two types of small RNAs, their biogenesis involves several conserved biochemical steps. First, a long double stranded RNA (dsRNA) or a single-stranded RNA with a hairpin structure is processed into one or more small RNA duplexes by RNase III endonucleases, Dicer-like proteins (DCL). Then a small RNA duplex is methylated by the methyltransferase HUA ENHANCER1 (HEN1). Finally, one small RNA strand is selectively incorporated into an ARGONAUTE (AGO)-containing effector complex, RNA induced silencing complex (RISC).

In plants, miRNA regulates target genes via two mechanisms: mRNA cleavage or translational inhibition (Reviewed in Bartel et al., 2004). A miRNA-RISC recognizes a target mRNA in a sequence specific manner to result in either cleavage of the mRNA at a defined position along the miRNA-mRNA duplex or translational inhibition. The mechanism of the mRNA cleavage event has been well understood. AGO1, the major effector in a miRNA-RISC, possesses endonucleolytic activity (Baumberger and Baulcombe, 2005; Fagard et al., 2000; Qi et al., 2005; Vaucheret et al., 2004). In *ago1*

mutants, miRNA target gene expression is increased and the amount of 3' cleavage products of target mRNAs is reduced. AGO1 has slicer activity *in vitro* and most miRNAs are associated with AGO1 *in vivo*.

However, the mechanism underlying translational inhibition is largely unknown. In animals, miRNAs mostly regulate target genes via translational inhibition (reviewed in Kim et al., 2009). Several possibilities have been suggested to understand how miRNAs cause translational inhibition. First, in vitro biochemical studies revealed that miRNAs inhibit the translational initiation of target mRNAs and the m^7G-cap of the mRNA is required for miRNA function. (Humphreys et al., 2005; Pillaiet al., 2005) Another study showed that some AGO proteins harbor a highly conserved motif that is similar to the m^7G-cap-binding motif of eukaryotic translation initiation factor 4E (eIF4E) (Kiriakidou et al., 2007). In turn, AGO1 can interact with the m^7G-cap of the mRNA and compete with eIF4E, which results in the inhibition of translation initiation of the mRNA. However, it is still controversial whether miRNA just affects the translational initiation step in the entire translational process (Maroney et al., 2006; Petersen et al., 2006). Second, it has been shown that the processing body (P body) is a functional place for miRNA-mediated translational inhibition (Eulalio et al., 2007; Frank and Lykke-Anersen, 2007). P bodies are cytoplasmic foci, which function as places for the storage of untranslated mRNAs and mRNA decay. Recent studies in animals showed that miRNAs and target mRNAs are found in P bodies (Liu et al., 2005; Pillai, 2005; Sen and Blau, 2005). In addition, AGO proteins are localized in P bodies (Liu et al., 2005). It suggests that miRNAs may sequester target mRNAs from the translational machinery into P

bodies. Furthermore, other pieces of evidence suggest that miRNAs can stimulate the degradation of the nascent polypeptide (Nottrott et al., 2006; Olsen and Ambros, 1999). In plants, although several genes required for miRNA-mediated translation inhibition, such as the microtubule-severing enzyme, KATANIN and the P-body component VARICOSE (VCS), have been identified, their mechanisms of action still need to be addressed (Brodersen et al., 2008). A recent study showed that a portion of mature miRNAs and AGO1 is associated with polysomes in *Arabidopsis* (Lanet et al., 2009).

STERILE APETALA (*SAP*) was first identified as a negative regulator of *AG* (Byzova et al., 1999). In *sap* mutants, petals in early-raising flowers are narrower and shorter compared to those in wild-type flowers. In later-raising flowers, petals are almost absent and sepals are transformed to carpels bearing ovules at the inner side. These phenotypes are very similar to those of *ap2* flowers. Interestingly, in *sap* mutants, *AG* expression is expanded into the two outer whorls, sepals and petals, which is also observed in *ap2* mutants (Bowman et al., 1991; Drews et al., 1991). *AG* and *AP2* are homeotic genes that specify the identities of the inner two whorls (stamens and carpels) and the outer two whorls, respectively. Although *AP2* mRNA is expressed in all four whorls, AP2 protein levels are highter in the outer two whorls because miR172, which negatively regulates *AP2* expression via translational inhibition, is present at higher levels in the inner two whorls (Chen, 2004). *SAP* was thought to be a transcription factor because a serine-rich stretch (STSSSSS) is present at the N terminus of the protein (Byzova et al., 1999). However, no functional study has been performed to prove it.

Here, we report that *SAP* is a negative regulator of miRNA activity for a subset of miRNAs. Despite no observed changes of miRNA accumulation, the expression of several miRNA target genes was at lower levels in the *sap* mutant. In addition, despite no detectable changes in mRNA levels, the levels of AP2 and AGO1 proteins were reduced in *sap* mutants. This result suggests that *SAP* could be involved miRNA-mediated mRNA cleavage or translational inhibition by impeding miRNA activity. We have tried to uncover the mechanism of action of SAP by testing several hypotheses but have been unsuccessful in defining its molecular function. Furthermore, we also showed that some hc-siRNA target loci were more repressed in *sap* mutants with no effects on hc-siRNA accumulation, which suggests that *SAP* also acts as a negative regulator in hc-siRNA-mediated transcriptional gene silencing.

RESULTS

Isolation and characterization of a loss of function mutant of *SAP*

Ethyl methanesulfonate (EMS) mutagenesis was performed to identify players with potential roles in modulating miRNA biogenesis or activity in *Arabidopsis*. The *sap-2* mutant was isolated based on the phenotypic similarity to the *hen1* mutant. HEN1, which methylates mature miRNA duplexes and is an essential factor in miRNA biogenesis. *hen1* mutants exhibit pleiotropic developmental defects such as reduced organ size, hyponastic leaves, compact inflorescence and reduced fertility. The *sap-2* mutant had smaller organ size, flat leaves, compact inflorescence and was sterile (Fig. 1B, D).

Genetic crosses indicated that the pleiotropic phenotypes were caused by a single, recessive mutation. The mutation was mapped close to the BAC MXH1 on Chromosome 5. Searching candidate genes in this region revealed that a previously known loss of function mutant of *STERILE APETALA* (*SAP*), which is located on MXH1, has very similar phenotypes to those of our mutant. Sequence analysis revealed a G-to-A mutation in the *SAP* gene, which is at the 276th nucleotide in the second exon and results in a premature stop codon (Fig. 2). In addition, we obtained two T-DNA mutant lines of *SAP*, *sap-3* (SALK_109129) and *sap-4* (SALK_001593). The *sap-3* mutant exhibited similar developmental defects in the reproductive organs, whereas the vegetative organs showed weaker phenotypes compared to that of *sap-2*. The *sap-4* mutant is a weak allele, as the T-DNA is inserted in the *SAP* promoter region (Fig. 2).

SAP was identified as a negative regulator of *AG*, a floral homeotic gene, in a previous study (Byzova et al., 1999). *AP2*, which is a target of miR172, is a floral homeotic gene that restricts the expression of *AG* to the inner two floral whorls. In *sap* mutants, like in *ap2* mutants, *AG* expression was expanded into the two outer whorls. Since this study, nothing further has been published regarding the molecular function of *SAP*.

The expression of a subset of miRNA target genes is reduced in *sap* mutants

sap mutants exhibit very similar morphological phenotypes as those of *hen1* mutants. In addition, *AG* is ectopically expressed in *sap* mutants, which is also observed in *ap2* mutants. *AP2* is negatively regulated by miR172 via translational inhibition. These

results suggest that *SAP* could be involved in miR172 biogenesis or miR172-mediated repression of *AP2*. If AP2 levels are lower in the *sap* mutants due to higher miR172 or more active miR172, the ectopic *AG* expression could be nicely explained. To test this possibility, first we determined the levels of several miRNAs in inflorescences. None of the miRNAs was affected in the *sap-2* mutant (Fig. 3). Next, the mRNA levels of miRNA target genes were determined by real-time RT-PCR. Interestingly, transcripts of several miRNA target genes were present at lower levels (Fig. 4A). Moreover, the protein levels of some miRNA target genes such as AGO1, AP2 and Copper Superoxide Dismutase (CSD2) were also at reduced levels in *sap* mutants (Fig. 4B, C). In particular, CSD2 protein levels were unaffected under Cu^2+-replete conditions and were only reduced in the *sap-4* mutants under a low concentration of Cu^{2+} (Fig. 4B). *CSD2* is the target of the miR398. miR398 is highly expressed under low Cu^{2+} conditions, but not expressed under high Cu^{2+} conditions. Therefore, the reduced CSD2 protein levels in *sap-4* depends on miR398 activity. We also examined the levels of the APS protein, which is encoded by a gene that is also regulated by miR398, in *sap-2*, but no difference was observed (data not shown).

A subset of miRNAs is more active in *sap* mutants

Our results show that the transcripts of several miRNA target genes are at lower levels in *sap* mutants despite no changes of miRNA levels. To investigate whether this result reflects more active activities of miRNAs in the mutants, we examined the accumulation of the 3' cleavage products of miRNA target mRNAs in *sap* mutants. The

functional miRNA-AGO1 RISC cleaves the target mRNA in a sequence-specific manner. If the miRNAs are more active, we expect to see higher levels of 3' cleavage products. Because the 3' cleavage products are subjected to degradation by the exonuclease XRN4 (Souret et al., 2004), we sought to determine the abundance of the 3' cleavage products in the *xrn4* mutant background. A mutation of *XRN4* was introduced into *sap-2*.

We determined the levels of the 3' cleavage products of seven miRNA target genes by Northern blot analysis (Fig. 5A). The transcript level of *ARF17* was the most reduced in *sap-2* mutant and the accumulation of the *ARF17* 3' cleavage product was higher in the *xrn4-1 sap-2* double mutant compared to the *xrn4-1* single mutant (Fig. 5A, B, C). This result indicates that reduced *ARF17* transcript level in *sap* mutants is possibly caused by enhanced miR160 activity. The accumulation of the PHB 3' cleavage product was also higher in the *xrn4-1 sap-2* double mutant as compared to the *xrn4-1* single mutant (Fig. 5A, B, C). Transcripts of other genes were present at slightly lower levels in the *sap* mutants and the accumulation of the 3' cleavage products was similar in *xrn4-1 sap-2* and *xrn4-1* (Fig. 5A, B, C).

ta-siRNAs are at higher levels in *sap* mutants

miRNA-mediated cleavage of the *TAS* transcripts is required to trigger ta-siRNA biogenesis. If miRNAs are more active in *sap* mutants, we would expect to observe higher levels of ta-siRNAs in *sap* mutants. Indeed, the ta-siRNAs siR255 and siR1511 were at higher levels in the *sap* mutant (Fig. 6A). Although the difference was not large, it was consistent in three biological replicates. An increase in the TAS3-5D8(+) level in

the *sap* mutant was observed in two independent experiments but not in two other experiments (Fig, 6A). In addition, the expression of some ta-siRNA target genes was reduced in *sap* mutants (Fig. 6B).

SAP is present in the cytoplasm as well as the nucleus

SAP was first identified as a putative transcriptional regulator. However, our results indicate that *SAP* may affect miRNA activity. In general, miRNAs are functional in the cytoplasm after being exported from the nucleus. If *SAP* is really involved in modulating miRNA activity rather than acting as a transcriptional regulator, SAP protein must be present in cytoplasm. To test it, we transiently expressed the *35S::SAP-YFP* transgene in *Nicotiana Benthaminana* leaves. YPF signal was detected in the nucleus as well as the cytoplasm (Fig. 7).

SAP does not directly bind to short or long RNA *in vitro*

We have shown that *SAP* is involved in negatively modulating the activity of at least a sub set of miRNAs. Then, how does SAP serve as a nagative regulator in miRNA activity? It is possible that SAP directly binds to miRNAs to modulate their activity negatively or directly interacts with target mRNAs to protect them from being accessed by miRNAs. To investigate this possibility, we tested whether SAP can directly bind to 21 nt short RNAs or long RNAs *in vitro*.

A GST-fused recombinant SAP protein was purified from *E. coli*. The GST-SAP protein is somehow unstable, resulting in always the presence of truncated forms (Fig.

8A). First, GST-SAP was incubated with miR172-^{32}pCp. Our result showed that there was no difference in miR172-^{32}pCp binding efficiency between GST alone and GST-SAP (Fig. 8C). Next, we incubated the GST-SAP protein with an in vitro transcribed *SCL6* RNA fragment containing a wild type or a mutated version of the miR171 binding site. We did not observe specific binding of GST-SAP to either *SCL6* RNA compared to GST alone (Fig. 8B). These results indicate that SAP does not directly bind to short or long RNAs in vitro.

AGO1 slicer activity is not affected in *sap* mutants

AGO1 has endonuclease activity (slicer activity), which carries out miRNA-mediated target mRNA cleavage. It is possible that SAP acts in the miRNA-mediated mRNA cleavage process, negatively affecting AGO1 slicer activity. To test this hypothesis, we performed AGO1 slicer assay in vitro. First, AGO1 was immunoprecipitated by an AGO1 antibody from wild type (L*er*) and the *sap-3* mutant (Fig. 9A). Then, the same amount of purified AGO1 complex from L*er* and *sap-3* was incubated with an *in vitro* transcribed, 250 nt *ARF17* RNA fragment containing the miR160 binding site. There was no obvious difference in AGO1 slicer activity between wild type and the *sap-3* mutant (Fig. 9B). This result indicates that SAP does not affect AGO1 endonuclease activity.

SAP is not localized into P bodies

AP2 and AGO1 proteins were at lower levels in the *sap* mutants although their mRNA levels were not affected. This raised the possibility that SAP could be involved in miRNA-mediated translational inhibition. Processing bodies (P bodies) are the cytoplasmic foci where untranslated mRNAs are stored and mRNA decay takes place. Recently, it has been shown that miRNA-mediated translational inhibition occurs in P bodies in animal systems. It has been proposed that plants may also use the same mechanism for miRNA-mediated translational inhibition. It is possible that SAP promotes the subcellular localization of target mRNAs into P bodies. To test this possibility, we examined whether SAP is localized in P bodies. One of the P body markers, *DCP1* fused with *CFP* was transiently coexpressed with *SAP* fused with *YFP* under the 35S promoter (Fig. 10A, B). The CFP and YFP signals were largely non-overlapping with each other (Fig. 10C). It indicates that SAP is not localized in P bodies.

***SAP* does not affect the distribution of *AP2* and *AGO1* mRNAs in polysomes**

Another molecular mechanism to explain miRNA-mediated translational inhibition is the effects of the miRNAs on the translational process itself. In animals, it has been suggested that miRNAs repress translational initiation or elongation. A recent study discovered that a portion of mature miRNA-AGO1 RISCs is associated with polysomes in *Arabidopsis*. To investigate whether *SAP* affects the translational process of *AP2* and *AGO1* mRNAs, we carried out polysome profiling in L*er* and the *sap-2* mutant. Sucrose gradient centrifugation was used to obtain fractions containing monosomes and

polysomes with various numbers of monosomes. First, we determined the distribution of *UBIQUITIN5* mRNA in the fractions as a control (Fig. 11A). The pattern was almost the same in L*er* and *sap-2* samples. Next, we examined *AP2* and *AGO1* mRNA distribution in the fractions in L*er* and the *sap-2* mutant. From the monosomes to the polysomes, *AP2* and *AGO1* mRNA distribution in *sap-2* was very similar to that in L*er* (Fig. 11B, C). This result indicates that the distribution of *AP2* and *AGO1* mRNAs in polysomes is not affected in the *sap-2* mutant.

SAP is required for the expression of endogenous hc-siRNA loci

We showed that *SAP* negatively affects the activities of a subset of miRNAs. To investigate whether *SAP* affects endogenous hc-siRNA biogenesis or activity, we first determined the levels of several hc-siRNAs in *sap* mutants. In general, hc-siRNA accumulation was not affected in the *sap* mutant (Fig. 12). However, intriguingly, the expression of hc-siRNA-generating loci was at reduced levels in the *sap* mutant (Fig. 13A, B), suggesting that these loci are further repressed in the *sap* mutant. At present, it is not clear whether *SAP* function is hc-siRNA dependant, but it is possible that *SAP* is a negative factor in hc-siRNA-mediated gene silencing.

DISCUSSION

Is *SAP* a transcription factor?

SAP does not contain any known conserved domains except for a WD40 domain. WD40 domains usually play a role in protein-protein interactions, which are obviously

involved in almost all molecular processes. Therefore, it is hard to deduce the mechanism of action of *SAP* based on its protein sequence. In *sap* mutants, *AG* expression is expanded into the two outer whorls like in *ap2* mutants. In addition, SAP possesses a serine-rich stretch, which is often found in eukaryotic transcription factors. Based on these observations, *SAP* was proposed to be a transcriptional regulator. However, no molecular evidence has been shown to support this hypothesis. Transcription factors are localized in the nucleus to activate or repress target gene transcription. We determined the subcellular localization of the SAP protein in a transient expression system. Intriguingly, SAP protein was localized in the cytoplasm as well as in the nucleus (Fig. 7). This result does not rule out the possibility of SAP being a transcription factor but suggests that SAP also acts in cytoplasm.

SAP acts as a negative modulator of the activities of a subset of miRNAs

We showed that the levels of several miRNA target mRNAs were at reduced levels in *sap* mutants. However, it is possible that *SAP* generally affects gene transcription rather than modulating miRNA-mediated gene regulation. To address this question, we determined the accumulation of the 3' cleavage products of miRNA target genes, which are generated as a result of AGO1's endonucleolytic activity. The overall accumulation of the 3' cleavage products was at higher levels in *sap* mutants. In particular, the expression of *ARF17* was most affected in *sap* mutants, showing reduced mRNA expression and increased levels of 3' cleavage products (Fig. 5A, B and C). *ARF17* is a target of miR160. Our northern results showed that the accumulation of

miR160 is not affected in *sap* mutants (Fig. 3). This indicates that miR160 activity is enhanced in *sap* mutants and *SAP* negatively regulates miR160 activity.

Another piece of evidence is that the negative regulation of CSD2 expression in *sap* mutants is dependant on miR398 activity. Under low Cu^{2+} conditions in which miR398 is expressed, the levels of CSD2 protein were low in the *sap* mutant. In contrast, CSD2 levels were not affected in *sap* mutants under high Cu^{2+} conditions in which miR398 is not expressed (Fig. 4B). This implies that *SAP* function depends on miR398 activity.

However, it is not clear, how broadly *SAP* affects miRNA activity. It is unlikely that *SAP* acts as a general modulator of miRNA action as there are several miRNA target genes whose mRNA or protein levels are not affected by *SAP* (Fig. 5).

Probing the molecular function of *SAP*

How does *SAP* function as a negative regulator of miRNA activities? We have tested several possibilities. First, SAP directly interacts with miRNAs or target mRNAs (Fig. 8). Second, *SAP* affects AGO1 endonuclease activity (Fig. 9). Third, *SAP* promotes the subcellular localization of target mRNAs into P bodies (Fig. 10). Finally, *SAP* affects translational efficiency of target mRNAs (Fig. 11). The experiments conducted towards testing these hypotheses all yielded negative results. However, this does not necessarily lead to the nullification of these hypotheses. For the first hypothesis, it is still possible that SAP indirectly interacts with miRNAs or target mRNAs in vivo. It could be addressed by conducting immunoprecipitation of the SAP protein followed by detection

for the presence of miRNAs. Although SAP is not localized in P bodies, it cannot be ruled out that it inhibits the sequesteration of miRNA target mRNAs in P bodies. In the absence of clues to the molecular function of *SAP*, perhaps the identification of SAP interacting proteins will provide leads for further investigation. We need to immunoprecipitate SAP and identify co-purifying components by mass spectrometry.

Functional relationship between *SAP* and hc-siRNA

We have shown that the expression of hc-siRNA target loci was reduced in *sap* mutants although hc-siRNA accumulation was not affected (Fig. 13). This raises two possibilities. First, *SAP* negatively modulates hc-siRNA activities. Second, *SAP* acts independently of hc-siRNAs to regulate heterochromatic gene expression. Whether *SAP* acts in the siRNA pathway can be addressed by introducing a mutation in hc-siRNA biogenesis genes such as RDR2 or Pol IV into *sap* mutants and determining the expression level of hc-siRNA target loci. If *SAP* acts in the same pathway as hc-siRNAs, the expression level of hc-siRNA target loci would not be affected in double mutants compared to single mutants of hc-siRNA biogenesis genes.

MATERIALS AND METHODS

Plant Materials

All mutants are in the L*er* background. *Arabidopsis* plants were grown at 24°C under continuous light. The T-DNA insertion lines *sap-3* and *sap-4* were obtained from the Salk Institute Genomic Analysis Laboratory. *xrn4-1* was a gift form Dr. Sablowski.

For CSD2 Western blot analysis, 9-day-old seedlings, which were grown on MS plates with or without Cu^{2+} (10uM), were harvested and the same amount of seedings was used for each experiment.

Map-based Cloning of *SAP*

sap-2 (L*er*) was crossed to Col. In the F2 population, plants showing *sap-2* phenotypes were collected as the mapping population. Initially, 25 *sap-2* plants were used for rough mapping, which revealed that *sap-2* was linked to the marker PHYC on chromosome 5. For the fine mapping, we designed new SSLP or CAPS markers in this region according to polymorphisms between L*er* and Col, using the Monsanto *Arabidopsis* polymorphism and L*er* sequence database (http://www.arabidopsis.org/Cereon). Using these markers, we mapped *SAP* to a region around the BAC MXH1. Then, sequencing analysis was conducted with candidate genes.

Genotyping

For the *sap-2* genotyping, genomic DNA was amplified with SAP-F2 (GAGTCTTTCATGCTTCGTTG) and SAP-R3 (AGAGGTCTGAGAGGGTGAGA) primers and PCR products from wild type could be digested by AluI, whereas those from *sap-2* could not. For *sap-3 and sap-4* genotyping, SALK_109129LP (TGGGCATTGGACTAAAGACTG)/SALK_109129RP (CCTTTTCTTGAATCTCTCG

CC) and SALK_001593LP (AAACACAGAAAGGGCGGTTAC)/ SALK_001593RP (GTCGAGATTTGGTGCTACGAG) primers, respectively, were used in combination with the LBa1 primer.

Plasmid Construction

For *35S::SAP-YFP* plasmid construction, *SAP* cDNA was amplified with SAP-F5 (caccggatccatgtctacctcctcctcttc)/SAP-R6 (tatctcgagtgcagtgcaccgaaatcccata) primers and cloned into the entry vector, pENTR1a (Invitrogen). Then, the entry clone was introduced into the pEG101 vector by LR reaction. DCP1-CFP was a gift from Dr. Chua (Xu et al., 2006)

Small RNA Northern Blot Analysis

RNA isolation and hybridization for miRNAs and endogenous siRNAs were performed as described (Park et al., 2002). 10ug total RNA and 5ug small RNA-enriched RNA from inflorescence were used for miRNAs and endogenous siRNAs northern blots, respectively. 5′-End-labeled ^{32}P antisense DNA oligonucleotides or LNA oligonucleotides were used to detect miRNAs and endogenous siRNAs. Oligo probes used are listed table 3.3.

RT-PCR

Total RNA from inflorescence was reverse-transcribed using SuperScriptII (Invitrogen) and oligo-d(T) primers according to the manufacturers' instructions. For pri-

miRNA detection, quantitative PCR was performed in triplicate on a Bio-Rad IQcycler apparatus with the Quantitech SYBR green kit (Bio-Rad). To determine the expression of endogenous siRNA loci, RT-PCR products were separated on agarose gels and stained with ethidium bromide. Primers used are listed in Table 3.1 and 3.4.

mRNA Northern Blot Analysis

Total RNA was isolated from inflorescence and then Poly(A)$^+$ mRNA was isolated according to manufacturers' instructions (Promega, PolyATtract® mRNA Isolation Systems). 1ug poly(A)$^+$ mRNA from each sample was resolved in 1.2% agarose formaldehyde gels, transferred to Nylon membranes, and hybridized to a labeled cDNA fragment for 16-18 hr. Then, the membrane was washed with 2X SSC/0.1% SDS and 1X SSC/0.1% SDS, respectively. To generate the probe, a gene-specific cDNA region was amplified and this product was labeled using the random priming method (GE health). Radioactive signals were quantified using a Phosphorimager. Primers used are listed in Table 3.2.

***In vitro* RNA binding assay**

RNA binding assays were performed as described (Trifillis P et al., 1999; Jiao X et al., 2002). Briefly, 5'-end-labeled miR172-^{32}pCp and *SCL6/SCL6m* RNA fragments, which were generated by *in vitro* transcription in the presence of [α-^{32}P] UTP, were incubated with sepharose beads-conjugated GST and GST-SAP protein (50ug each) at 4 °C and washed. Any remaining miR172 or *SCL6* RNA on the beads was resolved in 15%

and 5% polyacrylamide gels, respectively, and radioactive signals were quantified using a Phosphorimager.

Sucrose Density Gradient Analysis

Sucrose density gradient analysis was conducted as described (Mustroph A. et al., 2009). 2ml volumes of ground inflorescence tissues were combined with ice-cold polysome extraction buffer. After centrifugation at 4 °C, 16,000g for 15 min, the clarified extract was gently poured on the top of a sucrose cushion buffer. Then it was centrifuged at 4 °C, 116,000 g (35,000 rpm, TY 70T1 rotor) overnight. The polysome pellet was resuspended in ice-cold resuspension buffer and polysome profiles were generated by sucrose gradient ultracentrifugation at 4 °C, 237,000 g (50,000 RPM, SW55.1 rotor) for 1.5 hr. After centrifugation, 12 fractions were collected from the top to bottom. RNA was extracted from each fraction by the Trizol method and RNA distribution was determined by RT-PCR.

Transient Expression in *N. benthamiana*

Agrobacterium containing *35S::SAP-YFP* was cultured overnight at 28°C in 10ml LB media with antibiotics. Cells were pelleted by centrifugation at 1,000g for 10 min at room temperature and washed with infiltration media (10mM $MgCl_2$) two times. Finally, cells were resuspended in infiltration media at a final O.D. of 0.5-0.8. Then, the resuspended *Agrobacterium* was infiltrated into *Nicotiana Benthamiana* leaves. After 2-3

days, the expression of fluorescent fusion protein was detected by confocal microscopy on Zeiss 510.

AGO1 Slicer Assay

AGO1 slicer assay was performed as described (Baumberger and Balcombe, 2005). Flag-AGO1 was immunoprecipitated from the inflorescence of a *Flag-AGO1* transgenic line. The α-FLAG M2 agarose beads were washed twice in RNA-induced silencing complex (RISC) buffer (40 mM Hepes, pH7.4/100 mM KOAc/5 mM MgOAc/4 mM DTT), and Bead-conjugated FLAG-AGO1 was assembled in a reaction containing 1 mM ATP, RNase inhibitors, and ^{32}P-labeled *in vitro* transcribed target RNA.

REFERENCES

Bowman, J.L., Smyth, D.R., and Meyerowitz, E.M. (1991). Genetic interactions among floral homeotic genes of Arabidopsis. Development *112*, 1-20.

Byzova, M.V., Franken, J., Aarts, M.G.M., de Almeida-Engler, J., Engler, G., Mariani, C., Campagne, M.M.V., and Angenent, G.C. (1999). Arabidopsis *STERILE APETALA*, a multifunctional gene regulating inflorescence, flower, and ovule development. Genes Dev *13*, 1002-1014.

Chen, X. (2004). A microRNA as a translational repressor of *APETALA2* in Arabidopsis flower development. Science *303*, 2022-2025.

Cougot, N., Babajko, S., and Seraphin, B. (2004). Cytoplasmic foci are sites of mRNA decay in human cells. J Cell Biol *165*, 31-40.

Drews, G.N., Bowman, J.L., and Meyerowitz, E.M. (1991). Negative regulation of the Arabidopsis homeotic gene *AGAMOUS* by the *APETALA2* product. Cell *65*, 991-1002.

Eulalio, A., Behm-Ansmant, I., and Izaurralde, E. (2007). P bodies: at the crossroads of post-transcriptional pathways. Nat Rev Mol Cell Biol *8*, 9-22.

Franks, T.M., and Lykke-Andersen, J. (2007). TTP and BRF proteins nucleate processing body formation to silence mRNAs with AU-rich elements. Genes Dev *21*, 719-735.

Humphreys, D.T., Westman, B.J., Martin, D.I.K., and Preiss, T. (2005). MicroRNAs control translation initiation by inhibiting eukaryotic initiation factor 4E/cap and poly(A) tail function. Proc Natl Acad Sci U S A *102*, 16961-16966.

Jiao, X.F., Trifillis, P., and Kiledjian, M. (2002). Identification of target messenger RNA substrates for the murine deleted in azoospermia-like RNA-binding protein. Biol Reprod *66*, 475-485.

Kiriakidou, M., Tan, G.S., Lamprinaki, S., De Planell-Saguer, M., Nelson, P.T., and Mourelatos, Z. (2007). An mRNA m(7)G cap binding-like motif within human Ago2 represses translation. Cell *129*, 1141-1151.

Lanet, E., Delannoy, E., Sormani, R., Floris, M., Brodersen, P., Crete, P., Voinnet, O., and Robaglia, C. (2009). Biochemical Evidence for Translational Repression by Arabidopsis MicroRNAs. Plant Cell *21*, 1762-1768.

Liu, J.D., Valencia-Sanchez, M.A., Hannon, G.J., and Parker, R. (2005). MicroRNA-dependent localization of targeted mRNAs to mammalian P-bodies. Nat Cell Biol *7*, 719-U118.

Maroney, P.A., Yu, Y., Fisher, J., and Nilsen, T.W. (2006). Evidence that microRNAs are associated with translating messenger RNAs in human cells. Nat Struct Mol Biol *13*, 1102-1107.

Mustroph, A., Juntawong, P., Bailey-Serres, J. (2009). Isolation of plant polysomal mRNA by differential centrifugation and ribosome immuopurification methods. Methods Mol Biol *553*, 109-126.

Nottrott, S., Simard, M.J., and Richter, J.D. (2006). Human let-7a miRNA blocks protein production on actively translating polyribosomes. Nat Struct Mol Biol *13*, 1108-1114.

Olsen, P.H., and Ambros, V. (1999). The lin-4 regulatory RNA controls developmental timing in Caenorhabditis elegans by blocking LIN-14 protein synthesis after the initiation of translation. Dev Biol *216*, 671-680.

Park, W., Li, J.J., Song, R.T., Messing, J., and Chen, X. (2002). CARPEL FACTORY, a Dicer homolog, and HEN1, a novel protein, act in microRNA metabolism in Arabidopsis thaliana. Curr Biol *12*, 1484-1495.

Petersen, C.P., Bordeleau, M.E., Pelletier, J., and Sharp, P.A. (2006). Short RNAs repress translation after initiation in mammalian cells. Mol Cell *21*, 533-542.

Pillai, R.S. (2005). MicroRNA function: Multiple mechanisms for a tiny RNA? RNA *11*, 1753-1761.

Pillai, R.S., Bhattacharyya, S.N., Artus, C.G., Zoller, T., Cougot, N., Basyuk, E., Bertrand, E., and Filipowicz, W. (2005). Inhibition of translational initiation by Let-7 microRNA in human cells. Science *309*, 1573-1576.

Sen, G.L., and Blau, H.M. (2005). *Argonaute 2*/RISC resides in sites of mammalian mRNA decay known as cytoplasmic bodies. Nat Cell Biol *7*, 633-U628.

Sheth, U., and Parker, R. (2003). Decapping and decay of messenger RNA occur in cytoplasmic processing bodies. Science *300*, 805-808.

Souret, F.F., Kastenmayer, J.P., and Green, P.J. (2004). AtXRN4 degrades mRNA in Arabidopsis and its substrates include selected miRNA targets. Mol Cell *15*, 173-183.

Trifillis, P., Day, N., and Kiledjian, M. (1999). Finding the right RNA: Identification of cellular mRNA substrates for RNA-binding proteins. RNA *5*, 1071-1082.

Xu, J., Yang, J.Y., Niu, Q.W., and Chua, N.H. (2006). Arabidopsis DCP2, DCP1, and VARICOSE form a decapping complex required for postembryonic development. Plant Cell *18*, 3386-3398.

Zheng, B., Wang, Z., Li, S., Yu, B., Liu, J., and Chen, X. (2009). Intergenic transcription by RNA Polymerase II coordinates Pol IV and Pol V in siRNA-directed transcriptional gene silencing in Arabidopsis. Genes Dev (in press).

Figure 3.1 Phenotypes of *sap-2* mutants

(A) A L*er* seedling.

(B) A *sap-2* seedling with smaller organ size and flat leaves.

(C) A L*er* inflorescence.

(D) A *sap-2* inflorescence, which is more compact compared to that of L*er*.

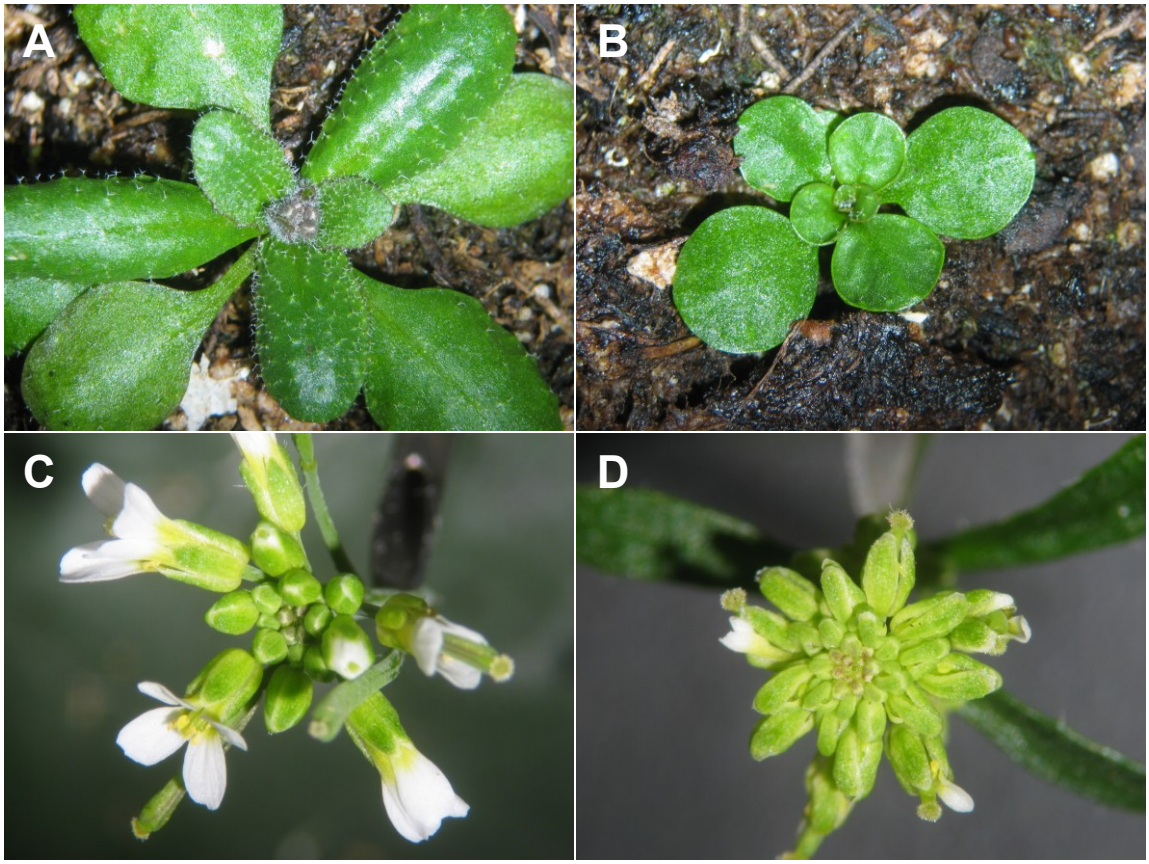
A
B
C
D

Figure 3.2 The structure of the *SAP* gene

A schematic diagram of the *SAP* gene showing the mutation (G to A) in the second exon (asterisk) in *sap-2*. Red triangles represent T-DNA insertions. *sap-3* (SALK_109129) has a T-DNA insertion in the first intron and *sap-4* (SALK_001593) has a T-DNA inserted in the promoter. The black rectangles represent protein-coding regions.


sap-4
sap-2
G→A
*
sap-3

Figure 3.3 The accumulation of miRNAs in the *sap-2* mutant

The accumulation of miRNAs was determined in L*er* and the *sap-2* mutant by small RNA Northern blotting. Total RNAs were extracted from inflorescences. Overall miRNA accumulation was not obviously different between L*er* and *sap-2*.

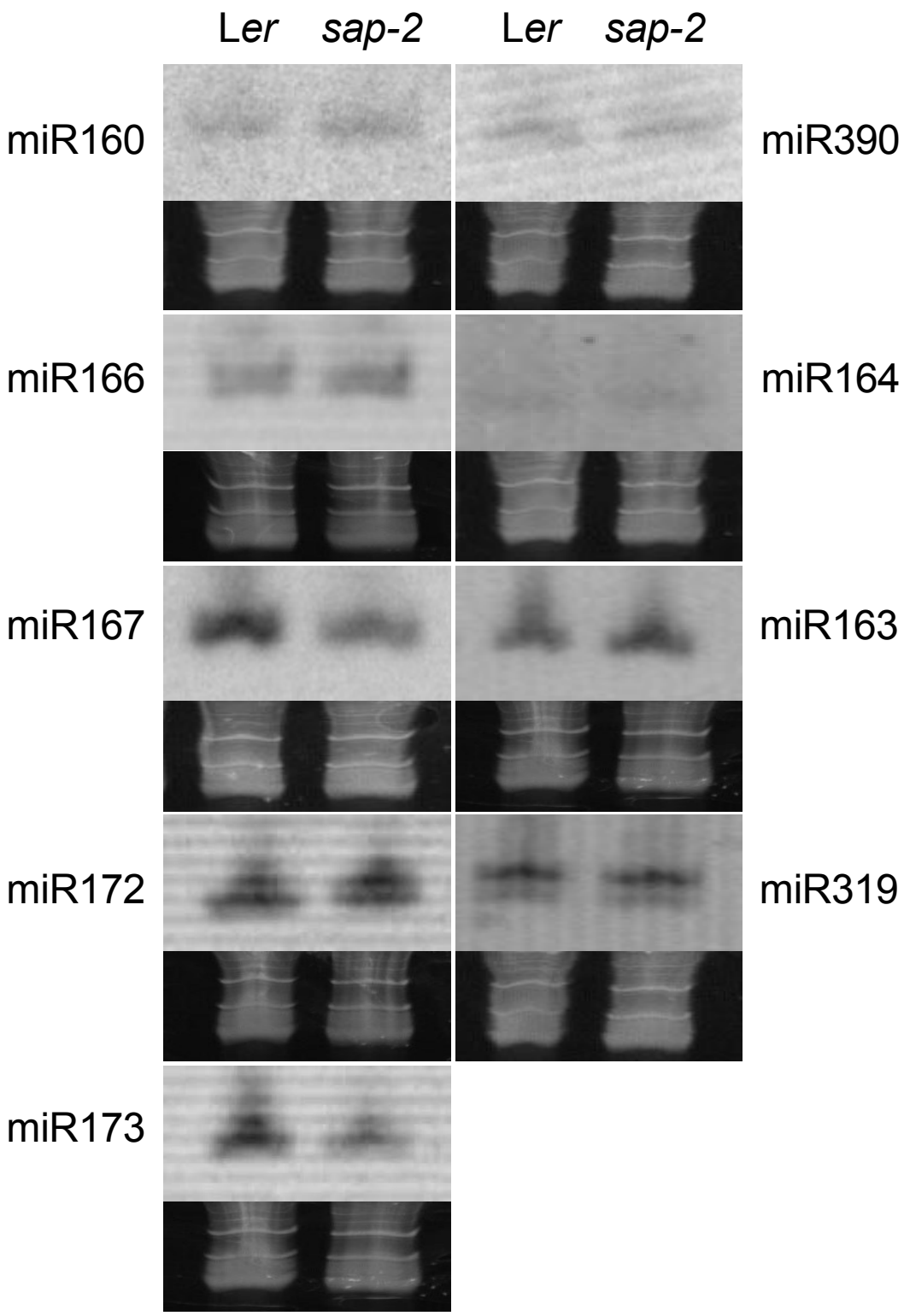
Ler
sap-2
Ler
sap-2
miR160
miR390
miR166
miR164
miR167
miR163
miR172
miR319
miR173

Figure 3.4 The mRNA and protein levels of several miRNA target genes in *sap-2*

(A) The transcript levels of several miRNA target genes were determined by real-time RT-PCR in L*er* and *sap-2*. The levels of all examined transcripts except *SPL10* were decreased in the *sap-2* mutant. The RNAs were extracted from inflorescences. The transcript levels of miRNA target genes were normalized to those of *UBIQUITIN* 5 and compared to Col.

(B) The protein levels of some miRNA targets were determined by Western Blotting in L*er*, *sap-3*, or *sap-4*. 9-day-old seedlings grown in MS plates with or without Cu2+ (10uM) were used to determine CSD2 levels. The levels of CSD2 were moderately reduced in the *sap-3* mutant. Inflorescence tissue was used to determine AGO1 and AP2 levels. The levels of AGO1 and AP2 were reduced in the *sap-3* mutant.

A

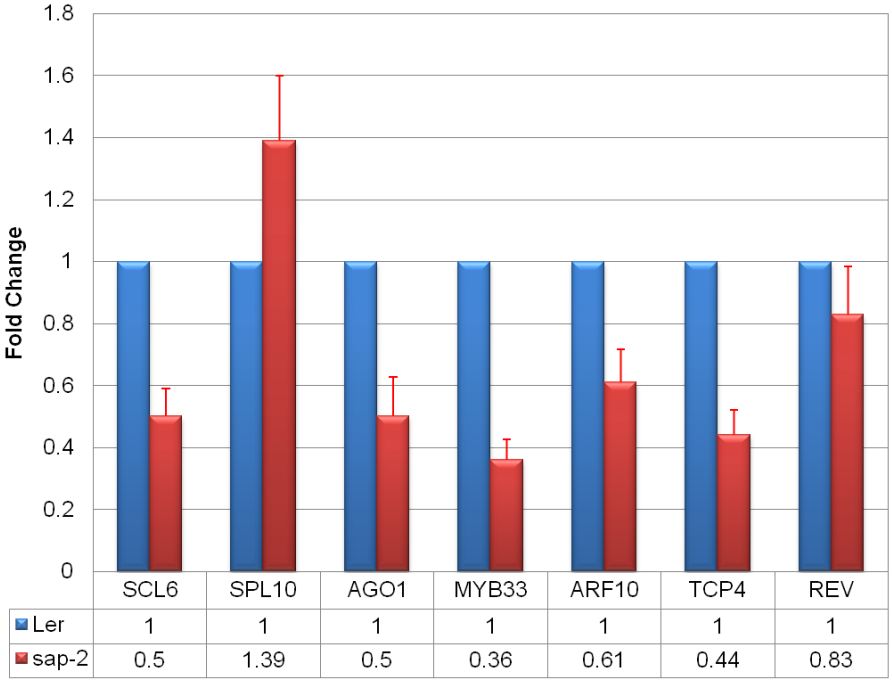

	SCL6	SPL10	AGO1	MYB33	ARF10	TCP4	REV
Ler	1	1	1	1	1	1	1
sap-2	0.5	1.39	0.5	0.36	0.61	0.44	0.83

B

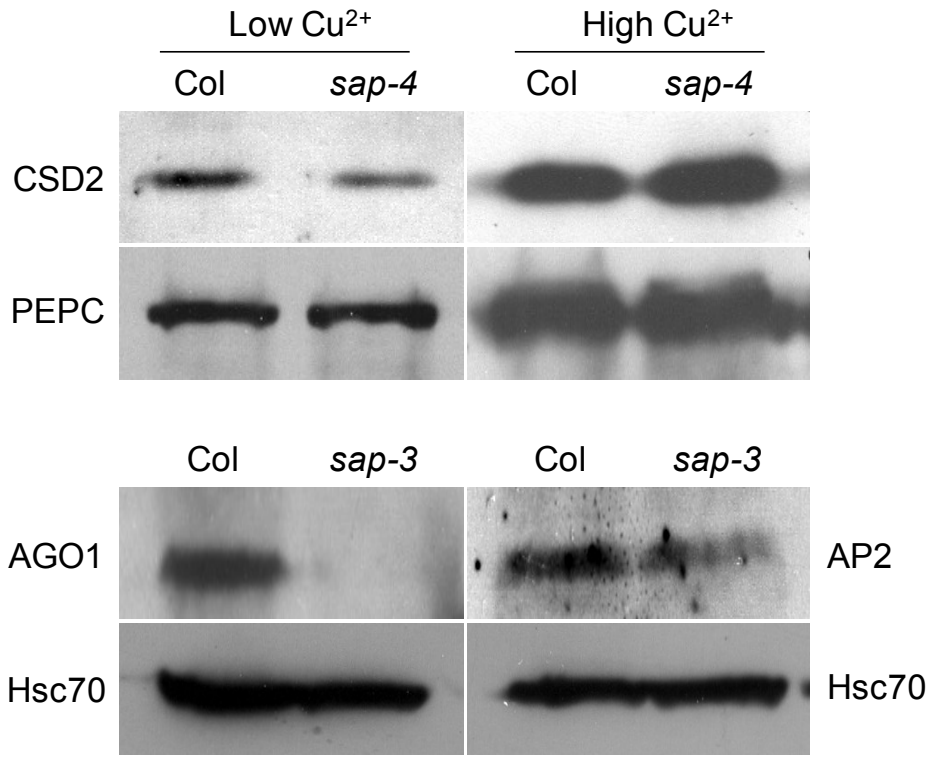

Figure 3.5 Transcripts of several miRNA target genes in L*er*, *sap-2*, *xrn4-1* and *xrn4-1 sap-2*

(A) The accumulation of full-length mRNAs and 3' cleavage products from several miRNA target genes was determined by Northern blot analysis. Total RNAs were isolated from inflorescences and poly(A)$^+$ RNA was isolated. 1ug poly(A)$^+$ RNA was resolved on 1.2% agarose/formaldehyde gels. *UBIQUITIN5* was used as an internal control. The red and blue asterisks indicate full length transcripts and 3' cleavage products, respectively.

(B) Real-time RT-PCR was performed to examine the levels of transcripts from miRNA target genes in L*er*, *sap-2, xrn4-1* and *xrn4-1 sap-2*. The primers flank the miRNA target sites in each gene such that levels of non-cleaved mRNAs were measured. The expression of *ARF17* was the most reduced in *sap-2* and *xrn4-1 sap-2* as compared to L*er* and *xrn4-1*, respectively, among the seven tested genes.

(C) The accumulation of 3' cleavage products in *sap-2* or *xrn4-1 sap-2* was compared to that of L*er* or *xrn4-1*, respectively. The relative level of the 3' cleavage product (*sap-2*/L*er* or *xrn4-1 sap-2/xrn4-1*) was divided by the relative level of the full-length mRNA (*sap-2*/L*er* or *xrn4-1 sap-2/xrn4-1*). The 3' cleavage product accumulation from *ARF17* was at the highest level in *sap-2* and *xrn4-1 sap-2* compared to L*er* and *xrn4-1*, respectively, among the genes tested.

A

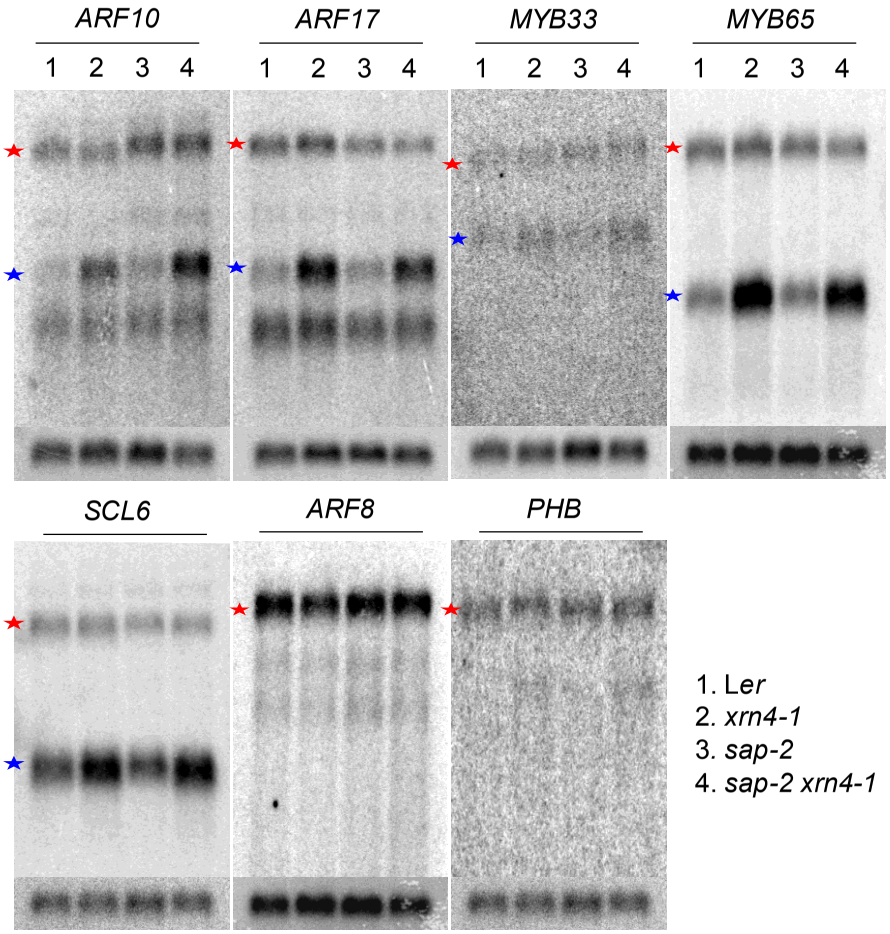

B

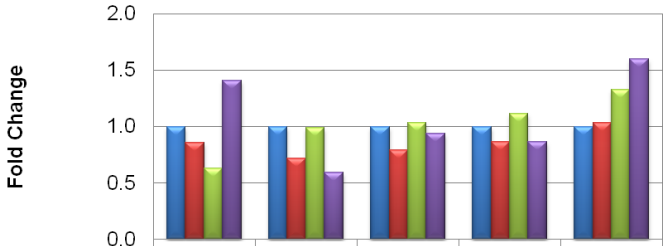

	ARF10	ARF17	MYB65	SCL6	MYB33
Ler	1	1	1	1	1
sap-2	0.8567	0.7204	0.7915	0.8625	1.0366
xrn4-1	0.6296	0.9881	1.0334	1.1128	1.3265
sap-2 xrn4-1	1.4099	0.5898	0.9412	0.8676	1.5981

C

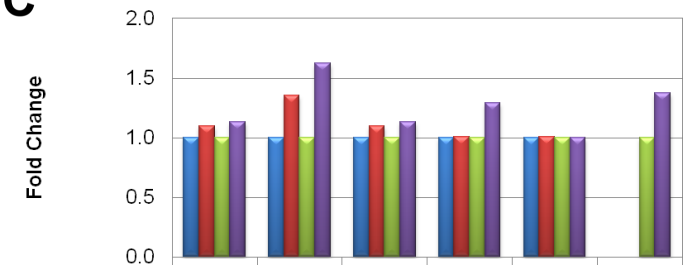

	ARF10	ARF17	MYB65	SCL6	MYB33	PHB
Ler	1	1	1	1	1	
sap-2	1.0967	1.3561	1.0967	1.0046	1.0090	
xrn4-1	1	1	1	1	1	1
sap-2 xrn4-1	1.1361	1.6283	1.1361	1.2894	1.0040	1.3749

Figure 3.6 The accumulation of ta-siRNAs and ta-siRNA target transcripts

(A) The levels of ta-siRNAs were determined in L*er* and *sap-2* by small RNA Northern blotting. The accumulation of ta-siRNAs was slightly increased in *sap-2*.

(B) The transcript levels of ta-siRNA target genes were determined by real-time RT-PCR. The expression of *ARF3* and *At4g19770* was at the lower levels in *sap-2*.

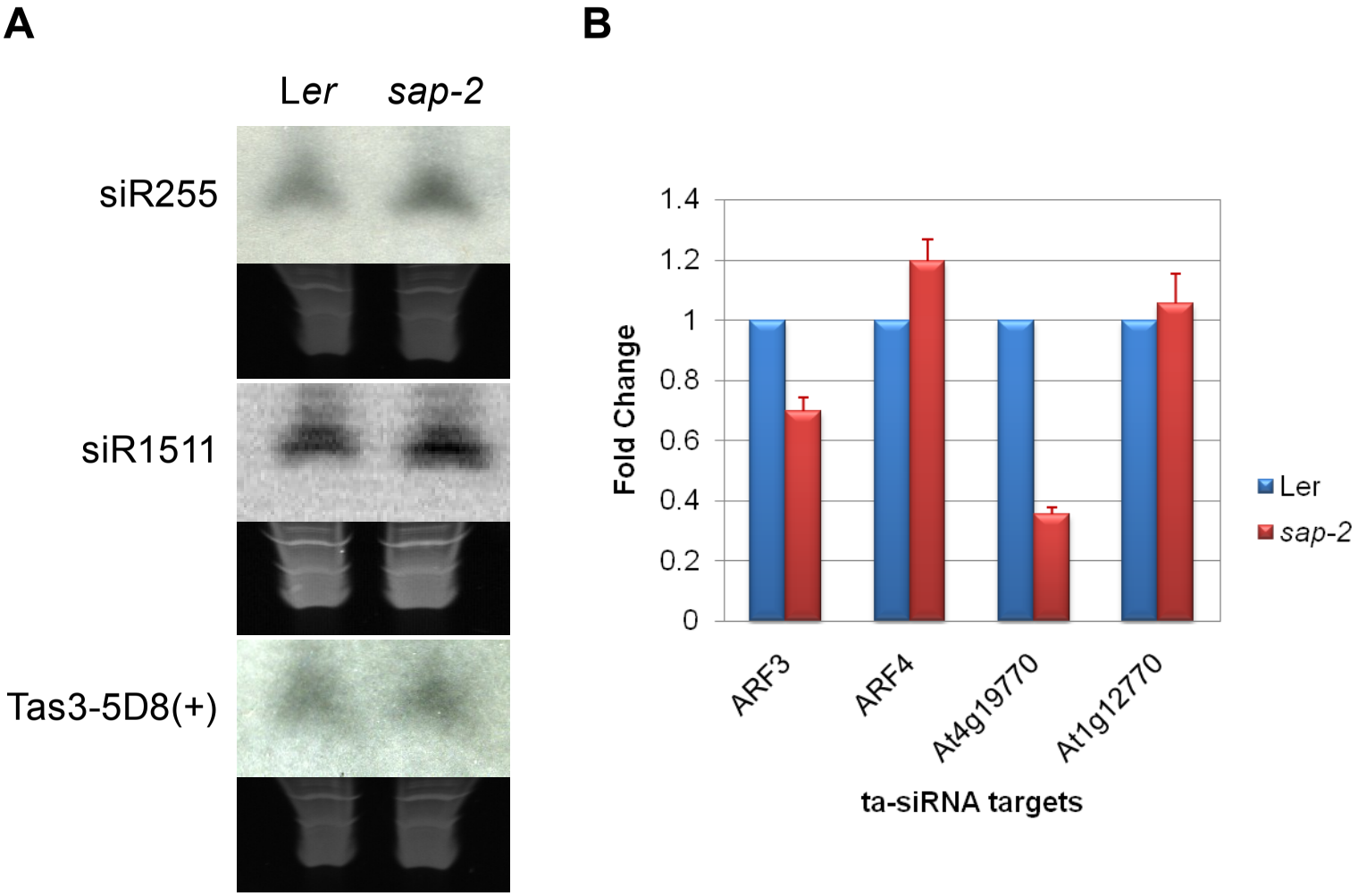
A
Ler
sap-2
siR255
siR1511
Tas3-5D8(+)
B
Fold Change
1.4
1.2
1
0.8
0.6
0.4
0.2
0
ARF3
ARF4
At4g19770
At1g12770
ta-siRNA targets
Ler
sap-2

Figure 3.7 Subcelluar localization of the SAP protein

35S::SAP-YFP was transiently expressed in *Nicotiana Benthaminana* leaves. YFP signal is localized in the cytoplasm and the nucleus.

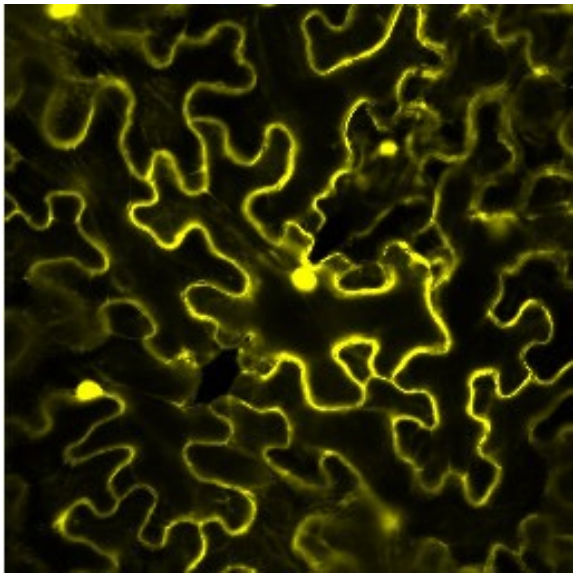

Figure 3.8 *In vitro* RNA binding assay

(A) GST and GST-SAP proteins were purified and resolved on an SDS/polyacrylamide gel. The red and blue arrowheads indicate the GST-SAP protein and the truncated GST-SAP, respectively.

(B) GST and GST-SAP proteins were incubated with *in vitro* transcribed ^{32}P-*SCL6/SCL6m* RNA fragments. SAP does not bind to either RNA *in vitro*.

(C) GST and GST-SAP proteins were incubated with ^{32}P-labeled miR172. SAP does not bind to miR172 *in vitro*.

A
GST
GST-SAP
BSA
B
SCL6
input
GST
GST-SAP
SCL6m
input
GST
GST-SAP
C
miR172
input
GST
GST-SAP

Figure 3.9 AGO1 slicer assay

(A) The AGO1 protein was purified by immunoprecipitation with anti-AGO1 antibodies. The amount of AGO1 in the IP was quantified by Western blot analysis.

(B) An *in vitro* transcribed ^{32}P-*ARF17* RNA fragment was incubated with AGO1 immunoprecipitates from Col and *sap-3* or from the FLAG-AGO1 transgenic line as a positive control. AGO1 slicer activity is not affected by the *sap-3* mutation.

A

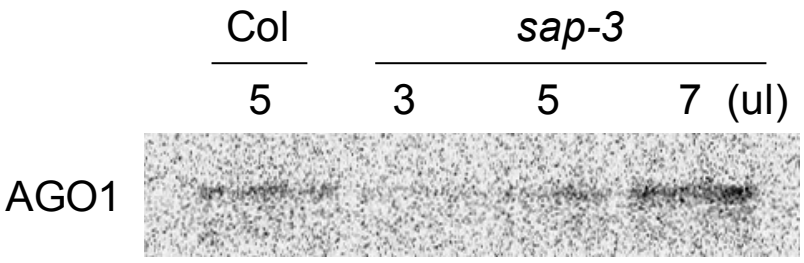
Col
sap-3
5
3
5
7 (ul)
AGO1

B

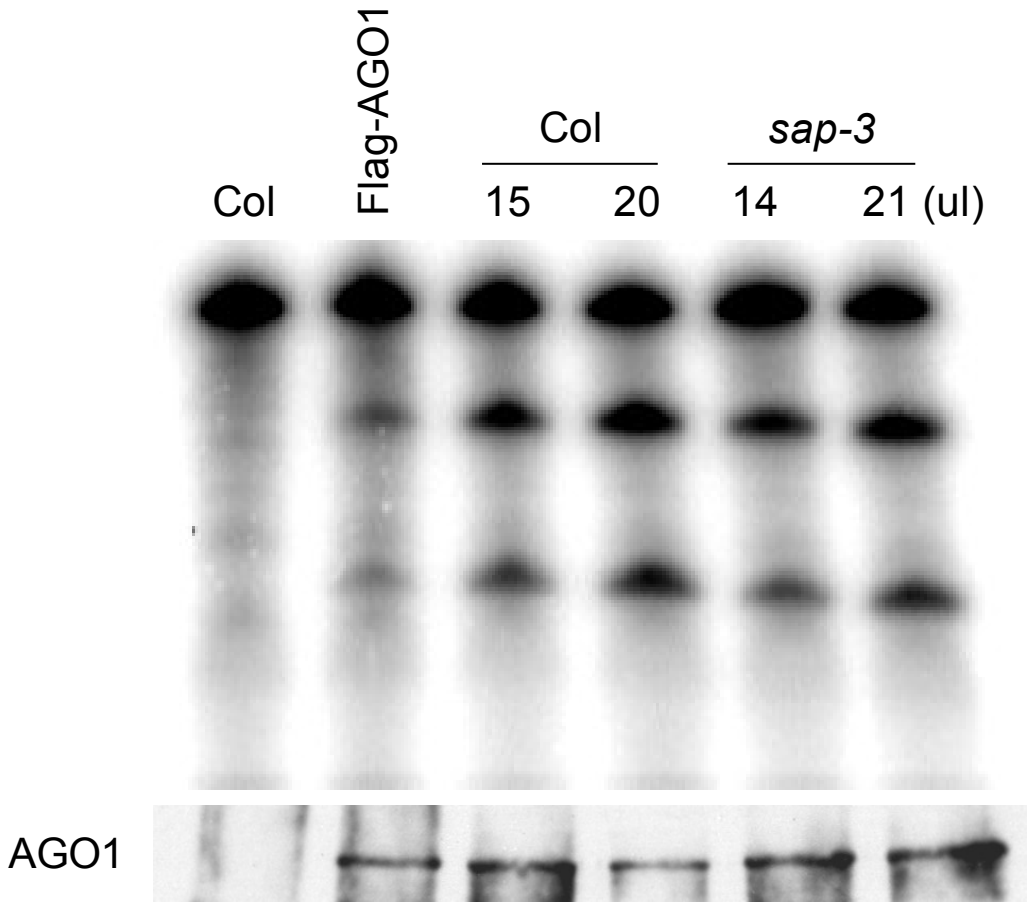
Col
Flag-AGO1
Col
sap-3
Col
15
20
14
21 (ul)
AGO1

Figure 3.10 Subcellular localization of DCP1 and SAP

Subcellular localization of SAP-YFP was compared with that of DCP1-CFP in tobacco epidermal cells. SAP is not co-localized with this P-body marker.

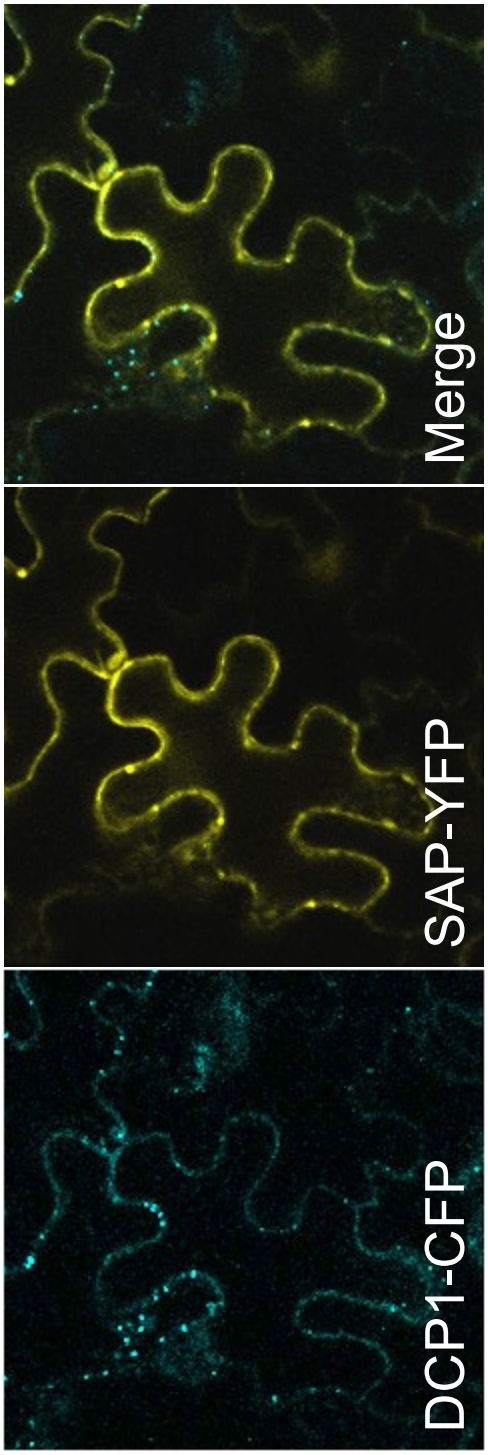
Merge
SAP-YFP
DCP1-CFP

Figure 3.11 Distribution of mRNAs in polysome fractions

In the top panel, absorbance at 254 nm is shown from the lighter (left) to the heavier (right) fractions of the continuous sucrose gradient. Polysomes were purified from inflorescences through sucrose gradients as described in Methods.

In the bottom panel, total RNA was extracted from each fraction and cDNA was synthesized. *AP2* and *AGO1* mRNA distribution was determined by RT-PCR from each fraction and the distribution pattern was compared to that of *UBIQUITIN* 5 as a control.

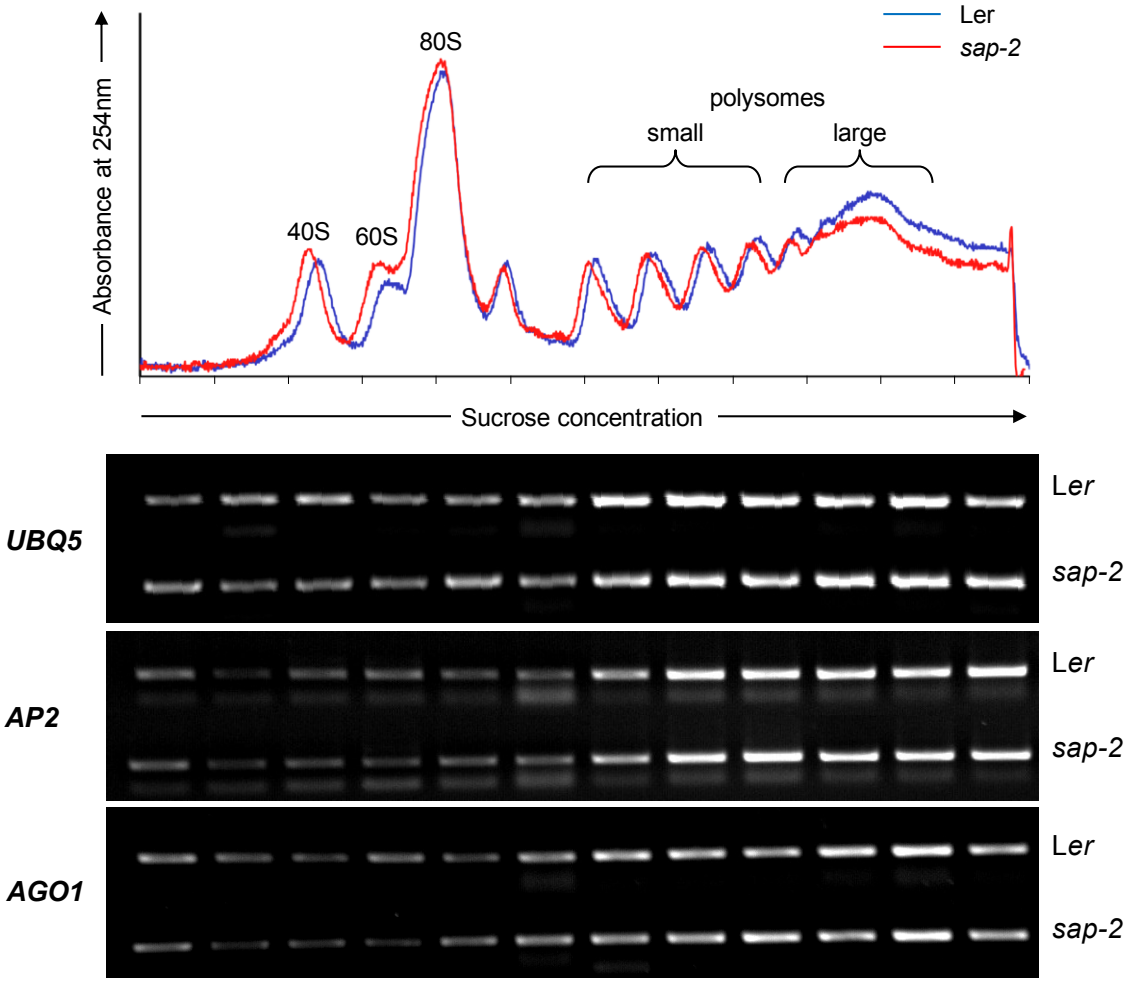
Ler
sap-2
80S
polysomes
small
large
40S
60S
Absorbance at 254nm
Sucrose concentration
UBQ5
AP2
AGO1
Ler
sap-2
Ler
sap-2
Ler
sap-2

Figure 3.12 The accumulation of hc-siRNAs in the *sap-2* mutant

The accumulation of hc-siRNAs was determined in L*er* and the *sap-2* by small RNA Northern blotting. Total RNAs were extracted from inflorescences. Overall hc-siRNA accumulation was not changed in the *sap-2* mutant.

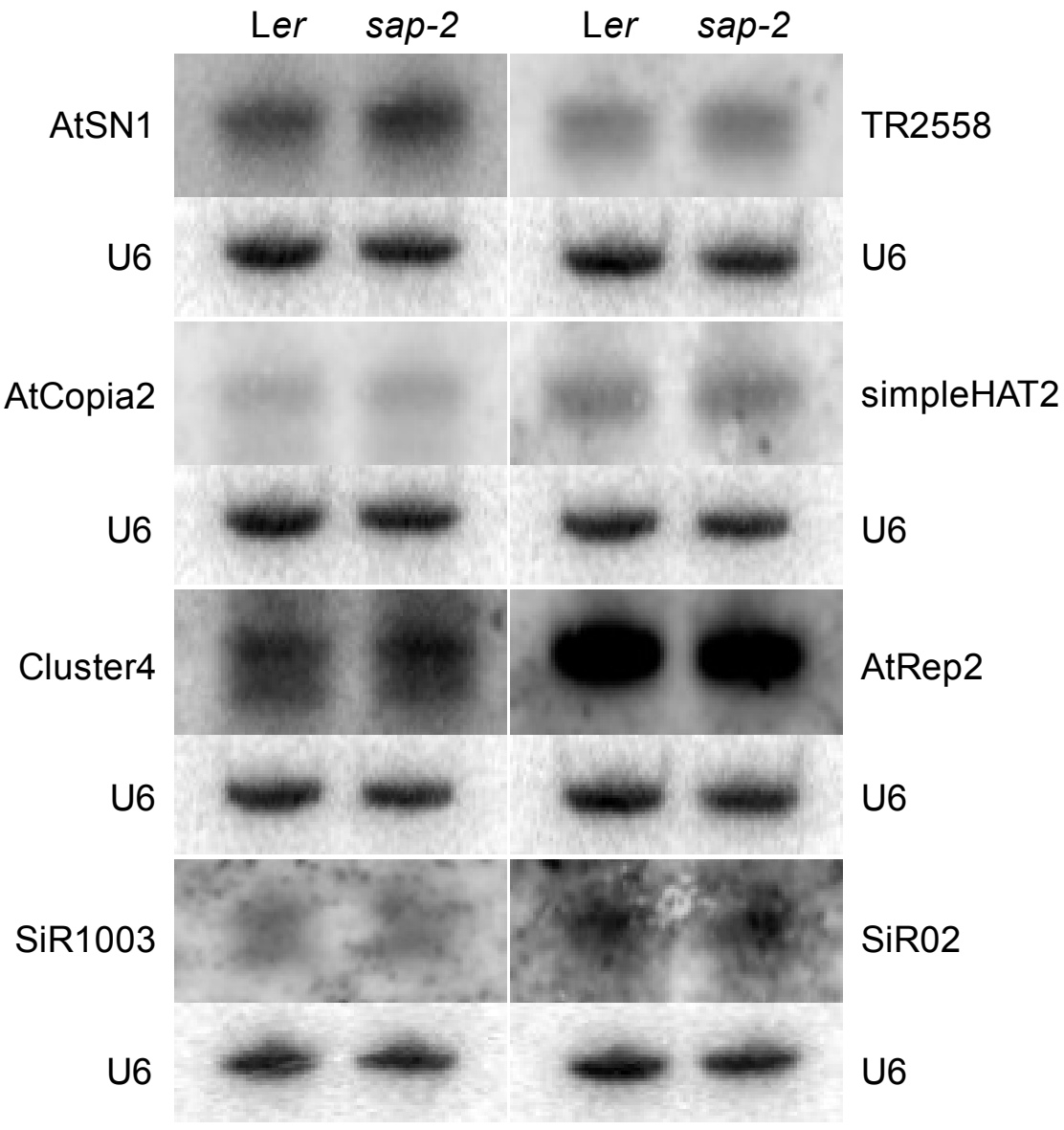
Ler
sap-2
Ler
sap-2
AtSN1
TR2558
U6
U6
AtCopia2
simpleHAT2
U6
U6
Cluster4
AtRep2
U6
U6
SiR1003
SiR02
U6
U6

Figure 3.13 The expression of hc-siRNA target loci in *sap* mutants

The expression of several hc-siRNA target loci was determined in L*er* and *sap-2* by real-time RT-PCR (A) and in Col and *sap-3* by semi-quantitative RT-PCR (B).

(A) The transcript levels of each locus were normalized to *UBIQUITIN 5* and compared to L*er*.

(B) Total RNAs were extracted from inflorescences. RT-PCR products were resolved on the 1.2% agarose gels and *UBIQUITIN 5* was used as an internal control.

A

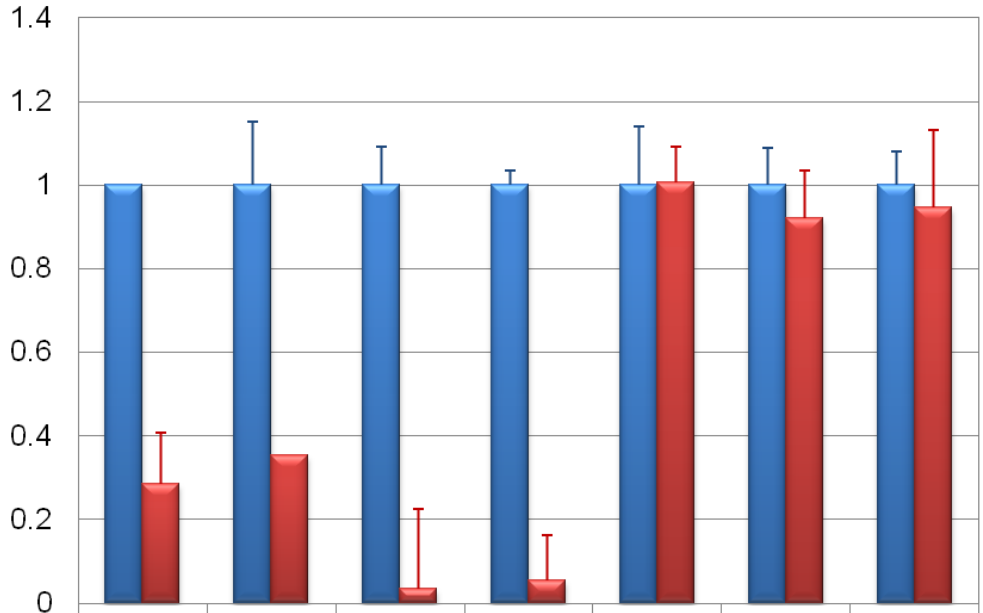

	AtSN1	AtMU1	AtLine4	AtGP1	Atcopia1	AGO4	RDR2
Ler	1	1	1	1	1	1	1
sap-2	0.2862	0.3536	0.0346	0.0552	1.0070	0.9202	0.9461

B

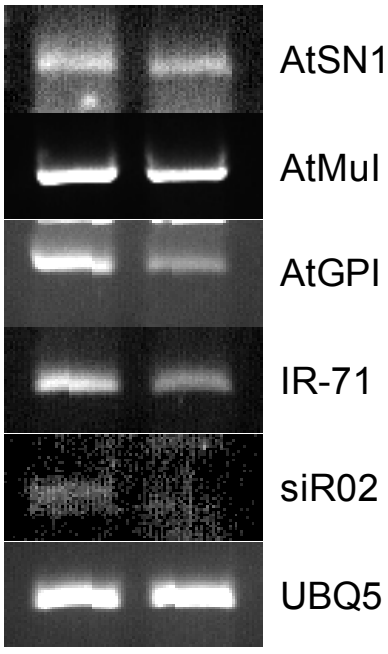

Table 3.1 Primers used for real-time RT-PCR

	5' primer	3' primer
SCL6	gaggtcatagagagcgacac	gaggtcatagagagcgacac
SPL10	tgagacaaagcctacacagatgga	gatgatgcaacccgacttttttatg
AGO1	tggaccaccgcagagacaat	catcatacgctggaagacgact
MYB33	agttgttgtatcctgggtgtagca	ccgttggtggtggtggagac
ARF10	accaagaattgtaccggaaa	cacgtctttctcacgttgtc
TCP4	ctgttcgctcctcctactc	agatggattggtgatgatg
REV	atctgtggtcacaactcc	tagcgacctctcacaaac
ARF3	ggtggcctggttcaaaatggag	cggaagagggtgatgatgatac
ARF4	gggcaggtttactggatact	gacacaagaactggatttgc
At4g19775	ccgtcaggtaatgaaacac	tgggatacagaagtcaacaa
At1g12770	gctttttctactatggggaag	atgagagtgggtttatgtcc
UBQ5	ggtgctaagaagaggaagaat	ctccttctttctggtaaacgt

Table 3.2 Primers used to generate probes for Northern blot analysis

	5' primer	3' primer
ARF17	gccatcagataacttatcgc	gaatcgtcacgtggcaaaga
ARF10	accaagaattgtaccggaaa	cacgtctttctcacgttgtc
Myb33	tcttgttcttggagcaacat	atcaaccacttcatcctcct
Myb65	tccgagttacaagtccctc	atgtaagccaggtgcatgaa
SCL6	actcaagacaacctcaagca	gatagatgcttcacgaaacg
ARF8	gagcctggacagattaactcgtcc	gtcatccaccaaggagaagaatatca
PHB	tgcttagctttcatgttcgt	ccatacaagatcagacattcg
UBQ5	ggtgctaagaagaggaagaat	ctccttctttctggtaaacgt

Table 3.3 Oligo probes used for small RNA Northern blot analysis

miR160	tggcataccagggagcccaggca
miR172	atgccagccatcatccaagattct
miR164	tgcacgtgcccctgcttcctcca
miR166	ccccaatgaatcctggtccgt
miR173	gtgatttctcctcctgtaagccgaa
miR163	atccgaagttccaagtcctccttcaa
miR167	taggtcatgttggcagtttca
miR390	ggcgctatccctcctgagctt
miR319	gggagcctcccttcagtccaa
siR255	tacgctatgttggaccttagaa
siR1511	aagtatcatcattccgccttgga
TAS3-5D8(+)	aaaggcccttacaaggtccaaga
LNA-AtSN1	acca+acg+tgttg+ttgg+cccagtg+gtaaa+tctctca+gat
LNA-Cluster4	aa+gatc+aaac+atca+gca+gcgtc+ag+agg+ctt
LNA-SimpleHAT2	t+ggg+tta+ccc+attt+tgac+accc+cta
LNA-siR1003	a+tgc+caa+gtt+tgg+cct+cac+cgt
LNA-AtREP2	g+cggg+acgg+gttt+ggca+ggac+gtta+ctt+aat
LNA-SiR02	g+ttg+acc+agt+ccg+cca+gcc+gat
LNA-AtCopia2	tc+atcta+gat+gtt+tcta+gggt+ttt+accc+tttt+ccttgt+actcc
LNA-TR2558	aa+gcta+tcgg+tcatg+ctgatg+aatatg+agg+agg+aa
U6	aggggcccatgctaatccttcctc

Table 3.4 Primers used to detect endogenous siRNA target transcript

	5' primer	3' primer
AtSN1	accaacgtgctgttggcccagtggtaaatc	aaaataagtggtggttgtacaagc
soloLTR	aactaacgtcattacatacacatcttg	aattaggatcttgtttgccagcta
AtMu1	ccgagaactggttgtggttt	gctcttgctttggtgatggt
AtGP1	tggtttttcctgtccagtttg	aacaatcctaaccgggttcc
siR02	caatatgttcttcaccatcg	atttgcgaacctaatggaag
IR-71	tatcatccttctggttttgg	aagcaacattcatttcagc
UBQ5	ggtgctaagaagaggaagaat	ctccttctttctggtaaacgt

CONCLUSION

In my thesis research, I have mainly focused on understanding the molecular mechanisms underlying floral meristem determinacy and small RNA biogenesis/function in *Arabidopsis*. Unlike the shoot apical meristem (SAM), a floral meristem is determinate. One of my goals was to understand the molecular mechanisms that confer floral meristem determinacy. Through the characterization of *CURLY LEAF* (*CLF*), I provide a link between epigenetic regulation and stem cell maintenance in the floral meristem. Another goal was to identify genes that act in small RNA biogenesis/function. microRNAs (miRNAs) and small interfering RNAs (siRNAs) play important roles in biological processes such as developmental patterning, stress signaling and genome stability in plants. I identified two genes, *MED20a* and *STERILE APETALA* (*SAP*) that promote small RNA biogenesis and modulate small RNA activities, respectively. The studies of these two genes extend our understanding of the dynamic control of small RNA biogenesis and function.

Epigenetic control in floral meristem determinacy

I characterized a Polycomb group (PcG) gene, *CLF*, as a factor required for floral meristem termination. Through a forward genetic screen, *clf-47* was isolated as an enhancer of *ag-10*, a weak allele of *AGAMOUS* (*AG*), which has defects in floral meristem determinacy but normal organ identity. *CLF* acts in the same genetic pathway as *AG* to confer floral determinacy because *ag-1* is epistatic to *clf-47*. In the *clf-47*

mutant, *WUSCHEL* (*WUS*) is continuously expressed from early stages until stage 8-9, suggesting that *CLF* is required for the initial repression of *WUS* by *AG*. In addition, the function of *CLF* reflects a role of the PcG complex in the control of floral meristem determinacy as a mutation in another PcG gene, *TFL2*, also enhances the floral determinacy defects of *ag-10*.

Identification of a positive factor in miRNA biogenesis

MED20a was identified as a factor that acts in small RNA biogenesis. MED20a is a subunit of Mediator, which is thought to bridge transcription factors and the RNA Polymerase II (Pol II) transcriptional machinery. In *med20a* and mutants in two other Mediator subunits, *med17* and *med18*, the levels of miRNAs are generally reduced. In the *med20a* mutant, the levels of pri-miRNAs are also lower and the promoter activity of *MIR167a* is reduced, suggesting that Mediator promotes miRNA gene expression at the transcriptional level. On the other hand, the accumulation of heterochromatic small interfering RNAs (hc-siRNAs) is not affected in the *med20a* mutant, suggesting that Mediator does not act with the plant-specific RNA polymerase Pol IV. However, some hc-siRNA loci were de-repressed in *med* mutants, raising the possibility that Mediator acts with the other plant-specific RNA polymerase, Pol V.

Identification of a negative regulator of miRNA function

SAP was identified as a negative regulator of the activities of a subset of miRNAs. In *sap* mutants, the mRNA and protein levels of several miRNA target genes are reduced

despite no changes in miRNA accumulation. In addition, some miRNAs are more active in *sap* mutants, resulting in more 3' cleavage products from target mRNAs. Moreover, SAP is present in the cytoplasm, where miRNAs act, as well as in the nucleus. To investigate how *SAP* modulates miRNA activities, I have tested several possibilities: 1) SAP directly interacts with miRNAs or target mRNAs; 2) SAP promotes the subcellular localization of target mRNAs into Processing bodies (P bodies); 3) SAP affects AGO1 endonuclease activity and 4) SAP affects the translational efficiency of target mRNAs. However, the experiments conducted towards testing these hypotheses all yielded negative results. In the absence of clues to the molecular function of *SAP*, perhaps the identification of SAP interacting proteins will provide leads for further investigation.